COUPLING THERMAL TREATMENT AND MICROBIAL REDUCTIVE DECHLORINATION FOR THE ENHANCED REMEDIATION OF CHLORINATED ETHENES

A Dissertation

Submitted by

Tyler F. Marcet

In partial fulfillment of the requirements for the degree of

Doctor of Philosophy

in

Civil and Environmental Engineering

TUFTS UNIVERSITY

February 2018

DISSERTATION COMMITTEE:

Natalie L. Cápiro, PhD, Advisor (*Tufts University*)
Kurt D. Pennell, PhD, Advisor (*Tufts University*)
Ayse Asatekin, PhD (*Tufts University*)
Frank E. Löffler, PhD (*University of Tennessee, Knoxville*

Abstract

The targeted, synergistic implementation of in situ thermal treatment (ISTT) with microbial reductive dechlorination (MRD) has potential to enhance biodegradation of tetrachloroethene (PCE), trichloroethene (TCE), and their chlorinated daughter products, while reducing remedial costs and cleanup time relative to conventional *in situ* remediation technologies. Growth rates and activity of reductively dechlorinating bacteria have been shown to increase during or following field-scale ISTT, but the causal mechanisms are poorly understood. Two of the most likely mechanisms were investigated: 1) increased availability of bioavailable substrates in the aqueous phase and 2) direct temperature stimulation of the microbial community. Through a series of laboratory-scale batch reactor and 1-D column studies, electron donors and fermentable precursors released from porous media during thermal treatment were identified, quantified, and evaluated for their ability to promote the complete microbial reductive dechlorination of PCE to non-toxic ethene. Column studies were also completed to elucidate the impacts of temperature on the growth and activity of a dechlorinating consortium under continuous flow conditions. Results indicate that compounds released from soil organic matter during thermal treatment can represent a substantial source of bioavailable reducing equivalents, capable of sustaining bacterial ethene formation even in the absence of an external electron donor source. Sustained ethene formation was also demonstrated at elevated temperatures previously believed to inactivate key

reductively dechlorinating bacteria. Collectively, results reaffirm the argument for the coupled implementation of ISTT and microbial reductive dechlorination technologies, and underscore the potential to improve contaminant degradation rates.

Acknowledgements

I would like to thank Dr. Natalie Cápiro for her guidance and unyielding support throughout my graduate career, and for allowing me to develop and argue my own opinions and ideas (even when I was clearly wrong).

Thank you to Dr. Kurt Pennell for helping to keep me focused, for continuing to fund me when the grant money *technically* ran out, and for tirelessly advocating for my fellow graduate students and me.

Thank you to Dr. Frank Löffler for telling me that I could do better and for recognizing it when I did.

Thank you to Dr. Ayse Asatekin for serving so enthusiastically on my PhD committee, and for asking thoughtful questions that made me reconsider what I thought I already knew.

Mom, Dad, Nate, and Grandma – I would never have finished my PhD without you because your unconditional love and support are what made it possible for me to begin it in the first place. Thank you. Also, I officially grant you permission to resume asking when I am going to graduate.

Jenny, Tom, Anjuliee, Matt, Kate, Nate, Tiffany, and everyone else who has helped me stay sane along the way – thank you.

List of tables

List of figures

List of abbreviations and acronyms

bvcA – vinyl chloride reductase gene

CERLA – Comprehensive Environmental Response, Compensation and Liability Act

cis-DCE – *cis*-1,2-dichloroethene

COOH – carboxyl group

DCE – dichloroethene

Dhc – *Dehalococcoides*

DNAPL – dense non-aqueous phase liquid

DOC – dissolved organic carbon

e^- – reducing equivalent

ERH – electrical resistance heating

FID – flame ionization detector

GC – gas chromatography

IC – ion chromatography

ISB – in situ bioremediation

ISTT – in situ thermal treatment

IHSS – International Humic Substances Society

LCFA – long-chain fatty acid

NPL – National Priorities List

OC – organic carbon

ORP – oxidation-reduction potential

PCE – tetrachloroethene

PV(s) – pore volume(s)

qPCR – quantitative polymerase chain reaction

RCRA – Resource Conservation and Recovery Act

RDase – reductive dehalogenase

TCD – thermal conductivity detector

TCE – trichloroethene

tceA – trichloroethene reductase gene

trans-DCE – *trans*-1,2-dichloroethene

USEPA – United States Environmental Protection Agency

VC – vinyl chloride

vcrA – vinyl chloride reductase gene

VFA(s) – volatile fatty acid(s)

COUPLING THERMAL TREATMENT AND MICROBIAL REDUCTIVE DECHLORINATION FOR THE ENHANCED REMEDIATION OF CHLORINATED ETHENES

1. Introduction

Although our understanding of pollutant fate, transport, and remediation has improved significantly over the past four decades, there are still 1,383 proposed or active sites on the National Priorities List (NPL), with only 391 sites having been removed since its creation in 1980.[1] The most common pollutants at these sites are chlorinated ethenes: toxic and carcinogenic solvents used heavily throughout the 20th century for their exceptional degreasing properties.[2] While existing technologies have been sufficient to remove the majority of pollutant mass at a relatively small number of contaminated sites, it has become clear to regulators, practitioners, and even product vendors that novel remediation approaches will be necessary to achieve reliable site closure at the increasingly complex contaminated sites that remain.[3-7]

In situ thermal and biological treatments have risen to the forefront of remedial technologies over the past decade as older technologies like pump-and-treat, surfactant flushing, and other standalone physical-chemical remedies have failed to reliably meet remedial goals in a timely and affordable manner. In situ thermal treatment (ISTT) technologies offer rapid removal of contaminant mass and are less sensitive to subsurface heterogeneities and low permeability zones than technologies relying upon in situ flushing or amendment delivery.[4, 5, 8] In situ bioremediation (ISB) typically cannot boast the same speed as ISTT, but it can be effective as a longer term solution, helping to control plume migration and

degrading dissolved contaminant mass or entrapped ganglia for a fraction of the cost of more aggressive technologies.[4, 9] Like all remedial approaches, ISTT and ISB technologies have weaknesses; however, the targeted, synergistic implementation of these technologies shows high potential for mitigating these weaknesses and achieving more complete, timely, and cost-efficient closure of contaminated sites.

The coupled implementation of ISTT with ISB has gained traction as more practitioners share their stories of successes in the field.[2, 10-12] However, though there are logical theories and assumptions about why ISTT seems to improve the microbial degradation of chlorinated solvents, the mechanism or mechanisms responsible for these effects are not fully understood. While there are many possible explanations as to why microbial reductive dechlorination activity often increases during or following ISTT, two stand out as the most likely: 1) increased substrate availability in the aqueous phase and 2) direct temperature stimulation of the microbial population. In order to grow, dechlorinating bacteria must have adequate access to electron acceptors, electron donors, vitamins, and a carbon source.[13] ISTT is known to cause chlorinated ethenes (i.e., electron acceptors) to desorb from the solid phase,[5] but recent research also suggests that soil heating can lead to increased aqueous concentrations of organic carbon (OC),[14-16] potentially improving microbial access to both a carbon source and bioavailable electron donors. Additionally, ISTT may also directly stimulate dechlorinating bacteria.[17-19] The

average groundwater temperature in the United States ranges from 3 °C in parts of Maine and Minnesota to 25 °C in southern Florida and Texas,[20] but all known dechlorinating bacteria are mesophilic, with optimal growth temperatures as high as 38 °C, as determined by batch culture studies.[13, 17-19, 21] Carefully controlled ISTT could close this temperature gap, providing dechlorinating bacteria with more optimal growth conditions and enhancing their activity.

The overarching goal of the research described in this dissertation was to develop a more complete understanding of the mechanisms by which in situ thermal treatment (ISTT) impacts microbial reductive dechlorination (MRD), with particular emphasis on identifying potential synergies between ISTT and MRD technologies so that they may be more effectively coupled at the field scale. A combination of exploratory and hypothesis-driven laboratory studies were designed and completed around the following major research objectives:

1) To determine whether thermal treatment of soils impacts aqueous concentrations of electron donors and fermentable electron donor precursors critical to the MRD process, and whether intrinsic soil properties or heating parameters may be predictive of compound release from the solid phase (Chapter 3).

2) To determine whether electron donors and fermentable electron donor precursors released from the solid phase during thermal treatment are sufficient to promote the growth and activity of a tetrachloroethene (PCE)-to-ethene dechlorinating consortium in a system otherwise lacking those compounds (Chapter 4).

3) To determine the impacts of low-temperature thermal treatment on the MRD of chlorinated ethenes, the growth and activity of a PCE-to-ethene dechlorinating consortium, and presence of *Dehalococcoides mccartyi* (*Dhc*) reductive dehalogenase (RDase) genes in a system incorporating dynamic flow through a porous media (Chapter 5).

2. Background

Background information broadly relating to chlorinated solvent contamination, remediation, and the coupling of remediation technologies are described in this chapter. Additional background information of specific relevance to studies described in Chapters 3, 4, and 5 are included in those chapters.

2.1 Chlorinated ethene contamination and impacts to human health

Chlorinated solvents are among the most widespread and persistent groundwater pollutants in the United States, posing a serious, long term threat to human and environmental health.[22, 23] The most common among these are chlorinated ethenes: tetrachloroethene (PCE), trichloroethene (TCE), and their degradation products 1,1-Dichloroethene (DCE), *cis*-1,2-Dichloroethene (*cis*-DCE), *trans*-1,2-Dichloroethene (*trans*-DCE), and vinyl chloride (VC). PCE and TCE are potent degreasers that have been used extensively in industrial, military, and dry cleaning applications,[2] while *cis*-DCE and VC are most commonly used as chemical intermediaries during the large-scale production of polyvinyl chloride (PVC).[24] Most chlorinated ethenes enter the natural environment as PCE or TCE, typically due to poor storage or disposal practices, though *cis*-DCE and VC are also commonly detected in groundwater as the result of natural degradation of the parent compounds.

Large-scale production of chlorinated ethenes began in the United States during the industrial revolution. Production increased steadily throughout the 20th century until the 1970s and 1980s,[2] when adverse impacts to human health prompted the federal government to begin regulation of hazardous wastes.[25] In 1976, the Resource Conservation and Recovery Act (RCRA) gave the United States Environmental Protection Agency (USEPA) the authority to regulate the handling and disposal of hazardous wastes.[26] In 1980, the passage of the Comprehensive Environmental Response, Compensation and Liability Act (CERCLA) led to the creation of the National Priorities List (NPL), also referred to as the Superfund, intended to aid in the cleanup of heavily contaminated sites.[27] Unfortunately, both the extent of contamination and the difficulty of remediation were drastically underestimated. Approximately 15,000 to 25,000 sites are still believed to be impacted by chlorinated ethene contamination in the United States,[28] and chlorinated ethenes are present at 1,383 proposed or active sites currently on the NPL.[1]

In the 1980s, the negative health impacts of chlorinated ethenes were returned to national attention when TCE contamination of drinking water wells in Woburn, MA was implicated as the primary cause of a series of leukemia clusters, primarily affecting children.[29] Since then, all chlorinated ethenes except the DCE isomers have been classified as known or probable human carcinogens with additional non-carcinogenic affects,[22, 24, 30, 31] including toxicity to the liver, kidneys, reproductive

system, and nervous system.[32] The most common routes of exposure are direct ingestion of contaminated water sources and inhalation of contaminated air.

2.2 Remediation of chlorinated ethenes

Chlorinated ethenes are difficult to remediate, due in part to the tendencies of PCE and TCE to sink below the water table as dense non-aqueous phase liquids (DNAPLs), where they sorb strongly to soil organic matter and slowly dissolve to create persistent contaminant source zones.[33] For the same reasons, excavation of chlorinated solvent sites is cost-prohibitive, and continuously pumping and treating contaminated groundwater is subject to diminishing returns that can extend the theoretical cleanup time to decades or even centuries.[34] Thus, the majority of remedial designs rely upon technologies that isolate, extract, or degrade the target compounds in situ. These technologies include flushing with surfactants or co-solvents to dissolve and mobilize contaminants, air sparging to strip volatile compounds for treatment above ground, injection of chemical oxidants to destroy contaminants in situ, heating of the subsurface to desorb, volatilize, and capture volatile contaminants, and augmentation with or stimulation of microorganisms capable of coupling contaminant degradation to their own metabolism.[33] Despite these and numerous other remedial innovations, and a substantially improved collective understanding of chlorinated ethene contamination as a whole since cleanup efforts began in the 1980s, complete removal of chlorinated solvent mass is still very rare. More commonly, rapid contaminant mass removal in early stages

of remediation is followed by an extended period characterized by persistent contaminant concentrations that are substantially lower than initial values, but remain above the target (Figure 2-1).[35] This remediation stall may be due to persistence of an existing or unidentified source zone, gradual desorption of contaminant mass that had previously been bound to soil organic matter, or back-diffusion of contaminant mass that had been driven into tightly packed, low permeability zones by a steep concentration gradient that was subsequently reversed upon elimination of the source zone.[36, 37]

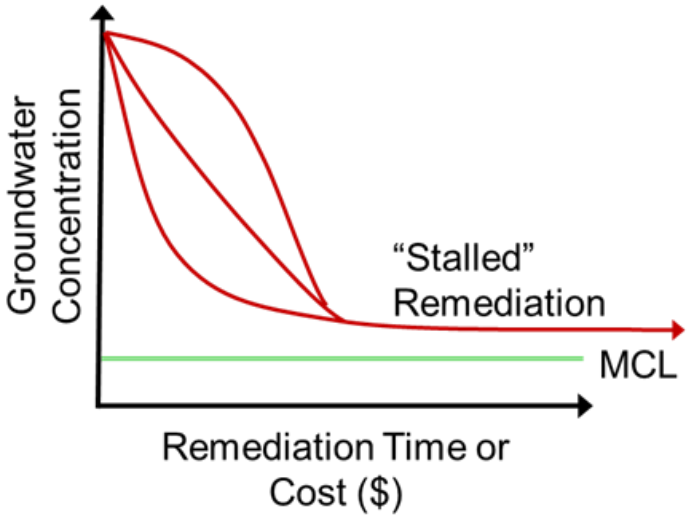

Figure 2-1: Typical concentrations of chlorinated ethenes in groundwater during application of in situ remediation technologies, demonstrating rapid mass removal in early phases, followed by long-term persistence of contaminant concentrations above the drinking water standard (MCL).

Some newer, aggressive technologies like in situ thermal treatment (ISTT) are capable of quickly removing more than 90% of chlorinated ethene mass,[4, 38] but even these technologies often leave behind contaminant concentrations well above the 2 – 5 µg/L drinking water standards set by the USEPA.[39]

In response to this failure of standalone technologies to reliably remediate sites contaminated with chlorinated ethenes, focus has shifted toward development and application of combined remedies, also referred to as the treatment train approach.[3, 4, 7, 40] Combined remedies are loosely defined as any of various complementary remediation technologies that are implemented in parallel or in series in an effort to improve contaminant mass removal while minimizing associated costs compared to a standalone technology. Treatment trains have been implemented with varying success at the laboratory, pilot, and field scales, and often consist of an aggressive technology (e.g., chemical oxidation, co-solvent flushing, steam injection) to remove the majority of chlorinated ethene mass, followed by a relatively passive, longer-term remedy (e.g., permeable reactive barrier, in situ bioremediation (ISB)) to degrade residual contaminant mass.[6, 41] Two classes of remediation technologies that have received substantial attention and seem particularly well-suited for field-scale coupling are ISTT and MRD.[3-5, 10, 15-18, 33, 42-44]

2.3 In situ thermal treatment

ISTT technologies are designed to increase the temperature of the contaminated subsurface, promoting the desorption, volatilization, and hydrolytic degradation of chlorinated ethenes and other volatile organic contaminants.[45, 46] The most commonly applied ISTT technologies include hot water injection, steam injection, conductive heating, and electrical resistance heating (ERH).[8, 47] While each of these ISTT technologies has been implemented with success at the field-scale, the reliability and versatility of ERH has made it the most popular and effective option in recent years.[47]

In an ERH system, electrodes are installed in the contaminated subsurface in a three-phase (Figure 2-2) or six-phase (Figure 2-3) configuration. In a three-phase configuration, electrodes are installed in a repeating triangular pattern so that each electrode is always adjacent to electrodes of a different electrical phase. Similarly, in a six-phase configuration, electrodes are installed in a repeating triangular pattern, with six electrodes each of different electrical phase surrounding a central, neutral electrode. Six-phase heating was primarily used during early pilot studies, but three-phase heating is most often applied during field-scale ERH because it is more likely to result in spatially consistent subsurface temperatures.[5]

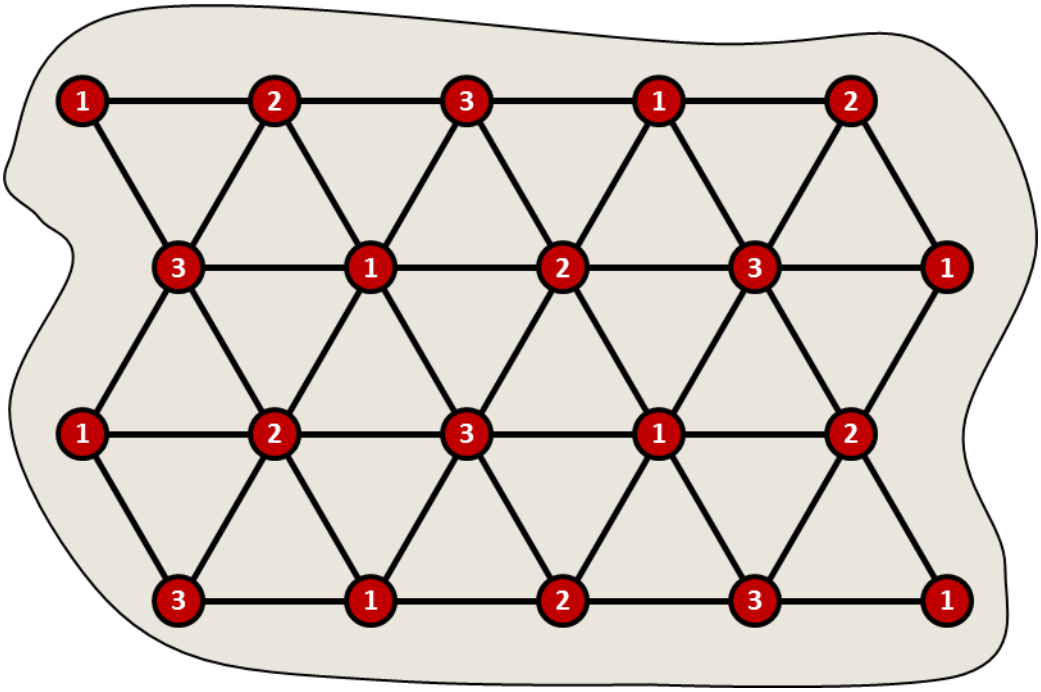

Figure 2-2: Electrode configuration typical of three-phase ERH, with numbers 1, 2, and 3 indicating electrodes of different electrical phases. Alternating current is passed between electrodes of different electrical phase and the resistance of the soil generates heat.

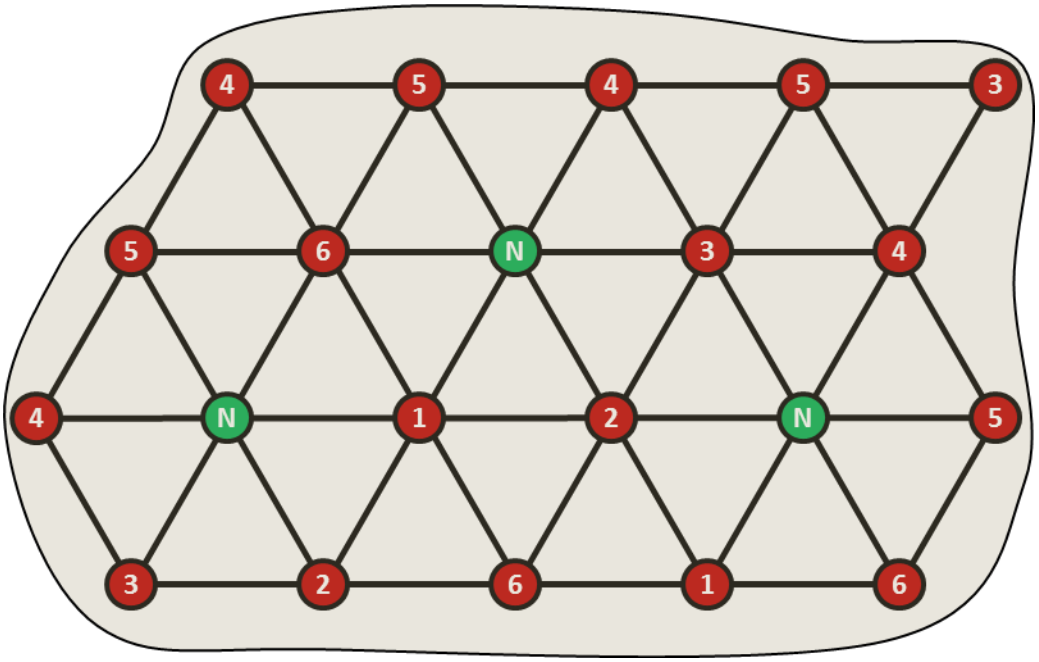

Figure 2-3: Electrode configuration typical of six-phase ERH, with numbers 1 – 6 indicating electrodes of different electrical phases and “N” indicating the neutral electrode. Alternating current is passed between electrodes of different electrical phase and the resistance of the soil generates heat.

In each configuration, alternating current is passed between electrodes of different electrical phase and the resulting electrical resistance of the soil generates heat.[5] Because ERH is not subject to the same hydraulic limitations as technologies reliant upon in situ flushing or amendment delivery, it can be successfully applied at low permeability and heterogeneous sites.[5, 47] As the technology has matured, contaminant mass reductions of more than an order of magnitude have become typical,[38] with some practitioners even offering guarantees that treatment goals will be achieved. In an assessment of six sites where ISTT was applied to chlorinated solvent DNAPL source zones, median contaminant mass reductions of more than 95% were reported.[38] However, due to high energy demands and rapidly diminishing returns upon source zone depletion, ERH systems are not typically applied to large, dissolved contaminant plumes, and are rarely operated for more than a year.[4, 38]

Most ERH systems to date have been designed with a target final temperature near the boiling point of water (80 – 110 °C),[47] ensuring rapid contaminant removal while preventing the system from drying out and becoming ineffective.[5] However, growing emphasis on sustainable remediation technologies has led to interest in low-temperature ISTT, which uses the same heating principles as traditional ERH, but with target temperatures significantly lower than 100 °C.[4, 11, 12] Although information in the literature is limited, field-scale experiments have demonstrated that low-temperature ERH can enhance degradation processes like ISB, while

reducing or eliminating the need for energy intensive components like soil vapor recovery systems.[10]

2.4 Microbial reductive dechlorination

Microbial reductive dechlorination is an ISB approach commonly applied at sites contaminated with chlorinated ethenes. In this redox process, anaerobic bacteria use chlorinated ethenes as electron acceptors, removing chlorine atoms in a stepwise manner until only non-toxic ethene remains.[9] Each step in the dechlorination process requires two moles of reducing equivalents (e^-), so complete dechlorination of one mole of PCE to non-toxic ethene consumes eight moles of reducing equivalents (Figure 2-4).[48, 49]

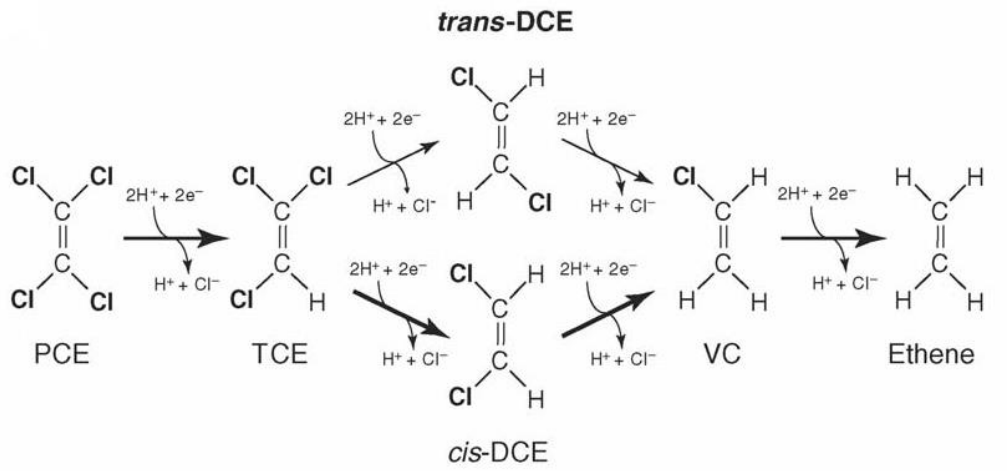

Figure 2-4: Microbial reductive dechlorination of chlorinated ethenes and subsequent release of hydrogen and chloride ions, reproduced from Löffler and Edwards (2006)

A small number of known pure strain bacteria are capable of reducing PCE all the way to ethene, but none can do so efficiently.[50-52] Instead, it is far more common for dechlorination to be carried out by a diverse bacterial consortium, with different species and strains catalyzing different steps in the MRD process. Consortia shown to fully dechlorinate PCE to ethene include Bio-Dechlor INOCULUM (BDI), KB-1®, SDC-9™, and associated subcultures, as well as other laboratory cultures.[53-57] While species capable of reducing PCE and TCE to *cis*-DCE are ubiquitous in the environment (Table 2-1),[58-66] only select strains of *Dehalococcoides mccartyi* (*Dhc*) are able to efficiently catalyze reduction of *cis*-DCE to VC and ethene.[13] Thus, all known PCE-to-ethene dechlorinating consortia contain at least one *Dhc* strain.

Table 2-1: Partial list of known species capable of MRD. Filled blocks represent proven metabolites and hatch blocks represent co-metabolites. Reproduced from Marcet (2014).

Species	PCE	TCE	DCEs	VC	Reference(s)
Sulfurospirillum multivorans	■	■			60, 62, 63
Desulfuromonas chloroethenica	■	■			59
Dehalobacter restrictus	■	■			58
Desulfitobacterium sp. strain Y51	■	■			66
Sulfurospirillum halorespirans	■	■			60
Desulfuromonas michiganensis	■	■			65
Geobacter lovleyi strain SZ	■	■			64
Dhc strains:					
195	■	■	■	▨	13, 52, 61
FL2		■	■		50
GT		■	■	■	68
BAV1	▨	▨	■	■	69, 70
VS			■	■	71

Degradation of chlorinated ethene mass via MRD is slow compared to more aggressive remediation technologies like ISTT. In addition to measurement of contaminant concentrations, performance of MRD is also assessed by measuring the total and relative abundances of genomic biomarkers that have previously been associated with ethene formation during MRD. For example, *Dhc* abundance exceeding 10^6 copies/L or 0.05% of total bacteria in groundwater samples are strong indicators of ethene production.[72] Not all *Dhc* strains are capable of MRD, however, so high *Dhc* 16S rRNA gene abundance is not necessarily indicative of potential for ethene formation.

In addition to the *Dhc* 16S rRNA gene, three reductive dehalogenase (RDase) genes (*tceA*, *vcrA*, and *bvcA*) have been directly implicated in ethene production and are expressed only by *Dhc* strains known to reduce *cis*-DCE or VC. Thus, knowledge of the aqueous abundances of these RDase genes can help to determine whether attempts to stimulate native dechlorinating populations could be successful. Of the five *Dhc* strains capable of *cis*-DCE and VC reduction, strains 195 and FL2 possess the *tceA* gene (TCE → DCEs → VC), strains VS and GT possess the *vcrA* gene (cis-DCE → VC → ethene), and strain BAV1 possesses the *bvcA* gene (DCEs → VC → ethene).[13] The *vcrA* gene is often targeted in addition to the *Dhc* 16S rRNA gene during quantitative real-time polymerase chain reaction (qPCR) analysis because of its frequent correlation with ethene formation.[73] However, studies have also implicated the *bvcA* and *tceA* genes in ethene formation.[74] In a study of RDase

and *Dhc* gene abundance in relation to geochemical parameters, *vcrA* abundance was highly correlated to VC and ethene formation under highly reducing conditions, but the *bvcA* and *tceA* genes were increasingly implicated in dechlorination under more oxidizing conditions.[74] Similarly, increased abundance of *bvcA* and *tceA* was reported following ISTT of a field site in Fort Lewis, WA.[10] These reports suggest that relevant reductive dechlorination biomarkers may vary depending upon site characteristics.

MRD systems are typically designed around *Dhc* because, in addition to their critical role in the dechlorination process, they have very strict growth requirements and are highly sensitive to their environment.[13] These requirements are often cited as reasons for "*cis*-DCE stall," or the tendency of MRD sites to accumulate *cis*-DCE while producing very limited amounts of VC and ethene.[75] In order for growth to occur, *Dhc* require chlorinated ethenes as electron acceptors, hydrogen (H_2) as electron donor, a carbon source (typically acetate), and vitamin B_{12}.[13] These substrates can be injected into the subsurface to stimulate native bacteria in a process called biostimulation. However, like all amendment delivery, the effectiveness of biostimulation can be limited by subsurface heterogeneities, and thus requires a thorough understanding of subsurface architecture to ensure that substrates reach the target microorganisms. Alternatively, bioaugmentation with an enriched, commercially available consortium is typically accompanied by substrate injection in the same inoculum and a higher likelihood of success.[76, 77]

In addition to their highly specific substrate requirements, *Dhc* are strict anaerobes, with oxygen and sulfite exposure leading to rapid cell death. Neutral pH and temperatures below 30 °C are also generally considered to be required for cell growth, though there are limited examples suggesting that exceptions to these pH and temperature requirements may exist;[17, 19] however, research on these topics is preliminary and largely unavailable in the literature.

Despite the challenges associated with establishing and maintaining a functioning system, the popularity of MRD continues to increase due to its high effectiveness and low operational and maintenance costs relative to other technologies.[78] However, it is a slow process, especially when compared to aggressive technologies like ISTT, and is usually applied to dissolved contaminant plumes instead of DNAPL source zones, as even dechlorinating bacteria can be subject to chlorinated ethene toxicity.[79-81]

2.5 Coupling in situ thermal treatment and microbial reductive dechlorination

In recent years, the traditional concept of applying standalone remedial technologies has given way to that of combined remedies, where two or more complimentary technologies are simultaneously or sequentially applied. The ideal combined remedy takes advantage of the strengths of each component, creating an effective, cost-efficient system capable of achieving remedial goals otherwise unattainable by a standalone technology. Combined remedies are considered by many practitioners, regulators, and even vendors to be the best chance at combating the remedial stalling and contaminant rebound effects often encountered at chlorinated solvent sites.[3-5, 7, 40]

ISTT and microbial reductive dechlorination are two technologies potentially well suited for simultaneous or sequential implementation: ISTT would provide the initial aggressive push necessary for rapid source zone removal, while dechlorinating microorganisms would degrade residual contaminants over a longer period.[3-5, 10, 15-18, 33, 42-44] Previous studies indicate that ISTT may also benefit microbial reductive dechlorination by eliminating competing bacterial communities,[42] thus providing a competitive advantage to native or amended dechlorinating bacteria.[43] Krauter, et al. (1995) reported that ISTT at a gasoline-impacted site led to a 90 – 98% reduction in the overall microorganism population. Yang and McCarty (1998) reported that dechlorinating bacteria compete for H_2

most effectively when concentrations are between 2 and 11 nM, but *Dhc* have also been reported to consume H_2 at concentrations as low as 0.061±0.016 nM,[50] three orders of magnitude lower than even the most competitive methanogens.[84]

Laboratory-scale studies have also demonstrated that heating of contaminated field materials may improve redox conditions for bacterial growth and increase availability of fermentable substrates in the aqueous phase. Friis, et al. (2005) reported that heating of Fort Lewis, WA field samples to 100 °C resulted in an increase of dissolved organic carbon (DOC) (14 mM) compared to unheated samples (2 mM). Most of this organic carbon (OC) was not identified as specific compounds and was assumed to be composed predominantly of long-chain fatty acids (LCFAs), which are too complex to be used directly as electron donors for microbial reductive dechlorination.[15] However, large organic compounds like LCFAs and humic materials are partly composed of simple acidic functional groups within their complex organic structures.[85] Thermal analyses of the structural composition of humic matter have demonstrated that carboxyl functional groups (COOH), the key components of readily bioavailable volatile fatty acids (VFAs), are heat-stable to approximately 300 °C,[86, 87] suggesting that partial degradation of organic material may provide a source of bioavailable organic substrates. In another study, incubation of material from the Fort Lewis, WA site at 25 to 95 °C led to limited accumulation of formate and acetate, [14] suggesting that subsurface temperatures commonly achieved during traditional ISTT can cause soil organic

matter to break down to bioavailable components. For example, *Geobacter lovleyi* strain SZ couples acetate oxidation to reduction of PCE and TCE to *cis*-DCE.[65, 70] Furthermore, VFAs like formate,[88] propionate, butyrate, and isovalerate can be oxidized to H_2 (

Table 2-2), thus providing strictly hydrogenotrophic *Dhc* with reducing equivalents necessary to convert *cis*-DCE and VC to ethene.

Table 2-2: Maximum theoretical H_2 (reducing equivalents) resulting from oxidation of organic compounds.

Oxidation of organic compounds	$C_xH_yO_z + (2x - z)H_2O \rightarrow \left(\frac{y}{2} + 2x - 2\right)H_2 + xCO_2$	(Equation 1)
Hydrogen half-reaction	$H_2 \rightarrow 2H^+ + 2e^-$	(Equation 2)
Equation 1 + Equation 2	$C_xH_yO_z + (2x - z)H_2O \rightarrow (4x + y - 4)(H^+ + e^-) + xCO_2$	(Equation 3)
Formic acid oxidation	$HCOOH \rightarrow 2H^+ + \mathbf{2}\boldsymbol{e}^- + CO_2$	(Equation 4)
Acetic acid oxidation	$CH_3COOH + 2H_2O \rightarrow 8H^+ + \mathbf{8}\boldsymbol{e}^- + 2CO_2$	(Equation 5)
Propionic acid oxidation	$C_2H_5COOH + 4H_2O \rightarrow 14H^+ + \mathbf{14}\boldsymbol{e}^- + 3CO_2$	(Equation 6)
Butyric acid oxidation	$C_3H_7COOH + 6H_2O \rightarrow 20H^+ + \mathbf{20}\boldsymbol{e}^- + 4CO_2$	(Equation 7)
Isovaleric acid oxidation	$C_4H_9COOH + 8H_2O \rightarrow 26H^+ + \mathbf{26}\boldsymbol{e}^- + 5CO_2$	(Equation 8)

In addition to the potential for to create an in situ electron donor source, ISTT may provide direct temperature stimulation of dechlorinating bacteria. All known dechlorinating bacteria are mesophilic, with results from various isolated and mixed culture batch studies suggesting optimal growth temperatures ranging from 22 – 38 °C,[13, 17-19, 21] significantly higher than average United States groundwater temperatures (Figure 2-5).[20] A narrower optimal range of 25 – 30 °C has also been identified for the highly sensitive *Dhc*,[13] though slow dechlorination of TCE to ethene has been reported during 40 °C incubation of the PCE-to-ethene dechlorinating Bio-Dechlor INOCULUM,[17] representing the highest temperature permissive of sustained *Dhc* activity available in the literature. This temperature differential suggests that the majority of MRD sites in the country could experience increased microbial degradation rates given a moderate increase in subsurface temperature.

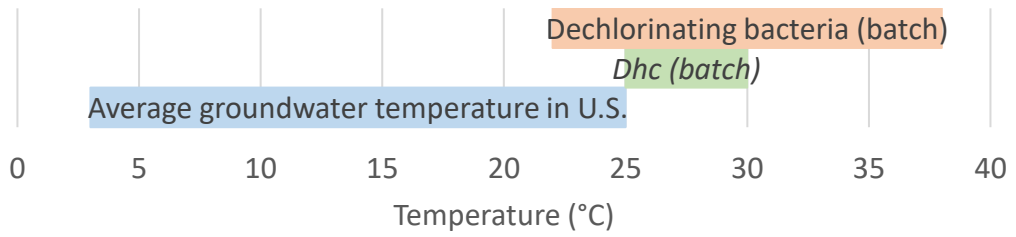

Figure 2-5: Optimal growth temperatures for dechlorinating bacteria and *Dhc* in batch studies compared to average groundwater temperature in the United States.

Finally, though the influence of temperature on MRD has been studied extensively in batch experiments, few studies have incorporated the simultaneous effects of flow through a porous media and variable temperature. In one such study, no PCE dechlorination occurred in batch studies at 10 °C, but dechlorination was complete to ethene and ethane in an anaerobic flow experiment completed at the same temperature.[21] Similarly, the dechlorination activity of *Dhc* was approximately 200 times greater in column experiments than in equivalent batch experiments, suggesting that flow conditions may have a dramatic effect on microbial activity.[89] Although laboratory- and field-scale studies have demonstrated increased activity of dechlorinating bacteria during or following ISTT, the reasons why are not fully understood. Because of this, results from even the most successful coupled implementation of in situ thermal and biological treatments must be considered at least in part fortuitous. Until the mechanisms responsible for the apparent thermally-induced increase in dechlorination activity are identified and understood, practitioners will be unable to effectively optimize remedial designs.

3. Release of fermentable substrates and direct electron donors during thermal treatment of soils

3.1 Abstract

Thermal treatment of soil and groundwater may provide an *in situ* source of bioavailable organic compounds that could stimulate microbial reductive dechlorination (MRD) at sites impacted by chlorinated solvents. The objectives of this study were to identify and quantify release of electron donors and fermentable precursors during soil heating, and to develop a correlation for estimating availability of these compounds following thermal treatment. 14 solids (quartz sand, aquifer material, natural soils, humic and fulvic acid standards) containing <0.01 to 63.81 wt% organic carbon (OC) were incubated at 30, 60, or 90 °C for up to 180 d. Total volatile fatty acids (VFAs) release, expressed as moles of carbon per gram solid, ranged from 5±0 × 10^{-9} molC/g_s during 30 °C incubation of quartz sand to 820±50 × 10^{-6} molC/g_s during 90 °C incubation of humic acid. Hydrogen (H_2) was detected in the gas phase at a maximum of 180±50 × 10^{-9} molH_2/g_s, accounting for less than 0.3% of reducing equivalents associated with VFAs released under the same conditions. These findings demonstrate that heating of solid materials leads to release of electron donors and fermentable precursors, identified primarily as VFAs. The observed VFAs release was positively correlated with incubation time, temperature, and solid-phase OC content, allowing for more reliable prediction and integration into the overall remedial strategy.

3.2 Introduction and background

Simultaneous or sequential implementation of remediation technologies may produce synergistic effects that reduce the cost and time required to achieve remedial objectives.[3, 4, 7, 90] For example, coupling of in situ thermal treatment (ISTT) with microbial reductive dechlorination (MRD) shows promise as a combined remedy at sites impacted by tetrachloroethene (PCE), trichloroethene (TCE), and their chlorinated daughter products.[3, 15, 16, 18, 42, 43] Both technologies are effective standalone methods for chlorinated solvent remediation, but complete contaminant mass removal with a single technology is rare.[5, 35, 38, 49] ISTT technologies such as electrical resistance heating (ERH) are typically designed to increase subsurface temperatures to 80 – 110 °C,[47] promoting rapid contaminant mass removal via desorption and volatilization; however, high energy requirements preclude prolonged operation, making the technology best suited for source zone removal.[5, 47] MRD is relatively inexpensive and effective for remediating contaminant plumes that may be economically infeasible to treat using aggressive methods like ERH.[78] However, MRD is comparatively slow and most effective when favorable geochemical conditions (e.g., circumneutral pH, anoxic conditions, substrate availability) are maintained.[13]

Insufficient electron donor availability often limits MRD, especially in low permeability zones where traditional biostimulation techniques (e.g., substrate amendment) are difficult to implement.[48, 91, 92] Previous studies have shown that

heating of aquifer material may increase availability of fermentable substrates in the aqueous phase and create geochemical conditions favorable for reductively dechlorinating bacteria.[14-16] For example, heating of Fort Lewis, WA field samples to 100 °C increased aqueous concentrations of OC compared to unheated samples (i.e., 14 versus 2 mM), which was primarily attributed to long-chain fatty acids (LCFAs) and water soluble humic matter. Similar increases in dissolved organic carbon (DOC) were reported at field sites undergoing ISTT.[16]

Neither LCFAs nor humic matter can be used directly as electron donors by reductively dechlorinating microbes,[15] but humic matter contains abundant carboxyl functional groups (COOH),[85] a defining component of all bioavailable VFAs, that can be separated from the bulk organic structure.[93] One of these VFAs, acetate, is used directly as an electron donor by some dechlorinating bacteria (e.g., *Geobacter lovleyi* strain SZ) to reduce PCE and TCE to *cis*-1,2-dichloroethene (*cis*-DCE),[64, 65] and, like all VFAs, can be converted to H_2,[88, 94-97] potentially stimulating the strictly hydrogenotrophic *Dehalococcoides mccartyi* (*Dhc*) and supporting complete reduction of chlorinated ethenes. These VFA-consuming, H_2-producing reactions are thermodynamically unfavorable under standard conditions (i.e., $\Delta G°' > 0$ kJ/reaction), but can proceed spontaneously (i.e., $\Delta G' < 0$ kJ/reaction) if H_2 does not accumulate ().

Table 3-1).

Table 3-1: VFAs-consuming, H_2-producing reactions and associated changes in Gibbs free energy under standard conditions and geochemical conditions relevant to microbial reductive dechlorination.

Reaction			$\Delta G°'_a$ (kJ/reaction)	$\Delta G'_b$ (kJ/reaction)	$\Delta G'_c$ (kJ/reaction)	
$formate^- + H_2O$	→	$HCO_3^- + H_2$	+1.3	-18.8	-2.3	(Equation 9)
$acetate^- + 4H_2O$	→	$2HCO_3^- + 4H_2 + H^+$	+104.5	-49.9	-69.5	(Equation 10)
$propionate^- + 3H_2O$	→	$acetate^- + HCO_3^- + 3H_2 + H^+$	+76.5	-57.8	-93.9	(Equation 11)
$butyrate^- + 2H_2O$	→	$2acetate^- + 2H_2 + H^+$	+48.3	-65.9	-118.5	(Equation 12)

Changes in Gibbs free energy ($\Delta G = \Delta G°' + RT\ln([C]^c[D]^d/[A]^a[B]^b)$) for a given equation $aA + bB \rightarrow cC + dD$, assuming 25 °C, pH 7, $[H_2O]$ = 1 M, and: (a) [VFAs] = 1 M, $[HCO_3^-]$ = 1 M, P_{H2} = 1 atm; (b) [VFAs] = 1 mM, $[HCO_3^-]$ = 30 mM; $P_{H2} = 10^{-5}$ atm; (c) [VFAs] = 10 nM, $[HCO_3^-]$ = 30 mM; $P_{H2} = 7.8 \times 10^{-8}$ atm.

Fortunately, *Dhc* can utilize H_2 at partial pressures as low as $78 \pm 20 \times 10^{-9}$ atm,[50] orders of magnitude lower than the minimum threshold for methanogenesis,[50, 84, 94, 98] thus helping to maintain reaction spontaneity even when VFAs are present at low concentrations (e.g., < 10 nM).

Various methods (e.g., acid/alkaline hydrolysis, pyrolysis, reductive cleavage, chemical oxidation) have been used to separate low molecular weight compounds, such as readily bioavailable VFAs, from the macromolecular organic structure; unfortunately, these harsh methods also degrade the liberated compounds themselves. Hydrolytic degradation at circumneutral pH is a comparatively mild separation method that results in lower recovery of organic constituents (0 – 4 wt% of initial organic matter), but is less likely to disrupt the molecular integrity of liberated compounds.[93] In two studies using aquifer material from the Fort Lewis, WA field site, VFAs (formate, acetate, and propionate) were detected following incubation at 25 – 100 °C,[14, 16] indicating that in situ hydrolysis of organic matter during ISTT could increase aqueous concentrations of VFAs that are known to stimulate beneficial anaerobic processes. However, the existing data are limited to site-specific conditions and are inconsistent in terms of the compounds released during heating.[14-16] Consequently, the benefits of this substrate release cannot be fully exploited, limiting the potential use of MRD as a combined remedy or polishing step during ISTT. A comprehensive effort to quantify substrate release as a function of key solid-phase properties and thermal treatment parameters will

allow for more reliable prediction of the rate, extent, and types of substrate release during ISTT. In this study, an extensive matrix of batch experiments was completed using sand, aquifer material, natural soils, and humic and fulvic acid standards (hereinafter referred to jointly as "solids" or "solid materials") possessing a wide range of OC contents (<0.01 – 63.81 wt%) incubated at 30, 60, or 90 °C for up to 180 d. The objectives of this work were: 1) to identify electron donors and fermentable precursors released during thermal treatment of solids, with focus on release of VFAs; 2) to quantify this release as a function of solid-phase properties (i.e., OC content, functional group abundance) and incubation parameters (i.e., time, temperature); and 3) to identify potential correlations for estimating substrate availability following ISTT of solids. Results provide more generalized, less site-specific information than previously available, and will allow remediation professionals to better anticipate and take advantage of thermally-induced substrate release to stimulate a concurrent or subsequent in situ bioremediation (ISB) phase.

3.3 Materials and methods

3.3.1 Materials

VFA standard solutions were prepared using reagent grade or higher purity sodium acetate (EMD Millipore, Burlington, MA), sodium butyrate (Alfa Aesar, Haverhill, MA), isobutyric acid, sodium formate, sodium propionate, valeric acid, and

isovaleric acid (Sigma-Aldrich, St. Louis, MO). Solid- and dissolved-phase OC standards were prepared using ACS reagent grade sucrose (Thermo Fisher, Waltham, MA) and potassium hydrogen phthalate (EMD Millipore), respectively. Nitric acid (Certified ACS Plus, 70%) used in batch experiment preparation and mercury (II) chloride ($HgCl_2$; ACS reagent, 99.5+%) used to inhibit microbial activity were purchased from Thermo Fisher. All gases used in batch experiment preparation, sampling, and analyses were of ultra-high purity and obtained from Airgas (Radnor, PA). Aqueous solutions were prepared with deionized (DI) water (18.2 MΩ cm^{-1}, total OC <5 µg/L) that had passed through a Milli-Q® Reference Water Purification System (EMD Millipore).

3.3.2 Porous media and humic acid standards

14 solid materials, representing a range of OC contents, were used in incubation experiments (

Table 3-2). Solids included Federal Fine Ottawa sand (US Silica, Frederick, MD), Groveland aquifer material (8.8 – 11.3 m depth, Groveland Wells Superfund site, MA),[99] Appling soil (<30 cm depth, University of Georgia Agricultural Experiment Station, Eastville, GA),[100, 101] Webster soil (<30 cm depth, Iowa State University Agricultural Experiment Station, Ames, IA),[100, 101] Arkport soil (114 – 142 cm depth, Orleans County, NY),[101] Hudson soil (60 – 104 cm depth, Allegany County, NY),[101] and Mardin soil (64 – 102 cm depth, Tompkins County, NY).[101] Also included were three solids obtained from the International Humic Substances Society (IHSS) (St. Paul, MN): Elliott silt loam soil (Joliet Army Ammunition Plant, Joliet, IL);[101, 102] Pahokee peat soil II (University of Florida Everglades Research & Education Center, Belle Glade, FL);[101, 102] and Gascoyne leonardite (Gascoyne Mine, Gascoyne, ND).[102] Highly characterized Suwannee River fulvic acid standard II, Pahokee peat humic acid standard, Elliott soil humic acid standard, and Leonardite humic acid standard were also obtained from the IHSS.[102] Humic and fulvic acid standards are rendered essentially sterile during the extraction process due to repeated hydrofluoric acid exposure and freeze-drying.[103]

Table 3-2: Solid-phase properties and mass per ampule in incubation experiments.

Solid phase	OC		pH	COOH	Solid mass per ampule in Set:				
	(wt%)	(mmol/ampule)		(mmol/g_s)	#1	#2	#3	#4	#5
Federal Fine Ottawa sand	0.01	0.1	7.7	nd	15 g	15 g	-	-	15 g
Groveland aquifer material	0.01	0.1	6.4	nd	15 g	15 g	-	-	15 g
Appling soil	0.66	5.5	4.6	0.02[b]	10 g	10 g	-	-	10 g
Webster soil	1.97	16.4	6.7	0.08[b]	10 g	10 g	-	-	10 g
Arkport soil	0.32	2.7	5.5	nd	-	-	-	-	10 g
Hudson soil	1.14	9.5	5.8	nd	-	-	-	-	10 g
Mardin soil	1.42	11.8	4.0	nd	-	-	-	-	10 g
Suwannee River fulvic acid standard II	52.34[a]	0.3	nd	5.81[a]	-	-	7 mg	-	-
Pahokee peat humic acid standard	56.37[a]	0.4	nd	5.02[a]	-	-	8 mg	-	-
Elliott soil humic acid standard	58.13[a]	0.4	nd	4.77[a] 4.51[b]	-	-	8 mg	-	-
Leonardite humic acid standard	63.81[a]	0.4	nd	4.64[a] 4.16[b]	-	-	8 mg	-	-
Elliott silt loam soil	2.86	19.0	6.1	0.07[b]	-	-	-	8 g	8 g
Pahokee peat soil II	46.90[a]	117.1	nd	nd	-	-	-	3 g	3 g
Gascoyne leonardite	50.11	125.2	nd	1.14[b]	-	-	-	3 g	3 g

nd = not determined. Values determined at Tufts University unless specified otherwise: (a) IHSS, (b) University of Georgia.

3.3.3 Batch experiments

Five sets of incubation experiments were performed in 20 mL borosilicate glass ampules (Kimble-Chase, Vineland, NJ). Set #1 consisted of ampules containing Federal Fine Ottawa sand, Groveland aquifer material, Appling soil, or Webster soil, and was designed to identify and quantify VFAs and H_2 release during heating of solids with OC contents (<0.01 – 1.97 wt%) likely to be encountered at a thermal remediation site.[104] Set #2 ampules contained the same solids as Set #1, but also contained 2 mM $HgCl_2$ so that VFAs and H_2 release could be assessed under microbially-inhibited conditions.[105] Set #3 was designed to assess VFAs and H_2 release during heating of Suwannee River fulvic acid standard II, Pahokee peat humic acid standard, Elliott soil humic acid standard, and Leonardite humic acid standard in the absence of potentially confounding factors (e.g., inorganic constituents and native microbial activity) present in the bulk source materials from which the standards were extracted. Set #4 ampules included the three available bulk source materials (Elliott silt loam soil, Pahokee peat soil II, Gascoyne leonardite) and, in conjunction with Set #3, was designed to elucidate the role of OC structure on thermally-induced VFAs and H_2 release. Set #5 included each of the solid materials from Sets #1, 2, and 4, as well as the Arkport, Hudson, and Mardin soils, and was designed to quantify VFAs and H_2 release following incubation under typical thermal remediation conditions (180 d at 90 °C).

Prior to loading, ampules were soaked overnight in a 1.6 M nitric acid solution, rinsed with DI water, covered with aluminum foil, steam-sterilized at 121 °C for 30 min, and oven-dried at 110 °C. Solids were dried for 48 h in a glass desiccator containing Drierite desiccant (Thermo Fisher) under a 750 mm Hg vacuum at room temperature. Solids, excluding humic and fulvic acid standards and bulk source materials, were then passed through a sterilized #30 stainless steel sieve (ASTM E-11) to remove large particles and debris. Ampules were loaded with each solid phase per

Table 3-2, followed by 10 mL of sterile, degassed DI water (Sets #1, 3 – 5) or 2 mM $HgCl_2$ (Set #2). Prepared solid samples were also set aside for determination of solid-phase OC content. Loaded ampules were then purged with filter-sterilized (0.22 µm) argon gas and flame-sealed using a BernzOmatic MAPP/oxygen torch (Worthington Industries, Columbus, OH) or a propane/air Twin Jet ampule sealer (Adelphi, Manchester, UK). Depending upon the volume of the solid phase in each ampule, the argon headspace volume ranged from 12 to 15 mL. Method blanks containing no solid phase were also prepared for each ampule set. All batch experiments were prepared in triplicate or greater. In total, 543 non-method blank ampules remained intact until sampling, representing 140 unique combinations of solid-phase and incubation conditions.

3.3.4 Incubation and destructive sampling

Sealed ampules were placed in a dark 30 °C constant temperature room, a 60 °C water bath or incubator (Thermo Fisher), or a 90 °C recirculating water bath (VWR, Radnor, PA) or oven (Thermo Fisher) for periods of: 28, 42, and 56 d (Set #1: Quartz sand, aquifer material, and natural soils and Set #2: Quartz sand, aquifer material, and natural soils with 2 mM $HgCl_2$); 7, 14, 21, and 28 d (Set #3: Humic and fulvic acid standards); 7, 21, 49, and 77 d (Set #4: Humic acid bulk source materials); or 180 d (Set #5: Quartz sand, aquifer material, natural soils, and humic acid bulk source materials). Ampules were not subject to mixing or agitation during

incubation. Following incubation, intact ampules were cooled for 12 h at room temperature, then destructively sampled following an established procedure.[106] Briefly, ampules were inverted and cracked open at the pre-scored neck, then a stainless-steel needle was inserted through the aqueous phase into the gas phase. A 5 mL headspace sample was collected over 0.5 min in a gastight syringe (Hamilton, Reno, NV), while argon gas (15 mL/min) was directed into the open neck of each ampule to prevent intrusion of ambient air. Headspace samples were injected into a gas chromatograph (GC) equipped with a thermal conductivity detector (TCD) for carbon dioxide (CO_2), methane (CH_4), and H_2 analysis. The aqueous phase from each ampule was stored in a -80 °C freezer pending VFAs and DOC analyses. Based on their Henry's law constants[107] ($K_H^{VFAs} \approx 0.9 – 2.2 \times 10^3$ M/atm, $K_H^{H_2} = 780 \times 10^{-6}$ M/atm), less than 1% of VFAs and H_2 masses were associated with the gas and aqueous phases, respectively, and were thus assumed to be negligible in those phases.

3.3.5 Data normalization and statistical analysis

Given the variability in solid:liquid:gas ratios between ampules and the different molecular weights of each VFA, reporting the absolute concentrations of each VFA released during incubation would not allow for quantitative comparisons. Therefore, VFAs concentrations are reported throughout on a carbon per gram solid ($molC/g_s$) basis.

The statistical significance of differences in total VFAs, DOC, and H_2 releases between incubation conditions was determined in STATA 14 (StataCorp, College Station, TX) using two-sample, two-tailed t-tests assuming unequal variance.

3.3.6 Analytical methods

Permanent gases

Concentrations of H_2, CO_2, and CH_4 in gas samples were measured using an Agilent 6890 GC equipped with a thermal conductivity detector TCD (Agilent, Santa Clara, CA). Gas samples were manually injected to fill a 250 µL sample loop connected to a six-port gas sampling valve operated at 120 °C. After 0.2 min, the gas sample was transferred to the inlet, operating at 200 °C with a 1:1 split ratio, then onto a Supelco Carboxen 1010 PLOT capillary column (Sigma-Aldrich, St. Louis, MO) with 320 µm mean outer diameter and 30 m length. The GC oven was held at an initial temperature of 30 °C for 4.5 min, followed by a +50 °C/min ramp to 130 °C, which was maintained for 3 min until the end of the run. Argon gas (2 mL/min) was used as the carrier gas to optimize H_2 sensitivity of the TCD, which was operated at 230 °C with argon reference and makeup flows of 20 and 7 mL/min, respectively. Calibration standards were prepared by diluting a custom gas mixture containing 5% H_2, 20% CO_2, 5% carbon monoxide, and 20% CH_4 in a 100 mL gas-tight syringe (Hamilton, Reno, NV) using argon as the diluent. The method detection limits for CO_2, CH_4, and H_2 were 6.0×10^{-5} atm (2.5×10^{-6} mol/L_{gas}), 1.3×10^{-4} atm (5.3×10^{-6} mol/L_{gas}), and 3.0×10^{-5} atm (1.2×10^{-6} mol/L_{gas}),

respectively, determined via the Hubaux and Vos method and assuming a total confidence level of 99%.

Volatile fatty acids

Concentrations of seven VFAs, formate, acetate, propionate, butyrate, isobutyrate, valerate, and isovalerate in aqueous samples were measured using a Dionex ICS-2000 or Thermo Fisher (Waltham, MA) ICS-2100 ion chromatography (IC) system. The IC was equipped with a Dionex IonPac AS11-HC analytical column (Thermo Fisher) maintained at a constant temperature of 35 °C with and an anion self-regenerating suppressor operated at 112 mA. The IC was operated with a constant flow rate of 1.5 mL/min and a variable potassium hydroxide eluent concentration that was held at an initial concentration of 1 mM for 25 min, ramped up to 30 mM from 25 to 54 min, then ramped down to 1 mM until the run ended at 56 min. Calibration standards were prepared by diluting a stock solution containing 2 mM of each VFA in deionized (DI) water (18.2 MΩ cm^{-1}, total OC <5 µg/L). The method detection limit for VFAs listed above was approximately 1 µM, determined via the Hubaux and Vos method and assuming a total confidence level of 99%.

Solid-phase organic carbon

The OC content of solids used in ampule incubation experiments was measured using a Shimadzu (Kyoto, JP) TOC-L Total Organic Carbon Analyzer equipped with a Shimadzu SSM-5000A Solid Sample Module. All solid samples were

analyzed in triplicate and were prepared identically to those used in ampule incubation experiments. Approximately 500 mg of each solid were added to a ceramic dish, which was then introduced to the Total Carbon Furnace of the SSM-5000A for combustion. The SSM-5000A combustion tube was operated at 800 °C with an oxygen gas flow rate of 500 mL/min. The resulting CO_2 gas was automatically transferred to the TOC-L for detection by a non-dispersive infrared (NDIR) gas analyzer. Calibration standards were prepared by adding 100 μL of DI water (18.2 MΩ cm^{-1}, total OC <5 μg/L) containing 0 – 300 g/L sucrose (Thermo Fisher) as carbon to the ceramic dish. The method detection limit was approximately 25 μg carbon, or 0.005 wt% carbon assuming a 500 mg solid sample.

Dissolved organic carbon

DOC content in aqueous samples was measured using a Shimadzu TOC-L Total Organic Carbon Analyzer equipped with a Shimadzu ASI-L Auto Sampler. Duplicate 100 μL injections of each aqueous sample were transferred from the ASI-L to the TOC-L for combustion. A third 100 μL sample was injected only if the coefficient of variation exceeded 2.0% for the first two injections. The TOC-L combustion tube was operated at 680 °C with 150 mL/min air serving as the carrier gas. The resulting CO_2 gas was detected by a NDIR gas analyzer. Calibration standards were prepared by diluting a stock solution containing 100 mg/L potassium hydrogen phthalate as carbon. A linear (R^2 = 1.000), 11-point calibration curve was obtained over a range of 0 – 100 mg/L as carbon. A detection limit of 4 μg/L as carbon is advertised for the TOC-L by the manufacturer.

Solid-phase pH

The pH of solids used in ampule incubation experiments was determined by the Standard Test Method for pH of Soils (ASTM D4972 – 13). Briefly, 10 g of each solid was suspended in 10 mL of a 0.01 M calcium chloride ($CaCl_2$) solution and allowed to equilibrate for 1 h. The pH of the resulting suspension was then measured using an Orion 9106BNWP Combination Ag/AgCl pH Electrode (Thermo Fisher) connected to an Orion 3-Star Benchtop pH Meter (Thermo Fisher). The pH meter was calibrated using pH 4.01, 7.00, and 10.01 standard solutions (Thermo Fisher).

3.4 Results

3.4.1 VFAs and gas release from quartz sand, aquifer material, and natural soils heated at 30 – 90 °C for 28 – 56 d (Ampule Set #1)

Set #1 consisted of 111 non-blank ampules (i.e., containing a solid phase) and was designed to assess VFAs and H_2 release during heating of Federal Fine Ottawa sand, Groveland aquifer material, Appling soil, and Webster soil (<0.01 – 1.97 wt% OC) incubated 30, 60, or 90 °C for 28 to 56 d. Analysis of aqueous samples confirmed the release of VFAs, with acetate, formate, propionate, or butyrate detected above the 1 µM detection limit (approximately 1×10^{-9} molC/g_s) in all 111 ampules. Isobutyrate, valerate, and isovalerate were not detected in Set #1, nor any subsequent set so all further references to "total VFAs" represent the sum of carbon associated with formate, acetate, propionate, and butyrate per gram solid. CO_2 was detected above the 60×10^{-6} atm detection limit (approximately 2×10^{-9} molC/g_s) in the headspace of 93 ampules. H_2 was detected above the 30×10^{-6} atm detection limit (approximately 1×10^{-9} molH_2/g_s) in the headspace of 30 ampules. CH_4 was detected above the 130×10^{-6} atm detection limit (approximately 10×10^{-9} molC/g_s) in the headspace of 7 ampules. Concentrations of VFAs, CO_2, CH_4, and H_2 were consistently below the detection limits in blanks containing no solid phase in Set #1 and all subsequent sets.

Acetate and formate were the most frequently detected and abundant VFAs in Set #1, appearing in all 111 ampules, followed by propionate (33 ampules), and butyrate (7 ampules) (Figure 3-1,

Table 3-3).

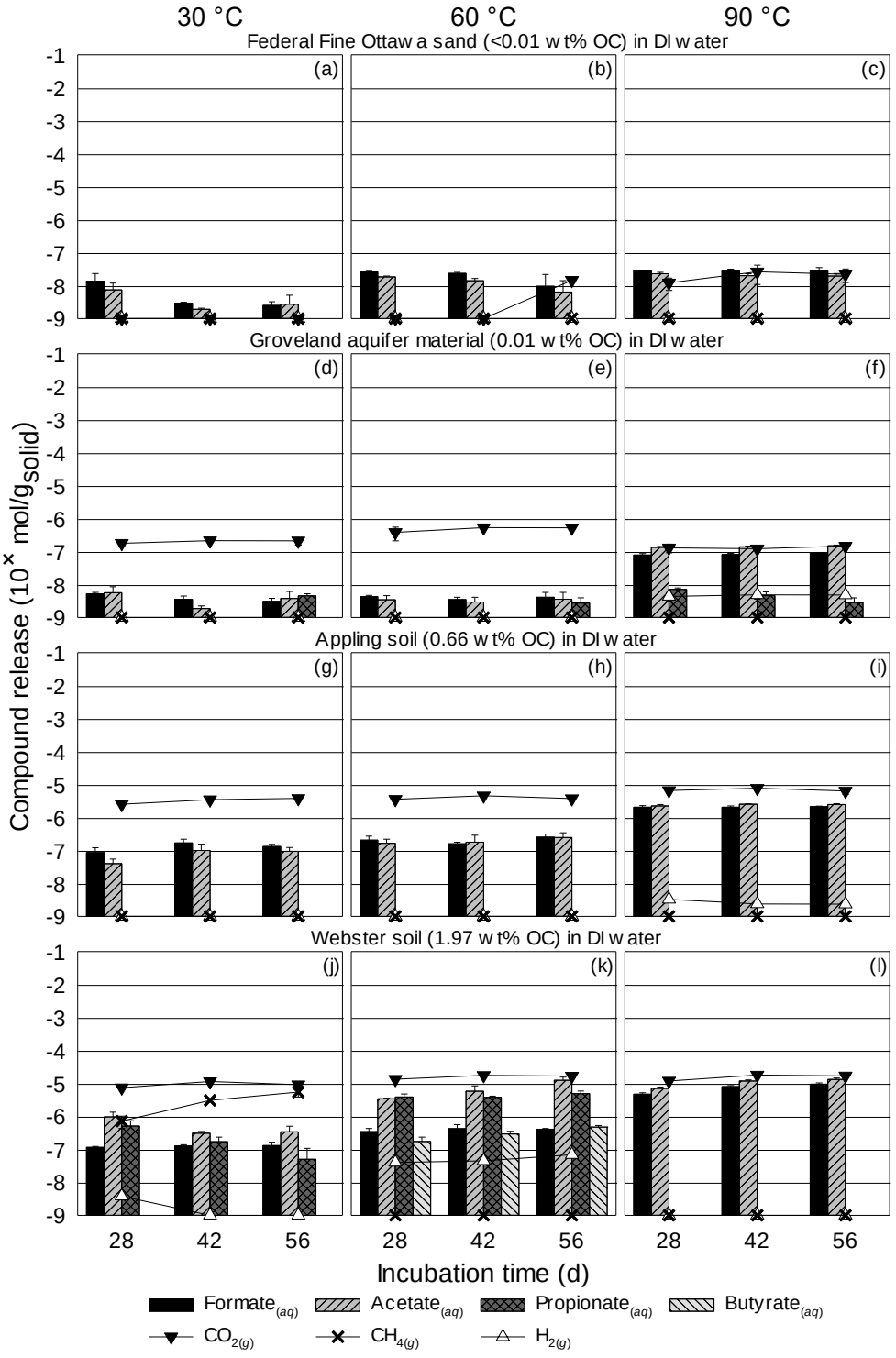

Figure 3-1: VFAs (as carbon), CO_2, CH_4, and H_2 release following 30, 60, and 90 °C incubation of: Federal Fine Ottawa sand (a, b, c); Groveland aquifer material (d,

e, f); Appling soil (g, h, i); and Webster soil (j, k, l) for 28, 42, and 56 d (Ampule Set #1). Error bars represent one standard deviation. Absence of a VFA bar or location of a symbol on the 10^{-9} line indicates that analysis was completed, but the corresponding compound was not detected. Absence of a symbol indicates that analysis of the corresponding compound was not completed.

Table 3-3: Data for Figure 3-1: VFAs (as carbon), CO_2, CH_4, and H_2 release following 30, 60, and 90 °C incubation of Federal Fine Ottawa sand, Groveland aquifer material, Appling soil, and Webster soil for 28, 42, and 56 days.

Federal Fine Ottawa sand (<0.01 wt% OC) in DI water

	30 °C (data for Figure 3-1a)			60 °C (data for Figure 3-1b)			90 °C (data for Figure 3-1c)		
	28 d	42 d	56 d	28 d	42 d	56 d	28 d	42 d	56 d
Formate(*aq*)	1E-8±1E-8	3E-9±2E-10	3E-9±7E-10	3E-8±1E-9	2E-8±2E-9	1E-8±1E-8	3E-8±9E-10	3E-8±4E-9	3E-8±7E-9
Acetate(*aq*)	7E-9±5E-9	2E-9±1E-10	3E-9±2E-9	2E-8±1E-9	1E-8±2E-9	6E-9±8E-9	2E-8±2E-9	2E-8±3E-9	2E-8±4E-9
Propionate(*aq*)	< det	< det	< det	< det	< det	< det	< det	< det	< det
Butyrate(*aq*)	< det	< det	< det	< det	< det	< det	< det	< det	< det
Total VFAs(*aq*)	2E-8±1E-8	5E-9±2E-10	5E-9±2E-9	4E-8±2E-9⊥	4E-8±3E-9⊥	2E-8±2E-8	5E-8±2E-9⊥,‖	5E-8±7E-9⊥	5E-8±4E-9⊥
CO_2(*g*)	< det	< det	< det	< det	< det	1E-8±2E-9	1E-8±5E-9	3E-8±2E-8	2E-8±1E-8
CH_4(*g*)	< det	< det	< det	< det	< det	< det	< det	< det	< det
H_2(*g*)	< det	< det	< det	< det	< det	< det	< det	< det	< det

Groveland aquifer material (0.01 wt% OC) in DI water

	30 °C (data for Figure 3-1d)			60 °C (data for Figure 3-1e)			90 °C (data for Figure 3-1f)		
	28 d	42 d	56 d	28 d	42 d	56 d	28 d	42 d	56 d
Formate(*aq*)	5E-9±5E-10	4E-9±9E-10	3E-9±7E-10	4E-9±4E-10	4E-9±6E-10	4E-9±2E-9	8E-8±8E-9	8E-8±7E-9	9E-8±4E-9
Acetate(*aq*)	6E-9±3E-9	2E-9±4E-10	4E-9±2E-9	3E-9±1E-9	3E-9±1E-9	4E-9±2E-9	1E-7±1E-8	1E-7±8E-9	2E-7±7E-9
Propionate(*aq*)	< det	< det	5E-9±7E-10	< det	< det	3E-9±1E-9	7E-9±8E-10	5E-9±1E-9	3E-9±1E-9
Butyrate(*aq*)	< det	< det	< det	< det	< det	< det	< det	< det	< det
Total VFAs(*aq*)	1E-8±3E-9	5E-9±1E-9	1E-8±4E-9	8E-9±2E-9	7E-9±2E-9	1E-8±3E-9	2E-7±2E-8⊥,‖	2E-7±2E-8⊥,‖	2E-7±1E-8⊥,‖
CO_2(*g*)	2E-7±3E-8	2E-7±2E-8	2E-7±5E-8	4E-7±2E-7	5E-7±6E-8	5E-7±4E-8	1E-7±4E-8	1E-7±2E-8	1E-7±1E-8
CH_4(*g*)	< det	< det	< det	< det	< det	< det	< det	< det	< det
H_2(*g*)	< det	< det	< det	< det	< det	< det	4E-9±1E-9	5E-9±1E-9	5E-9±9E-10

Appling soil (0.66 wt% OC) in DI water

	30 °C (data for Figure 3-1g)			60 °C (data for Figure 3-1h)			90 °C (data for Figure 3-1i)		
	28 d	42 d	56 d	28 d	42 d	56 d	28 d	42 d	56 d
Formate(*aq*)	9E-8±4E-8	2E-7±5E-8	1E-7±2E-8	2E-7±7E-8	2E-7±2E-8	3E-7±6E-8	2E-6±2E-7	2E-6±2E-7	2E-6±8E-8
Acetate(*aq*)	4E-8±2E-8	1E-7±6E-8	1E-7±3E-8	2E-7±6E-8	2E-7±1E-7	3E-7±1E-7	2E-6±2E-7	3E-6±8E-8	2E-6±1E-7
Propionate(*aq*)	< det	< det	< det	< det	< det	< det	< det	< det	< det
Butyrate(*aq*)	< det	< det	< det	< det	< det	< det	< det	< det	< det
Total VFAs(*aq*)	1E-7±5E-8	3E-7±1E-7	2E-7±4E-8	4E-7±1E-7$^{\perp}$	3E-7±1E-7	5E-7±2E-7	4E-6±5E-7$^{\perp,\perp\!\perp}$	5E-6±2E-7$^{\perp,\perp\!\perp}$	5E-6±2E-7$^{\perp,\perp\!\perp}$
CO_2(*g*)	3E-6±1E-7	3E-6±5E-7	4E-6±8E-8	4E-6±3E-7	5E-6±6E-7	4E-6±2E-7	7E-6±5E-7	8E-6±8E-7	6E-6±1E-6
CH_4(*g*)	< det	< det	< det	< det	< det	< det	< det	< det	< det
H_2(*g*)	< det	< det	< det	< det	< det	< det	3E-9±2E-10	2E-9±3E-10	2E-9±2E-10

Webster soil (1.97 wt% OC) in DI water

	30 °C (data for Figure 3-1j)			60 °C (data for Figure 3-1k)			90 °C (data for Figure 3-1l)		
	28 d	42 d	56 d	28 d	42 d	56 d	28 d	42 d	56 d
Formate(*aq*)	1E-7±7E-9	1E-7±1E-8	1E-7±3E-8	3E-7±8E-8	4E-7±1E-7	4E-7±2E-8	5E-6±5E-7	8E-6±6E-7	9E-6±8E-7
Acetate(*aq*)	1E-6±4E-7	3E-7±4E-8	3E-7±2E-7	3E-6±1E-7	6E-6±3E-6	1E-5±3E-6	7E-6±8E-7	1E-5±1E-6	1E-5±1E-6
Propionate(*aq*)	5E-7±2E-7	2E-7±6E-8	5E-8±6E-8	4E-6±9E-7	4E-6±3E-7	5E-6±1E-6	< det	< det	< det
Butyrate(*aq*)	< det	< det	< det	2E-7±6E-8	3E-7±6E-8	5E-7±5E-8	< det	< det	< det
Total VFAs(*aq*)	2E-6±6E-7	6E-7±7E-8	5E-7±3E-7	8E-6±1E-6	1E-5±2E-6$^{\perp}$	2E-5±4E-6	1E-5±1E-6$^{\perp,\perp\!\perp}$	2E-5±2E-6$^{\perp,\perp\!\perp}$	2E-5±2E-6$^{\perp}$
CO_2(*g*)	7E-6±6E-7	1E-5±3E-7	9E-6±2E-7	1E-5±1E-7	2E-5±4E-7	2E-5±1E-6	1E-5±2E-7	2E-5±6E-7	2E-5±1E-6
CH_4(*g*)	7E-7±3E-7	3E-6±3E-7	5E-6±2E-6	< det	< det	< det	< det	< det	< det
H_2(*g*)	4E-9±7E-10	< det	< det	4E-8±2E-9	4E-8±8E-9	7E-8±9E-9	< det	< det	< det

All values are presented in units of molC/g_{solid} except H_2(*g*), which is presented in units of molH_2/g_{solid}. Statistical differences between incubation temperatures were determined for Total VFAs(*aq*) only. < det = below detection limit; $^{\perp}$ = significantly greater release than for equivalent conditions at 30 °C; $^{\perp\!\perp}$ = significantly greater release than for equivalent conditions at 60 °C.

Total VFAs release was lowest in ampules containing Federal Fine Ottawa sand (<0.01 wt% OC) and never exceeded 55×10^{-9} molC/g_s for any replicate under any incubation condition (Figure 3-1a – c). Federal Fine Ottawa sand ampules (30 and 60 °C) also represent the only instances where no CO_2 was detected following incubation (Figure 3-1a and Figure 3-1b). Incubation of Webster soil (1.97 wt% OC) resulted in the greatest release of VFAs, CO_2, H_2, and CH_4 of any solid material in Set #1: $23\pm2 \times 10^{-6}$ molC/g_s total VFAs (56 d at 90 °C; Figure 3-1l); $18\pm1 \times 10^{-6}$ molCO_2/g_s (42 d at 90 °C; Figure 3-1l); $70\pm9 \times 10^{-9}$ molH_2/g_s (56 d at 60 °C; Figure 3-1k); and $5\pm2 \times 10^{-6}$ molCH_4/g_s (56 d at 30 °C; Figure 3-1j). Lower concentrations of H_2 were also detected following 90 °C incubation of Groveland aquifer material (0.01 wt% OC; Figure 3-1f) and Appling soil (0.66 wt% OC; Figure 3-1i), but CH_4 was only detected following 30 °C incubation of Webster soil. In general, increases in incubation temperature or solid-phase OC content corresponded to increases in total VFAs release. Total VFAs release also increased with incubation time for several of the solids, most notably Webster soil incubated at 60 and 90 °C (Figure 3-1k and Figure 3-1l), indicating time-dependent VFAs release.

3.4.2 Effect of microbial inhibition (2 mM $HgCl_2$) on VFAs and H_2 release at 60 and 90 °C (Ampule Set #2)

Set #2 consisted of 43 non-blank ampules containing Federal Fine Ottawa sand, Groveland aquifer material, Appling soil, or Webster soil. Unlike Set #1, the ampules in Set #2 were amended with 2 mM $HgCl_2$ to inhibit native microbial activity. VFAs were detected in all 43 ampules following incubation (Figure 3-2,

Table 3-4).

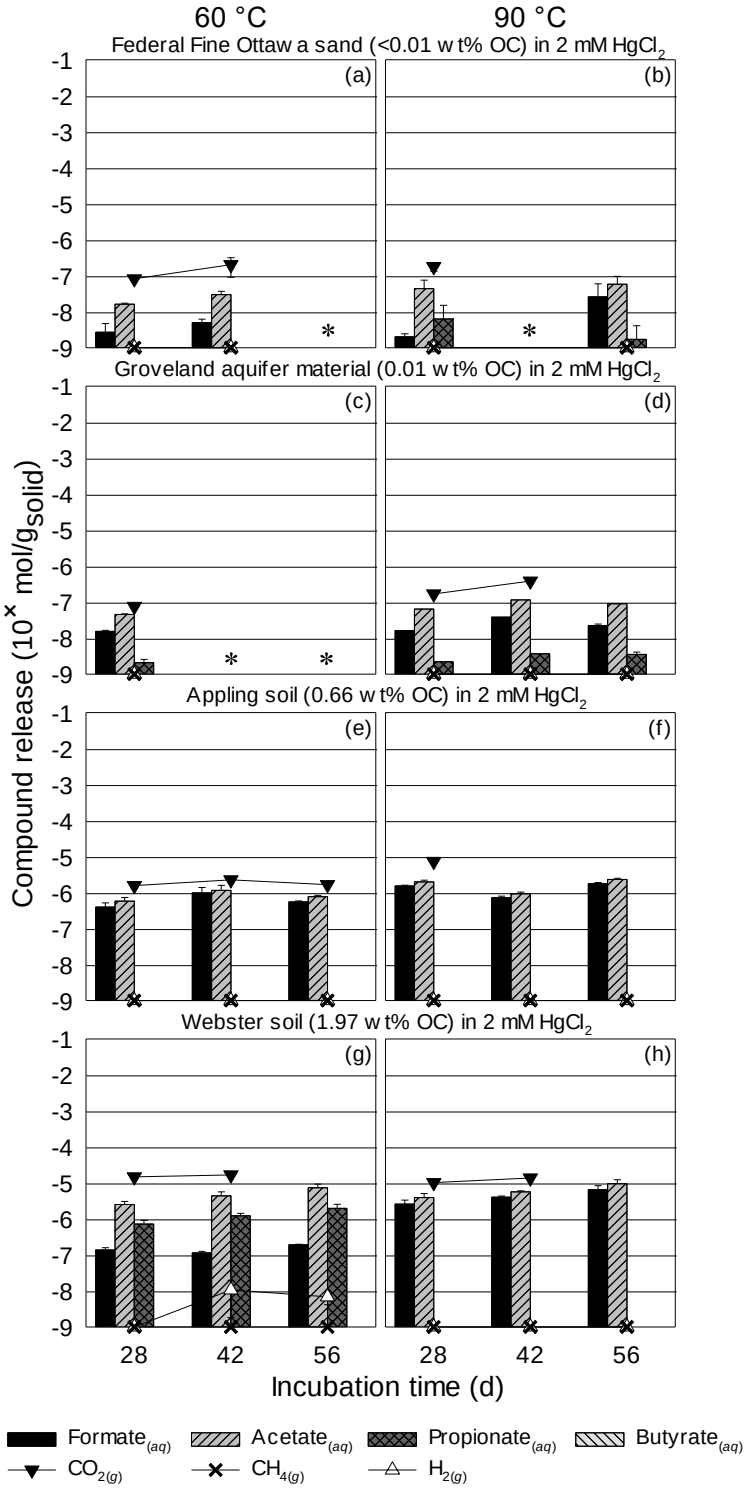

Figure 3-2: VFAs (as carbon), CO_2, CH_4, and H_2 release following 60 and 90 °C incubation of: Federal Fine Ottawa sand (a, b); Groveland aquifer material (c, d);

Appling soil (e, f); Webster soil (g, h) for 28, 42, and 56 days in ampules amended with 2 mM $HgCl_2$ to inhibit microbial activity (Ampule Set #2). Error bars represent one standard deviation. Absence of a VFA bar or location of a symbol on the 10^{-9} line indicates that analysis was completed, but the corresponding compound was not detected. Absence of a symbol indicates that analysis of the corresponding compound was not completed. A * symbol indicates that data was not collected for the corresponding incubation condition.

Table 3-4: Data for Figure 3-2: VFAs (as carbon), CO_2, CH_4, and H_2 release following 60 and 90 °C incubation of Federal Fine Ottawa sand, Groveland aquifer material, Appling soil, and Webster soil for 28, 42, and 56 days in ampules amended with 2 mM $HgCl_2$ to inhibit microbial activity.

	Federal Fine Ottawa sand (<0.01 wt% OC) in 2 mM HgCl2					
	60 °C (data for Figure 3-2a)			90 °C (data for Figure 3-2b)		
	28 d	42 d	56 d	28 d	42 d	56 d
Formate(*aq*)	3E-9±2E-9	5E-9±1E-9	*	2E-9±4E-10	*	3E-8±3E-8
Acetate(*aq*)	2E-8±1E-9	3E-8±7E-9	*	4E-8±3E-8	*	6E-8±4E-8
Propionate(*aq*)	< det	< det	*	6E-9±9E-9	*	2E-9±2E-9
Butyrate(*aq*)	< det	< det	*	< det	*	< det
Total VFAs(*aq*)	2E-8±1E-9	4E-8±8E-9	*	5E-8±4E-8	*	9E-8±9E-8
CO_2(*g*)	8E-8±7E-9	2E-7±1E-7	*	2E-7±5E-8	*	*
CH_4(*g*)	< det	< det	*	< det	*	< det
H_2(*g*)	< det	< det	*	< det	*	< det

	Groveland aquifer material (0.01 wt% OC) in 2 mM HgCl2					
	60 °C (data for Figure 3-2c)			90 °C (data for Figure 3-2d)		
	28 d	42 d	56 d	28 d	42 d	56 d
Formate(*aq*)	2E-8±1E-9	*	*	2E-8±ir	4E-8±ir	2E-8±3E-9
Acetate(*aq*)	5E-8±2E-9	*	*	6E-8±ir	1E-7±ir	9E-8±6E-10
Propionate(*aq*)	2E-9±5E-10	*	*	2E-9±ir	4E-9±ir	4E-9±6E-10
Butyrate(*aq*)	< det	*	*	< det	< det	< det
Total VFAs(*aq*)	6E-8±2E-9	*	*	8E-8±ir	2E-7±ir	1E-7±2E-9
CO_2(*g*)	8E-8±1E-8	*	*	2E-7±ir	4E-7±ir	*
CH_4(*g*)	< det	*	*	< det	< det	< det
H_2(*g*)	< det	*	*	< det	< det	< det

	Appling soil (0.66 wt% OC) in 2 mM HgCl2

	60 °C (data for Figure 3-2e)			90 °C (data for Figure 3-2f)		
	28 d	42 d	56 d	28 d	42 d	56 d
Formate(*aq*)	4E-7±1E-7	1E-6±4E-7	6E-7±4E-8	2E-6±8E-8	7E-7±7E-8	2E-6±1E-7
Acetate(*aq*)	6E-7±2E-7	1E-6±4E-7	8E-7±8E-8	2E-6±2E-7	9E-7±1E-7	2E-6±2E-7
Propionate(*aq*)	< det	< det	< det	< det	< det	< det
Butyrate(*aq*)	< det	< det	< det	< det	< det	< det
Total VFAs(*aq*)	1E-6±3E-7	2E-6±8E-7	1E-6±1E-7	4E-6±3E-7⇊	2E-6±2E-7	4E-6±3E-7⇊
$CO_2(g)$	2E-6±3E-7	2E-6±8E-8	2E-6±ir	7E-6±4E-7	*	*
$CH_4(g)$	< det	< det	< det	< det	< det	< det
$H_2(g)$	< det	< det	< det	< det	< det	< det

Webster soil (1.97 wt% OC) in 2 mM HgCl2

	60 °C (Figure 3-2g)			90 °C (Figure 3-2h)		
	28 d	42 d	56 d	28 d	42 d	56 d
Formate(*aq*)	1E-7±2E-8	1E-7±1E-8	2E-7±9E-9	3E-6±8E-7	4E-6±3E-7	6E-6±2E-6
Acetate(*aq*)	3E-6±5E-7	4E-6±1E-6	7E-6±2E-6	4E-6±1E-6	6E-6±4E-7	9E-6±3E-6
Propionate(*aq*)	7E-7±2E-7	1E-6±2E-7	2E-6±6E-7	< det	< det	< det
Butyrate(*aq*)	< det	< det	< det	< det	< det	< det
Total VFAs(*aq*)	3E-6±7E-7	6E-6±1E-6	9E-6±3E-6	6E-6±2E-6	1E-5±7E-7⇊	2E-5±5E-6
$CO_2(g)$	1E-5±8E-7	2E-5±9E-8	*	1E-5±1E-6	1E-5±6E-8	*
$CH_4(g)$	< det	< det	< det	< det	< det	< det
$H_2(g)$	< det	1E-8±9E-9	7E-9±3E-9	< det	< det	< det

All values are presented in units of molC/g_{solid} except $H_2(g)$, which is presented in units of molH_2/g_{solid}. Statistical differences between incubation temperatures were determined for Total VFAs(*aq*) only. < det = below detection limit; * = data not collected; ir = insufficient replicates to determine standard deviation and/or statistical difference between incubation conditions; ⊥ = significantly greater release than for equivalent conditions at 30 °C; ⇊ = significantly greater release than for equivalent conditions at 60 °C.

Total VFAs release was significantly greater in $HgCl_2$-amended (Set #2) ampules than in corresponding ampules containing no $HgCl_2$ (Set #1) for one incubation condition, significantly less for four incubation conditions, and was not significantly different for 11 incubation conditions ($p < 0.05$;

Table 3-5). H_2 was not detected in ampules containing 2 mM $HgCl_2$ except for those containing Webster soil incubated at 60 °C (Figure 3-2g). Mean H_2 releases in these 60 °C Webster soil ampules were 76 and 90% lower after 42 and 56 d (Figure 3-2g), respectively, than in Set #1 counterparts containing no $HgCl_2$ ($p < 0.05$; Figure 3-1k).

Table 3-5: Comparison of total VFAs release between ampules with and without 2 mM $HgCl_2$.

Total VFAs release from Federal Fine Ottawa sand (× 10^{-9} molC/g_{solid})						
	60 °C			90 °C		
[$HgCl_2$]	28 d	42 d	56 d	28 d	42 d	56 d
0 mM	**45±2**	38±3	16±20	52±2	48±7	47±4
2 mM	19±1	35±8	*	53±41	*	87±90

Total VFAs release from Appling soil (× 10^{-9} molC/g_{solid})						
	60 °C			90 °C		
[$HgCl_2$]	28 d	42 d	56 d	28 d	42 d	56 d
0 mM	375±120	341±110	507±161	4,316±478	**4,585±231**	4,617±221
2 mM	980±275	2,140±841	**1,326±99**	3,520±315	1,657±175	4,120±302

Total VFAs release from Webster soil (× 10^{-6} molC/g_{solid})						
	60 °C			90 °C		
[$HgCl_2$]	28 d	42 d	56 d	28 d	42 d	56 d
0 mM	**8±1**	10±2	18±4	12±1	**20±2**	23±2
2 mM	3±1	6±1	9±2	6±2	10±1	16±4,1

Values significantly ($p < 0.05$) greater than the corresponding incubation condition with/without 2 mM $HgCl_2$ are in **bold**. A * symbol indicates that data was not collected for the corresponding incubation condition.

3.4.3 VFAs release from humic and fulvic acid standards incubated at 30 – 90 °C to 7 – 28 d (Ampule Set #3)

Set #3 consisted of 161 non-blank ampules, and was designed to elucidate the role of organic constituents in VFAs and H_2 release during thermal treatment. Suwannee River fulvic acid II, Pahokee peat humic acid, Elliott soil humic acid, and Leonardite humic acid were used as the solid phases to confirm VFAs release trends (i.e., dependence on incubation temperature, time, OC content) observed during incubation of solids in previous sets, and to explore the influence of organic functional groups on the extent of VFAs release. H_2 and CH_4 were not detected in any ampule in Set #3, but the same four VFAs were detected at relative abundances similar to Sets #1 and 2 (i.e., release of acetate > formate > propionate and butyrate) (Figure 3-3,

Table 3-6).

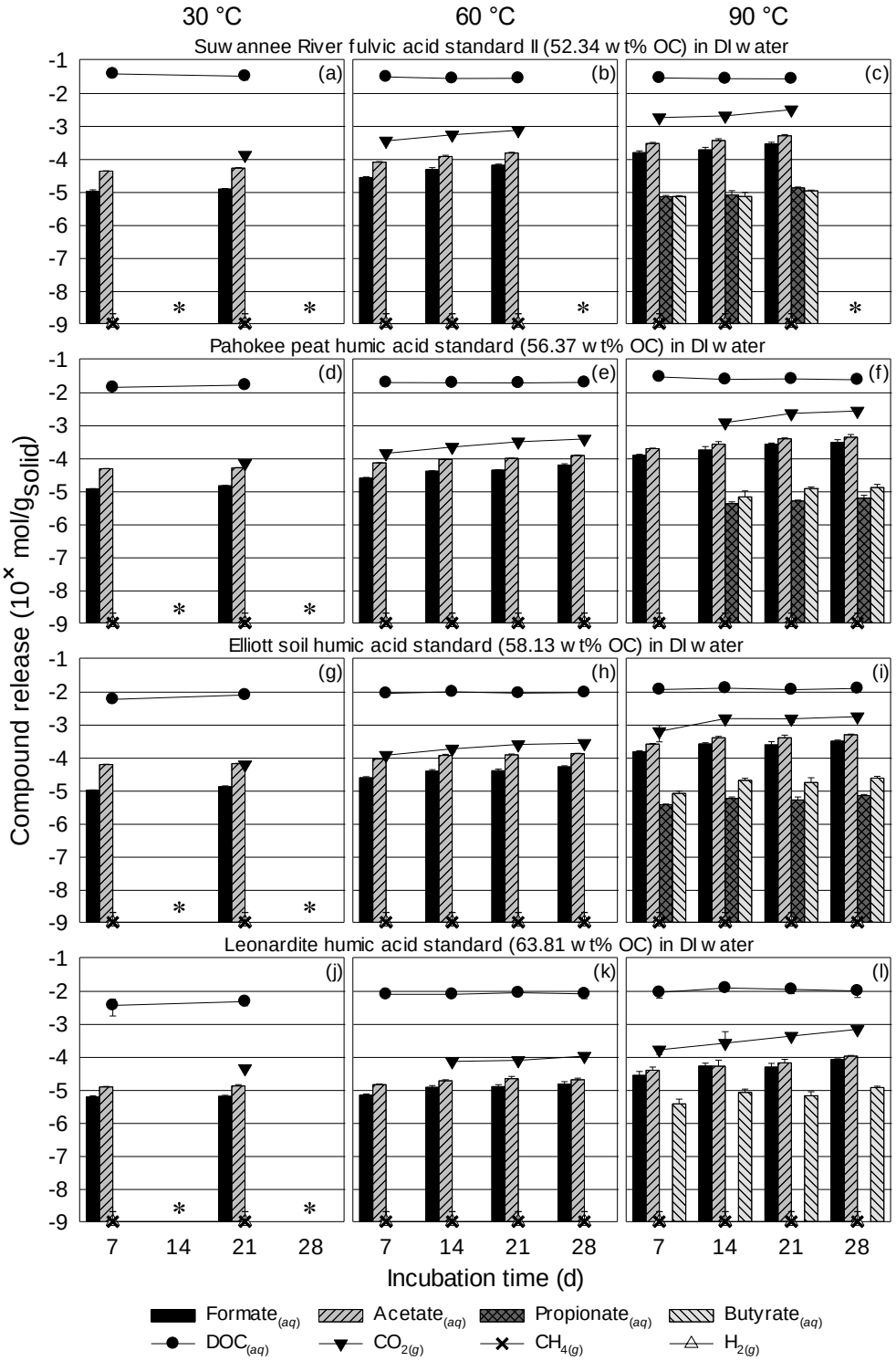

Figure 3-3: VFAs (as carbon), DOC, CO_2, CH_4, and H_2 release following 30, 60, and 90 °C incubation of: Suwannee River fulvic acid standard II (a, b, c); Pahokee

peat humic acid standard (d, e, f); Elliott soil humic acid standard (g, h, i); and Leonardite humic acid standard (j, k, l) for 7, 14, 21, and 28 d (Ampule Set #3). Error bars represent one standard deviation. Absence of a VFA bar or location of a symbol on the 10^{-9} line indicates that analysis was completed, but the corresponding compound was not detected. Absence of a symbol indicates that analysis of the corresponding compound was not completed. A * symbol indicates that data was not available for the corresponding incubation condition.

Table 3-6: Data for Figure 3-3: VFAs (as carbon), DOC, CO_2, CH_4, and H_2 release following 30, 60, and 90 °C incubation of Suwannee River fulvic acid standard II, Pahokee peat humic acid standard, Elliott soil humic acid standard, and Leonardite humic acid standard for 7, 14, 21, and 28 days.

Suwannee River fulvic acid standard II (52.34 wt% OC) in DI water

	30 °C (data for Figure 3-3a)				60 °C (data for Figure 3-3b)				90 °C (data for Figure 3-3c)			
	7 d	14 d	21 d	28 d	7 d	14 d	21 d	28 d	7 d	14 d	21 d	28 d
Formate(*aq*)	1E-5±1E-6	*	1E-5±5E-7	*	3E-5±2E-6	5E-5±7E-6	6E-5±5E-6	*	2E-4±2E-5	2E-4±3E-5	3E-4±3E-5	*
Acetate(*aq*)	4E-5±7E-7	*	5E-5±2E-6	*	8E-5±3E-6	1E-4±1E-5	1E-4±8E-6	*	3E-4±2E-5	4E-4±5E-5	5E-4±4E-5	*
Propionate(*aq*)	< det	*	< det	*	< det	< det	< det	*	7E-6±7E-7	8E-6±3E-6	1E-5±9E-7	*
Butyrate(*aq*)	< det	*	< det	*	< det	< det	< det	*	7E-6±5E-7	7E-6±2E-6	1E-5±6E-7	*
Total VFAs(*aq*)	5E-5±2E-6	*	6E-5±3E-6	*	1E-4±4E-6⊥	2E-4±2E-5	2E-4±1E-5⊥	*	5E-4±4E-5⊥,‖	6E-4±9E-5‖	8E-4±8E-5⊥,‖	*
DOC(*aq*)	4E-2±2E-3	*	3E-2±8E-3	*	3E-2±4E-3	3E-2±8E-4	3E-2±7E-4	*	3E-2±3E-3┬	3E-2±2E-3	3E-2±4E-3	*
CO_2(*g*)	*	*	1E-4±ir	*	3E-4±8E-6	5E-4±7E-5	7E-4±ir	*	2E-3±2E-4	2E-3±3E-4	3E-3±5E-5	*
CH_4(*g*)	< det	*	< det	*	< det	< det	< det	*	< det	< det	< det	*
H_2(*g*)	< det	*	< det	*	< det	< det	< det	*	< det	< det	< det	*

Pahokee peat humic acid standard (56.37 wt% OC) in DI water

	30 °C (data for Figure 3-3d)				60 °C (data for Figure 3-3e)				90 °C (data for Figure 3-3f)			
	7 d	14 d	21 d	28 d	7 d	14 d	21 d	28 d	7 d	14 d	21 d	28 d
Formate(*aq*)	1E-5±2E-7	*	1E-5±3E-7	*	2E-5±1E-6	4E-5±2E-6	4E-5±1E-6	6E-5±5E-6	1E-4±9E-6	2E-4±5E-5	3E-4±2E-5	3E-4±6E-5
Acetate(*aq*)	5E-5±6E-7	*	5E-5±1E-6	*	7E-5±1E-6	9E-5±3E-6	1E-4±2E-6	1E-4±6E-6	2E-4±8E-6	3E-4±5E-5	4E-4±3E-5	4E-4±9E-5
Propionate(*aq*)	< det	*	< det	*	< det	< det	< det	< det	< det	4E-6±5E-7	5E-6±3E-7	6E-6±1E-6
Butyrate(*aq*)	< det	*	< det	*	< det	< det	< det	< det	< det	7E-6±3E-6	1E-5±1E-6	1E-5±3E-6
Total VFAs(*aq*)	6E-5±5E-7	*	6E-5±1E-6	*	1E-4±2E-6⊥	1E-4±4E-6	1E-4±2E-6⊥	2E-4±1E-5	3E-4±2E-5⊥,‖	4E-4±1E-4‖	7E-4±5E-5⊥,‖	7E-4±2E-4‖
DOC(*aq*)	1E-2±1E-3	*	2E-2±2E-3	*	2E-2±1E-3⊥	2E-2±8E-4	2E-2±5E-4	2E-2±1E-3	3E-2±3E-3⊥,‖	2E-2±2E-3‖	2E-2±2E-3⊥,‖	2E-2±2E-3‖
CO_2(*g*)	*	*	7E-5±ir	*	1E-4±2E-6	2E-4±2E-5	3E-4±ir	4E-4±ir	*	1E-3±3E-5	2E-3±3E-4	3E-3±ir
CH_4(*g*)	< det	*	< det	*	< det	< det	< det	< det	< det	< det	< det	< det
H_2(*g*)	< det	*	< det	*	< det	< det	< det	< det	< det	< det	< det	< det

Elliott soil humic acid standard (58.13 wt% OC) in DI water

	30 °C (data for Figure 3-3g)				60 °C (data for Figure 3-3h)				90 °C (data for Figure 3-3i)			
	7 d	14 d	21 d	28 d	7 d	14 d	21 d	28 d	7 d	14 d	21 d	28 d
Formate(*aq*)	1E-5±3E-7	*	1E-5±9E-7	*	2E-5±2E-6	4E-5±4E-6	4E-5±4E-6	5E-5±4E-6	1E-4±1E-5	3E-4±2E-5	2E-4±6E-5	3E-4±2E-5
Acetate(*aq*)	6E-5±2E-6	*	6E-5±1E-6	*	9E-5±4E-6	1E-4±8E-6	1E-4±7E-6	1E-4±3E-6	3E-4±1E-5	4E-4±4E-5	4E-4±8E-5	5E-4±3E-5
Propionate(*aq*)	< det	*	< det	*	< det	< det	< det	< det	4E-6±2E-7	6E-6±6E-7	5E-6±1E-6	7E-6±5E-7
Butyrate(*aq*)	< det	*	< det	*	< det	< det	< det	< det	8E-6±1E-6	2E-5±3E-6	2E-5±7E-6	2E-5±3E-6
Total VFAs(*aq*)	7E-5±1E-6	*	8E-5±2E-6	*	1E-4±6E-6$^{\perp}$	2E-4±1E-5	2E-4±1E-5$^{\perp}$	2E-4±6E-6	4E-4±2E-5$^{\perp,\Vdash}$	7E-4±6E-5$^{\Vdash}$	6E-4±1E-4$^{\perp,\Vdash}$	8E-4±5E-5$^{\Vdash}$
DOC(*aq*)	6E-3±5E-5	*	8E-3±2E-3	*	9E-3±5E-4$^{\perp}$	1E-2±7E-4	9E-3±2E-4	9E-3±4E-4	1E-2±1E-3$^{\perp,\Vdash}$	1E-2±8E-4$^{\Vdash}$	1E-2±1E-3$^{\perp,\Vdash}$	1E-2±1E-3$^{\Vdash}$
CO_2(*g*)	*	*	6E-5±ir	*	1E-4±1E-5	2E-4±4E-5	2E-4±ir	3E-4±ir	6E-4±3E-4	1E-3±2E-4	1E-3±3E-4	2E-3±ir
CH_4(*g*)	< det	*	< det	*	< det	< det	< det	< det	< det	< det	< det	< det
H_2(*g*)	< det	*	< det	*	< det	< det	< det	< det	< det	< det	< det	< det

Leonardite humic acid standard (63.81 wt% OC) in DI water

	30 °C (data for Figure 3-3j)				60 °C (data for Figure 3-3k)				90 °C (data for Figure 3-3l)			
	7 d	14 d	21 d	28 d	7 d	14 d	21 d	28 d	7 d	14 d	21 d	28 d
Formate(*aq*)	6E-6±5E-7	*	6E-6±5E-7	*	7E-6±5E-7	1E-5±2E-6	1E-5±2E-6	1E-5±3E-6	3E-5±9E-6	5E-5±1E-5	5E-5±1E-5	8E-5±5E-6
Acetate(*aq*)	1E-5±4E-7	*	1E-5±1E-6	*	1E-5±7E-7	2E-5±1E-6	2E-5±4E-6	2E-5±2E-6	4E-5±9E-6	5E-5±3E-5	6E-5±2E-5	1E-4±5E-6
Propionate(*aq*)	< det	*	< det	*	< det	< det	< det	< det	< det	< det	< det	< det
Butyrate(*aq*)	< det	*	< det	*	< det	< det	< det	< det	4E-6±1E-6	8E-6±2E-6	6E-6±2E-6	1E-5±1E-6
Total VFAs(*aq*)	2E-5±9E-7	*	2E-5±2E-6	*	2E-5±6E-7$^{\perp}$	3E-5±3E-6	3E-5±5E-6$^{\perp}$	3E-5±5E-6	7E-5±2E-5$^{\perp,\Vdash}$	1E-4±1E-5$^{\Vdash}$	1E-4±3E-5$^{\perp,\Vdash}$	2E-4±1E-5$^{\Vdash}$
DOC(*aq*)	4E-3±2E-3	*	5E-3±1E-3	*	8E-3±8E-4	8E-3±1E-3	9E-3±1E-3$^{\perp}$	8E-3±2E-3	9E-3±3E-3$^{\perp}$	1E-2±2E-3$^{\Vdash}$	1E-2±3E-3$^{\perp}$	1E-2±3E-3
CO_2(*g*)	*	*	4E-5±ir	*	< det	7E-5±6E-6	8E-5±ir	1E-4±ir	2E-4±4E-5	3E-4±3E-4	4E-4±ir	7E-4±ir
CH_4(*g*)	< det	*	< det	*	< det	< det	< det	< det	< det	< det	< det	< det
H_2(*g*)	< det	*	< det	*	< det	< det	< det	< det	< det	< det	< det	< det

All values are presented in units of molC/g_{solid} except H_2(*g*), which is presented in units of molH_2/g_{solid}. Statistical differences between incubation temperatures were determined for Total VFAs(*aq*) and DOC(*aq*) only. < det = below detection limit; * = data not collected; ir = insufficient replicates to determine standard deviation and/or statistical difference between incubation conditions; $^{\perp}$ = significantly greater release than for equivalent conditions at 30 °C; $^{\Vdash}$ = significantly greater release than for equivalent conditions at 60 °C.

Total VFAs release ranged from $20\pm1 \times 10^{-6}$ molC/g_s for the Leonardite humic acid standard (63.81 wt% OC; 7 d at 30 °C; Figure 3-3j) to $820\pm50 \times 10^{-6}$ molC/g_s for the Elliott soil humic acid standard (58.13 wt% OC; 28 d at 90 °C; Figure 3-3f), 2.7 orders of magnitude greater than release from Webster soil (1.97 wt% OC) under the same incubation conditions (Figure 3-1l). These findings support the positive correlation between total VFAs release and solid-phase OC content, but inspection of results from only the humic and fulvic acid standard ampules revealed that this correlation was not universal. For example, total VFAs released from humic and fulvic acid standards accounted for 0.1 – 6.8% of post-incubation DOC in each ampule, which itself accounted for 7 – 84% of initial OC in each ampule (

Table 3-7).

Table 3-7: Mean DOC (left) and mean total VFAs (right) in the aqueous phase of ampules containing humic and fulvic acid standards.

Solid phase	Temperature (°C)	DOC (mol% of initial ampule OC) Time (d)				VFAs (mol% of DOC) Time (d)			
		7	14	21	28	7	14	21	28
Suwannee River	30	84	-	▼ 72	-	0.1	-	▲ 0.2	-
fulvic acid	60	69	▼ 61	▲ 62	-	0.4	▲ 0.6	▲ 0.8	-
standard II	90	64	▼ 60	60	-	1.6	▲ 2.1	▲ 3.1	-
Elliott soil	30	12	-	▲ 16	-	1.2	-	▼ 1.0	-
humic acid	60	18	▲ 20	▼ 18	▲ 19	1.3	▲ 1.6	▲ 1.8	▲ 2.0
standard	90	23	▲ 26	▼ 23	▲ 25	3.6	▲ 5.4	▲ 5.8	▲ 6.8
Pahokee peat	30	29	-	▲ 35	-	0.4	-	0.4	-
humic acid	60	41	▼ 40	40	▲ 41	0.5	▲ 0.7	0.7	▲ 0.9
standard	90	60	▼ 51	▲ 53	▼ 50	1.1	▲ 1.9	▲ 2.6	▲ 3.2
Leonardite	30	7	-	▲ 9	-	0.5	-	▼ 0.4	-
humic acid	60	14	14	▲ 16	▼ 15	0.3	▲ 0.4	0.4	▲ 0.5
standard	90	16	▲ 22	▼ 20	▼ 18	0.8	▲ 0.9	▲ 1.1	▲ 2.0

▲ = increase from previous, ▼ = decrease from previous.

Despite containing the most OC, the Leonardite humic acid standard (63.81 wt% OC) ampules accounted for the low end of both ranges, with post-incubation DOC accounting for only 7 – 22% of initial ampule OC and VFAs making up only 0.3 – 2.0% of that DOC. In ampules containing the comparatively low-OC Elliott soil humic acid standard (58.13 wt% OC), DOC accounted for 12 – 26% of initial OC and VFAs made up 1.0 – 6.8% of that DOC. This represents an apparent disruption of the positive relationship between VFAs release and solid-phase OC content observed following incubation of Federal Fine Ottawa sand, Groveland aquifer material, Appling soil, and Webster soil in Sets #1 and 2. Total VFAs release from the Leonardite humic acid standard (63.81 wt% OC) reached only $200\pm11 \times 10^{-6}$ molC/g_s after 28 d of incubation at 90 °C (Figure 3-3l), compared to $740\pm160 \times 10^{-6}$ and $820\pm50 \times 10^{-6}$ molC/g_s from the Pahokee peat (56.37 wt% OC) and Elliott soil (58.13 wt% OC) humic acid standards, respectively (Figure 3-3f and Figure 3-3i). These findings indicate that VFAs release from solids during heating is not governed solely by OC content, but also by the structure of the organic matter.

3.4.4 VFAs and gas release from humic acid source materials incubated at 30 – 90 °C for 7 – 77 d (Ampule Set #4)

Set #4 consisted of 179 non-blank ampules containing the Elliott silt loam soil, Pahokee peat soil II, and Gascoyne leonardite from which the humic acid standards used in Set #3 were extracted. Incubation of these bulk source materials was

intended to further investigate the influence of organic functional groups on VFAs release, and to explain the decoupling of the relationship between solid-phase OC content and total VFAs release observed during incubation of humic and fulvic acids (Set #3). Total VFAs release trends among the bulk materials (Figure 3-4,

Table 3-8) were similar to those observed for humic and fulvic acid standards (Figure 3-3).

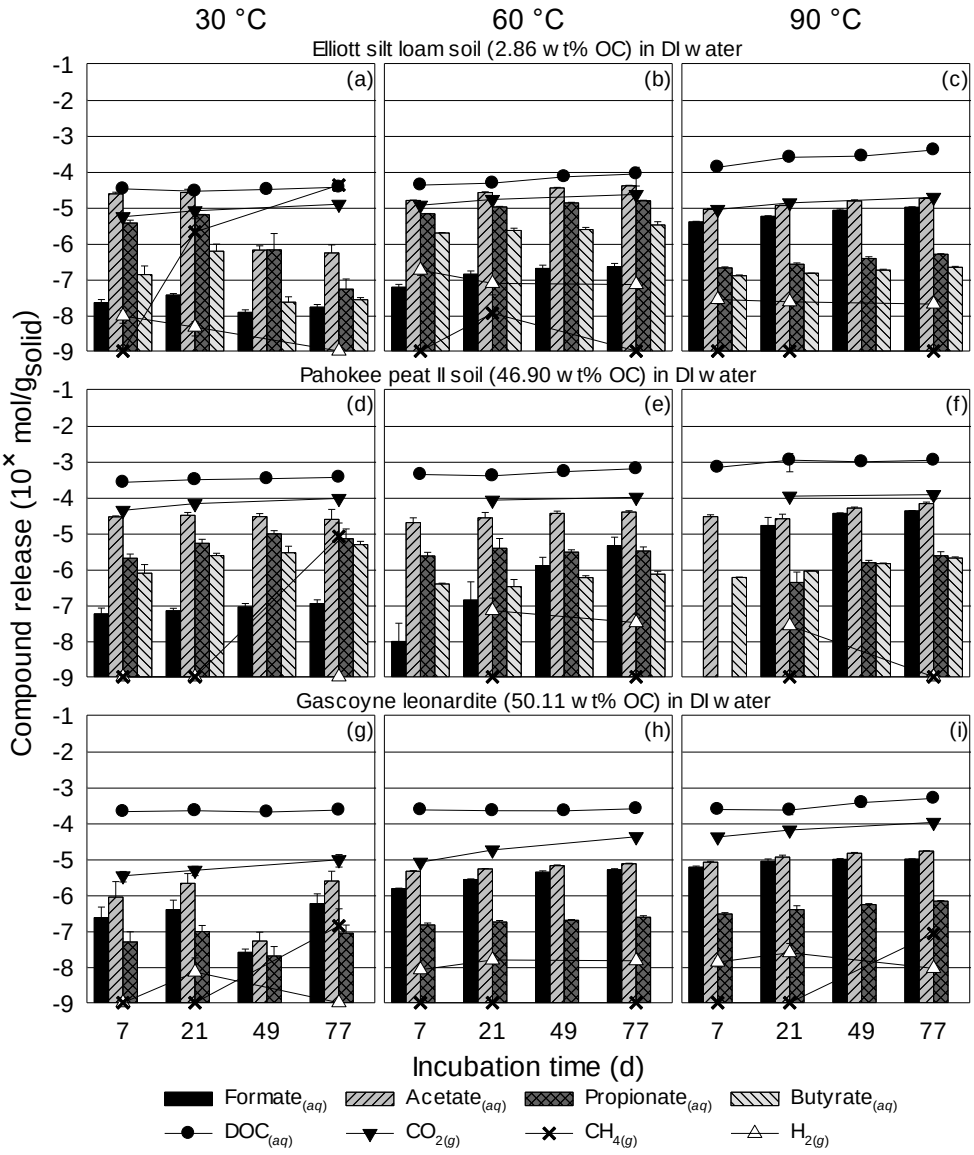

Figure 3-4: VFAs (as carbon), DOC, CO_2, CH_4, and H_2 release following 30, 60, and 90 °C incubation of: Elliott silt loam soil (a, b, c); Pahokee peat soil II (d, e, f); and Gascoyne leonardite (g, h, i) for 7, 21, 49, and 77 d (Ampule Set #4). Error bars represent one standard deviation. Absence of a VFA bar or location of a symbol on

the 10^{-9} line indicates that analysis was completed, but the corresponding compound was not detected. Absence of a symbol indicates that analysis of the corresponding compound was not completed.

Table 3-8: Data for Figure 3-4: VFAs (as carbon), DOC, CO_2, CH_4, and H_2 release following 30, 60, and 90 °C incubation of Elliott silt loam soil, Pahokee peat II soil, and Gascoyne leonardite for 7, 21, 49, and 77 days.

Elliott silt loam soil (2.86 wt% OC) in DI water

	30 °C (data for Figure 3-4a)				60 °C (data for Figure 3-4b)				90 °C (data for Figure 3-4c)			
	7 d	21 d	49 d	77 d	7 d	21 d	49 d	77 d	7 d	21 d	49 d	77 d
Formate(*aq*)	2E-8±5E-9	4E-8±4E-9	1E-8±2E-9	2E-8±3E-9	6E-8±1E-8	1E-7±3E-8	2E-7±5E-8	2E-7±5E-8	4E-6±2E-7	6E-6±2E-7	8E-6±7E-7	1E-5±3E-7
Acetate(*aq*)	2E-5±3E-6	3E-5±6E-6	7E-7±2E-7	5E-7±4E-7	2E-5±4E-7	3E-5±1E-6	3E-5±1E-6	4E-5±1E-6	9E-6±6E-7	1E-5±4E-7	2E-5±1E-6	2E-5±6E-7
Propionate(*aq*)	4E-6±7E-7	6E-6±2E-7	7E-7±1E-6	5E-8±5E-8	7E-6±1E-7	1E-5±4E-7	1E-5±5E-7	2E-5±6E-7	2E-7±1E-8	3E-7±2E-8	4E-7±4E-8	5E-7±2E-8
Butyrate(*aq*)	1E-7±1E-7	6E-7±3E-7	2E-8±9E-9	3E-8±4E-9	2E-6±5E-8	2E-6±4E-7	2E-6±3E-7	3E-6±7E-7	1E-7±6E-9	1E-7±3E-9	2E-7±1E-8	2E-7±1E-8
Total VFAs(*aq*)	3E-5±4E-6	3E-5±6E-6	1E-6±1E-6	6E-7±4E-7	2E-5±5E-7	4E-5±2E-6	5E-5±1E-6[⊥]	6E-5±2E-6[⊥]	1E-5±8E-7[┬,╥]	2E-5±7E-7[┬,╥]	2E-5±2E-6[⊥,╥]	3E-5±9E-7[⊥,╥]
DOC(*aq*)	3E-5±2E-6	3E-5±6E-7	3E-5±6E-6	4E-5±1E-6	4E-5±6E-6[⊥]	5E-5±2E-6[⊥]	7E-5±1E-5[⊥]	9E-5±5E-5	1E-4±2E-5[⊥,╨]	2E-4±3E-5[⊥,╨]	3E-4±6E-5[⊥,╨]	4E-4±9E-6[⊥,╨]
CO_2(*g*)	5E-6±2E-7	8E-6±4E-7	*	1E-5±4E-7	1E-5±7E-7	2E-5±5E-7	*	2E-5±2E-6	9E-6±2E-7	1E-5±9E-7	*	2E-5±8E-7
CH_4(*g*)	< det	2E-6±3E-6	*	4E-5±1E-6	< det	1E-8±3E-8	*	< det	< det	< det	*	< det
H_2(*g*)	1E-8±4E-9	5E-9±2E-9	*	< det	2E-7±5E-8	8E-8±6E-9	*	7E-8±1E-8	3E-8±7E-9	2E-8±2E-9	*	2E-8±9E-10

Pahokee peat II soil (46.90 wt% OC) in DI water

	30 °C (data for Figure 3-4d)				60 °C (data for Figure 3-4e)				90 °C (data for Figure 3-4f)			
	7 d	21 d	49 d	77 d	7 d	21 d	49 d	77 d	7 d	21 d	49 d	77 d
Formate(*aq*)	6E-8±3E-8	7E-8±1E-8	9E-8±2E-8	1E-7±3E-8	1E-8±2E-8	1E-7±3E-7	1E-6±9E-7	5E-6±3E-6	< det	2E-5±1E-5	4E-5±1E-6	4E-5±1E-6
Acetate(*aq*)	3E-5±2E-6	3E-5±6E-6	3E-5±6E-6	2E-5±2E-5	2E-5±7E-6	3E-5±1E-5	4E-5±6E-6	4E-5±4E-6	3E-5±4E-6	3E-5±9E-6	5E-5±4E-6	7E-5±7E-6
Propionate(*aq*)	2E-6±6E-7	5E-6±2E-6	1E-5±2E-6	7E-6±6E-6	2E-6±6E-7	4E-6±3E-6	3E-6±5E-7	3E-6±1E-6	< det	4E-7±4E-7	2E-6±2E-7	2E-6±7E-7
Butyrate(*aq*)	8E-7±6E-7	2E-6±4E-7	3E-6±1E-6	5E-6±1E-6	4E-7±2E-8	3E-7±2E-7	6E-7±8E-8	7E-7±1E-7	6E-7±1E-8	9E-7±4E-8	1E-6±7E-8	2E-6±2E-7
Total VFAs(*aq*)	3E-5±2E-6	4E-5±6E-6	4E-5±7E-6	4E-5±3E-5	2E-5±8E-6	3E-5±1E-5	4E-5±5E-6	5E-5±5E-6	3E-5±4E-6	4E-5±3E-6	9E-5±4E-6[⊥,╨]	1E-4±8E-6[⊥,╨]
DOC(*aq*)	3E-4±8E-6	3E-4±1E-5	3E-4±1E-5	4E-4±3E-5	4E-4±6E-5[⊥]	4E-4±4E-5[⊥]	5E-4±9E-5[⊥]	6E-4±7E-5[⊥]	7E-4±6E-5[⊥,╨]	1E-3±6E-4	1E-3±1E-4[⊥,╨]	1E-3±5E-5[⊥,╨]
CO_2(*g*)	4E-5±3E-6	7E-5±2E-6	*	9E-5±5E-6	*	8E-5±2E-6	*	1E-4±7E-6	*	1E-4±3E-6	*	1E-4±3E-5
CH_4(*g*)	< det	< det	*	8E-6±1E-5	*	< det	*	< det	*	< det	*	< det
H_2(*g*)	< det	< det	*	< det	*	7E-8±9E-8	*	3E-8±2E-8	*	3E-8±5E-10	*	< det

Gascoyne leonardite (50.11 wt% OC) in DI water

	30 °C (data for Figure 3-4g)				60 °C (data for Figure 3-4h)				90 °C (data for Figure 3-4i)			
	7 d	21 d	49 d	77 d	7 d	21 d	49 d	77 d	7 d	21 d	49 d	77 d
Formate(*aq*)	2E-7±2E-7	4E-7±3E-7	3E-8±6E-9	6E-7±5E-7	1E-6±6E-8	3E-6±1E-7	4E-6±4E-7	5E-6±3E-7	6E-6±5E-7	9E-6±1E-6	1E-5±5E-7	1E-5±4E-7
Acetate(*aq*)	9E-7±1E-6	2E-6±2E-6	5E-8±4E-8	2E-6±2E-6	5E-6±1E-7	5E-6±2E-7	6E-6±3E-7	7E-6±3E-7	8E-6±5E-7	1E-5±2E-6	1E-5±7E-7	2E-5±4E-7
Propionate(*aq*)	5E-8±4E-8	9E-8±4E-8	2E-8±2E-8	9E-8±6E-8	1E-7±2E-8	2E-7±2E-8	2E-7±1E-8	2E-7±3E-8	3E-7±2E-8	4E-7±1E-7	5E-7±4E-8	7E-7±3E-8
Butyrate(*aq*)	< det	< det	< det	< det	< det	< det	< det	< det	< det	< det	< det	< det
Total VFAs(*aq*)	1E-6±2E-6	3E-6±2E-6	1E-7±5E-8	3E-6±3E-6	6E-6±2E-7$^{\perp}$	8E-6±2E-7$^{\perp}$	1E-5±7E-7$^{\perp}$	1E-5±5E-7$^{\perp}$	1E-5±1E-6$^{\perp,\shortparallel}$	2E-5±3E-6$^{\perp,\shortparallel}$	2E-5±1E-6$^{\perp,\shortparallel}$	3E-5±8E-7$^{\perp,\shortparallel}$
DOC(*aq*)	2E-4±1E-5	2E-4±1E-5	2E-4±8E-6	2E-4±2E-5	2E-4±2E-5	2E-4±2E-5	2E-4±1E-5$^{\perp}$	2E-4±5E-5	2E-4±3E-5	2E-4±6E-5	4E-4±9E-5$^{\perp,\shortparallel}$	5E-4±4E-5$^{\perp,\shortparallel}$
CO_2(*g*)	3E-6±1E-6	5E-6±1E-6	*	1E-5±4E-6	8E-6±3E-7	2E-5±1E-6	*	4E-5±4E-6	4E-5±3E-6	6E-5±4E-6	*	1E-4±3E-6
CH_4(*g*)	< det	< det	*	1E-7±3E-7	< det	< det	*	< det	< det	< det	*	8E-8±4E-9
H_2(*g*)	< det	7E-9±1E-8	*	< det	8E-9±8E-10	2E-8±3E-9	*	1E-8±2E-9	1E-8±4E-9	2E-8±2E-8	*	9E-9±8E-10

All values are presented in units of molC/g_{solid} except H_2(*g*), which is presented in units of molH_2/g_{solid}. Statistical differences between incubation temperatures were determined for Total VFAs(*aq*) and DOC(*aq*) only. < det = below detection limit; * = data not collected; $^{\perp}$ = significantly greater release than for equivalent conditions at 30 °C; $^{\shortparallel}$ = significantly greater release than for equivalent conditions at 60 °C; $^{\top}$ = significantly lower release than for corresponding incubation conditions at 30 °C; $^{\pi}$ = significantly lower release than for corresponding incubation conditions at 60 °C.

The maximum total VFAs release was 60±2 × 10^{-6} molC/g_s from Elliott silt loam soil (77 d at 60 °C; Figure 3-4b); 110±8 × 10^{-6} molC/g_s from Pahokee peat soil II (77 d at 90 °C; Figure 3-4f); and 30±1 × 10^{-6} molC/g_s from Gascoyne leonardite (77 d at 90 °C; Figure 3-4i). Total VFAs release was unexpectedly low in 90 °C Elliott soil ampules, representing the only case where 90 °C incubation yielded significantly ($p < 0.05$) lower VFAs release than 60 °C incubation (Figure 3-4b); however, total VFAs release still increased with time, and post-incubation DOC was significantly ($p < 0.05$) higher at 90 °C (130±16 – 400±9 × 10^{-6} molC/g_s; Figure 3-4c) than at 30 °C (30±2 – 40±1 × 10^{-6} molC/g_s; Figure 3-4a) and 60 °C (40±6 – 90±50 × 10^{-3} molC/g_s; Figure 3-4b) at all time points, indicating that other, undetected soluble organic compounds were released. H_2 and CH_4 production also occurred in ampules containing all three IHSS bulk source materials. The highest H_2 production was measured in Elliott soil ampules incubated at 60 °C (180±50 × 10^{-9} molH_2/g_s; Figure 3-4b), but H_2 was present above the detection limit for all solid-temperature combinations except 30 °C incubation of Pahokee peat soil II (Figure 3-4). CH_4 production was highest in Elliott soil ampules (40±1 × 10^{-6} molCH_4/g_s; Figure 3-4a) after 77 d at 30 °C.

Long-term (180 d) incubation of quartz sand, aquifer material, natural soils, and humic acid source materials at 90 °C (Ampule Set #5). Set #5 consisted of 49 non-blank ampules containing 10 solid materials and was designed to quantify VFAs and H_2 release following long-term (180 d) incubation at 90 °C, similar to

conditions at an ERH field site application.[47] VFAs release occurred in all ampules and, except for Gascoyne leonardite ampules, increased with solid-phase OC content (Figure 3-5,

Table 3-9).

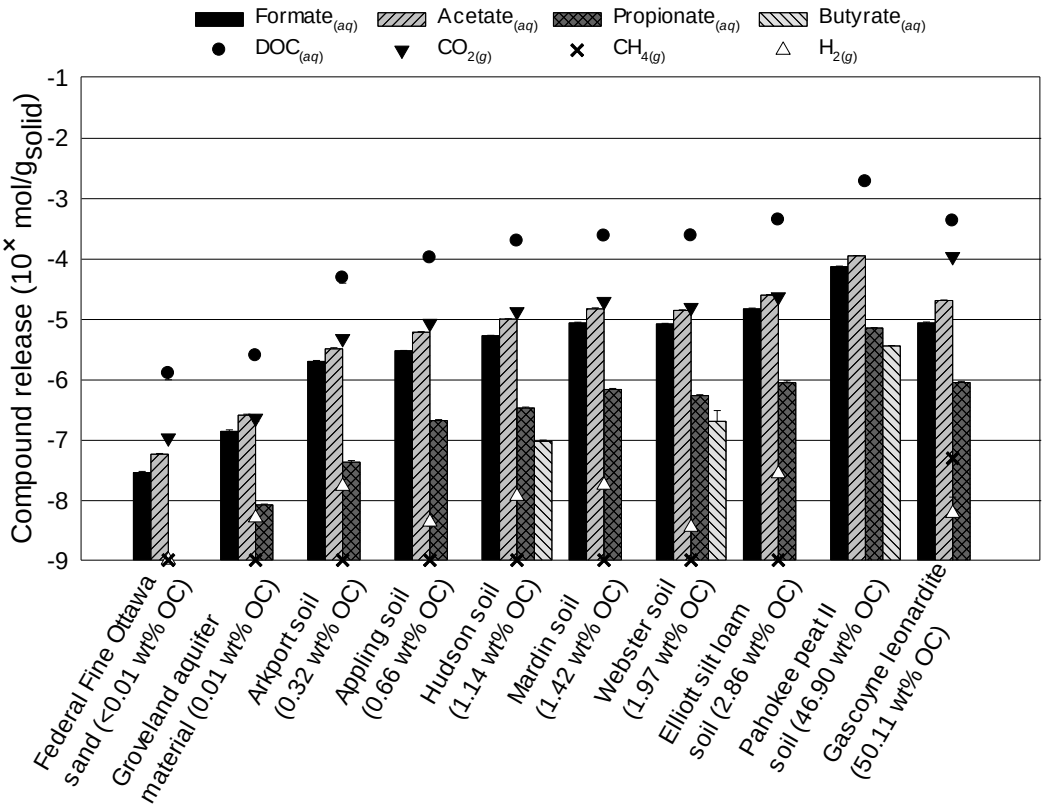

Figure 3-5: VFAs (as carbon), DOC, CO_2, CH_4, and H_2 release following incubation of Federal Fine Ottawa sand, Groveland aquifer material, Arkport soil, Appling soil, Hudson soil, Mardin soil, Webster soil, Elliott silt loam soil, Pahokee peat soil II, and Gascoyne leonardite at 90 °C for 180 d (Ampule Set #5). Error bars represent one standard deviation. Absence of a VFA bar or location of a symbol on the 10^{-9} line indicates that analysis was completed, but the corresponding compound was not detected. Absence of a symbol indicates that analysis of the corresponding compound was not completed.

Table 3-9: Data for Figure 3-5: VFAs (as carbon), DOC, CO_2, CH_4, and H_2 release following incubation of Federal Fine Ottawa sand, Groveland aquifer material, Arkport soil, Appling soil, Hudson soil, Mardin soil, Webster soil, Elliott silt loam soil, Pahokee peat II soil, and Gascoyne leonardite at 90 °C for 180 d.

	Federal Fine Ottawa sand (<0.01 wt% OC)	Groveland aquifer material (0.01 wt% OC)	Arkport soil (0.32 wt% OC)	Appling soil (0.66 wt% OC)	Hudson soil (1.14 wt% OC)	Mardin soil (1.42 wt% OC)	Webster soil (1.97 wt% OC)	Elliot silt loam soil (2.86 wt% OC)	Pahokee peat II soil (46.90 wt% OC)	Gascoyne leonardite (50.11 wt% OC)
Formate(*aq*)	3E-8±1E-9	1E-7±8E-9	2E-6±8E-8	3E-6±6E-8	5E-6±7E-8	8E-6±3E-7	8E-6±1E-7	1E-5±4E-7	7E-5±2E-6	8E-6±3E-7
Acetate(*aq*)	6E-8±2E-9	3E-7±8E-9	3E-6±1E-7	6E-6±1E-7	1E-5±1E-7	1E-5±5E-7	1E-5±2E-7	2E-5±7E-7	1E-4±2E-6	2E-5±5E-7
Propionate(*aq*)	< det	8E-9±2E-10	4E-8±2E-9	2E-7±8E-9	3E-7±1E-8	7E-7±3E-8	5E-7±2E-8	9E-7±7E-8	7E-6±9E-8	9E-7±4E-8
Butyrate(*aq*)	< det	< det	< det	< det	9E-8±4E-9	< det	2E-7±1E-7	< det	4E-6±5E-8	< det
Total VFAs(*aq*)	8E-8±2E-9	4E-7±2E-8	5E-6±2E-7	9E-6±2E-7	2E-5±2E-7	2E-5±8E-7	2E-5±5E-7	4E-5±1E-6	2E-4±3E-6	3E-5±8E-7
DOC(*aq*)	1E-6±3E-7	2E-6±8E-8	5E-5±8E-6	1E-4±3E-6	2E-4±1E-5	2E-4±2E-5	2E-4±6E-6	4E-4±2E-5	2E-3±4E-5	4E-4±1E-5
$CO_2(g)$	1E-7±8E-9	2E-7±3E-8	5E-6±7E-8	8E-6±6E-7	1E-5±1E-7	2E-5±9E-7	2E-5±4E-7	2E-5±1E-6	*	1E-4±5E-6
$CH_4(g)$	< det	< det	< det	< det	< det	< det	< det	< det	*	5E-8±4E-9
$H_2(g)$	< det	5E-9±2E-10	2E-8±7E-10	4E-9±6E-10	1E-8±8E-11	2E-8±2E-9	3E-9±2E-10	3E-8±2E-9	*	6E-9±5E-9

All values are presented in units of molC/g_{solid} except $H_2(g)$, which is presented in units of molH_2/g_{solid}. < det = below detection limit; * = data not collected.

DOC accounted for 0.1 – 2.4% of initial ampule OC and 6.9 – 16.4% of that DOC consisted of VFAs. The highest total VFAs release was $190\pm0 \times 10^{-6}$ $molC/g_s$, measured in ampules containing Pahokee peat soil II (46.90 wt% OC). Low levels of H_2 were detected in all ampules except for those containing Federal Fine Ottawa sand, ranging from $4\pm1 \times 10^{-9}$ $molH_2/g_s$ in Appling soil ampules to $30\pm2 \times 10^{-9}$ $molH_2/g_s$ in Elliott soil ampules. CH_4 ($50\pm4 \times 10^{-9}$ $molCH_4/g_s$) was detected only in Gascoyne leonardite ampules. Results reinforce the positive relationship between capacity for VFAs release and solid-phase OC content.

3.5 Discussion

3.5.1 VFAs release during thermal treatment of solids

Formate, acetate, propionate, and butyrate were consistently detected following thermal treatment of 14 different solids, including quartz sand, aquifer material, soils, and humic and fulvic acid standards. The extent of VFAs release was impacted by incubation temperature (Figure 3-1 and Figure 3-3), incubation time (Figure 3-3), and solid-phase OC content (Figure 3-5) and structure (Figure 3-3 and Figure 3-4). Because all VFAs contain carbon, release of VFAs requires that carbon must initially be present in the solid material itself. Similarly, the maximum potential VFAs release is limited by solid-phase carbon content. Experimental results demonstrated a relationship between incubation temperature and VFAs

release. After 56 d at 90 °C, total VFAs released from Federal Fine Ottawa sand, Groveland aquifer material, Appling soil, and Webster soil (Figure 3-1) were 796 – 4,293% greater ($p < 0.05$) than at 30 °C, and 25 – 2,235% greater ($p < 0.05$ in most cases;

Table 3-3) than at 60 °C. Similarly, total VFAs release from humic and fulvic acid standards (Figure 3-3) were 523 – 1,159% and 256 – 371% greater ($p < 0.05$) after 21 d at 90 °C than at 30 and 60 °C, respectively.

The extent of VFAs release was generally associated with longer incubation times; results from the incubation of humic and fulvic acids exemplify this temporal dependence (Figure 3-3). The stable DOC concentrations observed between 7 and 28 d of incubation (

Table 3-7) indicate that most soluble organic matter dissolved within the first 7 d. However, the DOC fraction identifiable as VFAs increased over time, particularly during 60 and 90 °C incubation, suggesting that the rate-limiting process resulted from the decomposition of larger dissolved compounds to VFAs, rather than gradual dissolution or cleaving of individual VFA molecules from the bulk organic structure. The time- and temperature-dependencies are consistent with hydrolytic degradation, which, as discussed previously, can separate VFAs and other low molecular weight constituents from humic matter without compromising the molecular integrity of the liberated compounds.

While incubation time and temperature influenced VFAs release from each solid material, the greatest variations in release were observed when comparing different solids, and thus OC contents, to one another. As noted previously, solid-phase OC content dictates the maximum potential release of VFAs. When considering all 140 unique incubations simultaneously (543 ampules), VFAs accounted for 0.0 – 4.8% of solid-phase OC content (Figure 3-6). This 0.0 – 4.8% recovery is consistent with the 0 – 4 wt% recovery rate that is typical during pH-neutral hydrolysis of organic matter, as discussed previously.

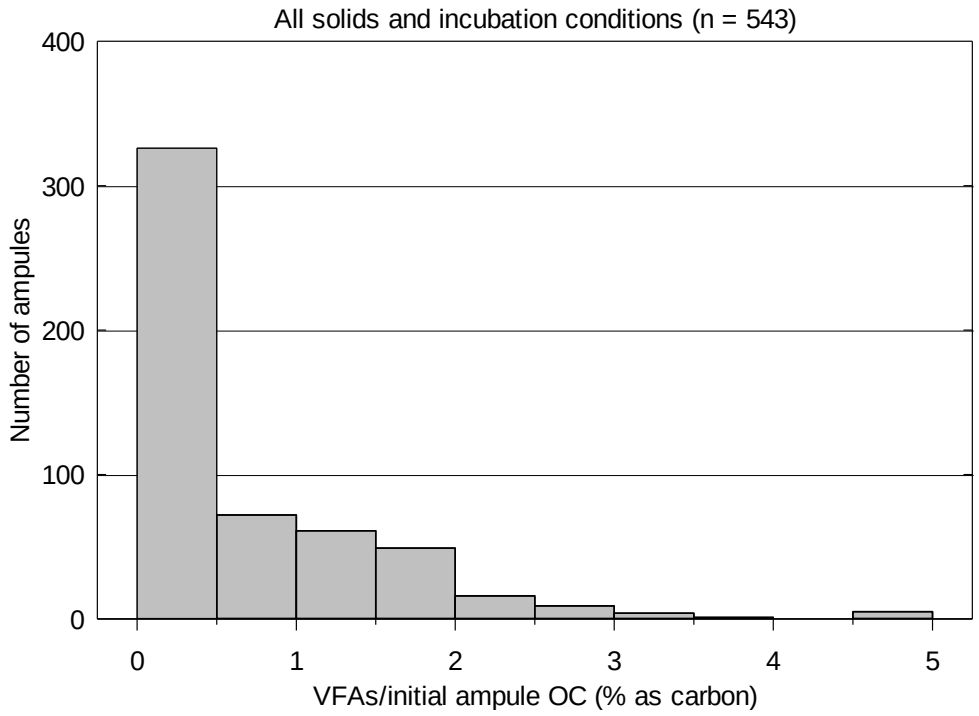

Figure 3-6: Distribution of initial ampule OC detected as VFAs (as carbon) following incubation of all solids and incubation conditions.

This relationship is confirmed by results of incubation experiments designed to imitate conditions typical of an ERH field site (Ampule Set #5). Eight of the 10 solids included in these long-term (180 d), high-temperature (90 °C) experiments contain OC at concentrations representative of aquifer materials; VFAs release from these eight solids accounted for a narrower range of solid-phase OC content (1.4 – 4.8%; Figure 3-7) than when all incubation conditions were assessed simultaneously (Figure 3-6). A linear regression model of total VFAs release as a function of solid-phase OC content (Equation 12; Figure 3-8) clearly demonstrates the correlation.

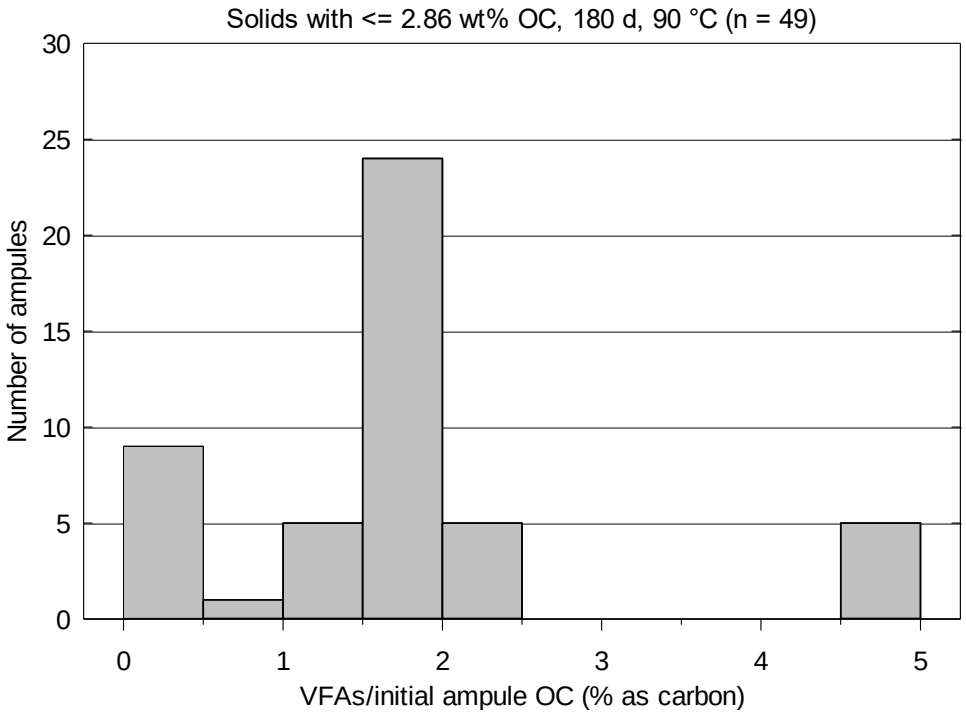

Figure 3-7: Distribution of initial ampule OC detected as VFAs (as carbon) following incubation of solids representative of aquifer materials incubation for 180 d at 90 °C.

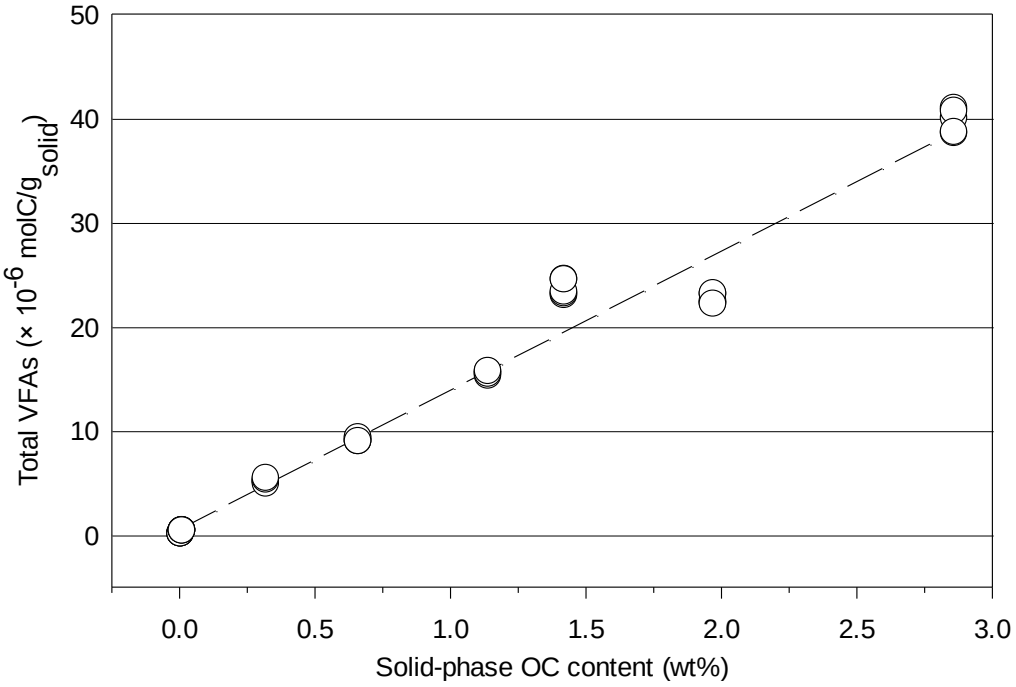

Figure 3-8: Total VFAs release (as carbon) as a function of solid-phase OC content ($p < 0.0005$) for solids representative of aquifer materials incubation for 180 d at 90 °C.

Despite its simplicity, the high statistical significance ($p < 0.0005$; adjusted R^2 = 0.97) of the model indicates that exposure of solid materials to typical ISTT parameters can result in a highly predictable release of bioavailable VFAs.

$$\widehat{VFAs}\ (\times 10^{-6}\ molC/g_s) = 13.4 \times OC\ (wt\%) \qquad \text{(Equation 12)}$$

Pahokee peat soil II (46.90 wt% OC) and Gascoyne leonardite (50.11 wt% OC) were excluded from the regression model because they are unrepresentative of aquifer materials due to their exceptionally high OC contents and distinctive origins.[101, 102] It must be acknowledged, however, that decoupling of the relationship between VFAs release and OC content makes the Equation 12 regression model unsuitable for most solids with exceptionally high OC content (e.g., humic and fulvic acids). Application of the regression model to Pahokee peat soil II and Gascoyne leonardite yielded total VFAs releases of 628 × 10^{-6} and 671 × 10^{-6} molC/g_s, respectively; these estimated values are 227 and 2,196% greater than the mean total VFAs releases measured from these solids after 180 d of incubation at 90 °C.

Given that pH-neutral hydrolysis is unlikely to disrupt the molecular integrity of liberated compounds, VFAs detected following incubation must initially have been part of the bulk organic structure of the solid phase. However, the OC content of each VFA ranges from 27% (formate) to 55% (butyrate) on a mass basis. For

Pahokee peat soil II, Gascoyne leonardite, and the humic and fulvic acid standards to contain such abundant OC (46.90 – 63.81 wt%), a substantial portion of that OC must be associated with organic compounds other than VFAs and the COOH groups that define them. These non-COOH compounds, such as highly stable phenol groups (76.6 wt% OC), would inflate the overall solid-phase OC content, but would not contribute to VFAs release under the incubation conditions described. For example, the Leonardite humic acid standard (63.81 wt% OC; $200\pm11 \times 10^{-6}$ molC/g_s maximum VFAs release) contains 4.64 mmol COOH/g_s, which accounts for only 8.7 % of total OC. By comparison, COOH groups in the Elliott soil humic acid standard (58.13 wt% OC), Pahokee peat humic acid standard (56.37 wt% OC), and Suwannee River fulvic acid standard II (52.34 wt% OC) account for 9.9, 10.7, and 13.3 % of total OC, respectively. Despite containing less OC overall than the Leonardite humic acid standard, the greater abundances of COOH-associated OC in these solids are consistent with their higher maximum VFAs releases (740 ± 160 – $820\pm50 \times 10^{-6}$ molC/g_s). While COOH abundance cannot be used to predict VFAs release as effectively as solid-phase OC content (Figure 3-8; Equation 12), these data help to reconcile the decoupling of the relationship between solid-phase OC content and total VFAs release during incubation of high-OC solids.

3.5.2 Production of H_2 during thermal treatment of solids

H_2 was produced during thermal treatment of all solid materials except Federal Fine Ottawa sand (<0.01 wt% OC) and the humic and fulvic acid standards (52.34 – 63.81 wt% OC), but production was relatively low compared to VFAs release. For example, 60 °C incubation of Elliott soil yielded the greatest overall H_2 production ($180\pm50 \times 10^{-9}$ molH_2/g_s; Figure 3-4b), equal to $360\pm100 \times 10^{-9}$ mol reducing equivalents per gram solid, but accounted for less than 0.3% of reducing equivalents associated with VFAs under the same incubation conditions. The lack of correlation with incubation parameters or solid-phase properties also indicates that this H_2 production was not a direct consequence of thermal treatment. Instead, multiple lines of evidence indicate that H_2 was produced by microorganisms. For example, Appling and Webster soils yielded H_2 when incubated in DI water (Figure 3-1), but H_2 was absent or significantly ($p < 0.05$) reduced following incubation with 2 mM $HgCl_2$ (Figure 3-2). H_2 was also absent following incubation of the microbially-inactive humic and fulvic acid standards (Figure 3-3), but was detected at up to $180\pm50 \times 10^{-9}$ molH_2/g_s following incubation of the non-sterile bulk source materials (Figure 3-4) from which the standards were extracted. Finally, the eight conditions yielding the most H_2 involved 60 °C incubation of Webster soil, Elliott soil, and Pahokee peat soil II (1.97 – 46.90 wt% OC), and no addition of microbial inhibitor (i.e., $HgCl_2$). These conditions provided abundant substrate by inducing VFAs release, while remaining within the upper temperature bounds (35 – 60 °C)[108] permissive of fermentative H_2 production.

3.5.3 Implications for chlorinated solvent remediation

The coupling of ISTT with MRD is a promising alternative to conventional chlorinated solvent remediation, but successful implementation requires a more thorough understanding of the interactions between the parent technologies. Thermal treatment has been shown to produce favorable conditions for reductively dechlorinating bacteria, effectively priming the system for a simultaneous or sequential ISB phase, but available data limits extrapolation to different field sites. This study demonstrates consistent release of specific bioavailable compounds from varied solid materials, and provides an empirical relationship to estimate the magnitude of this release under typical thermal remediation conditions. These findings will enable remediation professionals to better anticipate thermally-induced changes to aquifer geochemistry, allowing for more effective exploitation of organic substrate release and optimization of remedial designs.

4. Bioavailability and utilization of thermally-released substrates for the microbial reductive dechlorination of chlorinated ethenes

4.1 Abstract

In situ thermal treatment (ISTT) of soil and groundwater has been shown to induce release of bioavailable volatile fatty acids (VFAs) to the aqueous phase, providing a potential source of electron donors that could stimulate microbial reductive dechlorination (MRD) at sites contaminated with chlorinated solvents. The objectives of this study were to assess VFA mobility and availability downgradient of a heated zone during thermal treatment, and to determine the extent to which KB-1®, a tetrachloroethene (PCE)-to-ethene dechlorinating microbial consortium, can utilize liberated substrates to drive MRD of PCE in the absence of an external electron donor and carbon source. A series of 1-D flow studies was completed, wherein an upgradient zone packed with Webster soil (1.97 wt % organic carbon (OC)) or Hudson soil (1.14 wt% OC) was heated to mimic typical ISTT conditions, while VFAs release, transport, consumption, and resultant MRD activity were assessed downgradient in an unheated zone packed with Federal Fine Ottawa sand (<0.01 wt% OC). A stepwise heating regime in the Webster soil column (+10 °C/3.3 pore volumes (PVs)) led to pronounced spikes in VFAs concentrations of up to 2.5 mM total VFAs as carbon following a temperature increase in the heated

zone from 38 to 51 °C. These spikes in VFAs concentrations were not apparent during gradual heating of the Hudson soil columns (+2 °C/PV), indicating that heating regime may impact the rate and longevity of VFAs release during soil heating. Total VFAs concentrations of up to 10.6 mM as carbon were detected downgradient of the heated zone in Hudson column studies, and complete dechlorination to ethene occurred for up to 40 PV post-inoculation. These findings demonstrate that substrates released during thermal treatment of soils can provide dechlorinating bacteria with the necessary electron donor and carbon sources to sustain complete MRD of PCE to ethene.

4.2 Introduction and background

The coupled implementation of two or more complementary remediation technologies, sometimes referred to as a treatment-train approach, has gained support among remediation professionals in recent years as traditional standalone remediation technologies have failed to adequately address widespread chlorinated solvent contamination of soil and groundwater.[3, 4, 6, 7] By implementing complementary remediation technologies simultaneously or in series, practitioners aim to achieve contaminant mass removal or degradation that would not be attainable using a standalone technology. The coupling of ISTT with in situ bioremediation (ISB) has received substantial attention from practitioners and regulators as a potentially viable option for remediating sites contaminated with chlorinated ethenes,[3, 15, 16, 18, 42, 43] but has not yet translated into regular field-scale

implementation. However, a growing volume of literature based largely upon laboratory-scale batch studies has demonstrated that ISTT can help to optimize redox conditions for a subsequent ISB phase, and can promote release of organic compounds capable of serving as electron donor and carbon sources for reductively dechlorinating bacteria.[14-16]

In a recent study (Chapter 3), results of an extensive matrix of ampule batch experiments demonstrated conclusively that heating of solid materials leads to the release of organic substrates to the aqueous phase, specifically as the VFAs formate, acetate, propionate, and butyrate. This release was attributed to the hydrolytic degradation of organic matter, and was positively correlated with incubation time, incubation temperature, and the OC content of the solid phase. Although batch studies allow for rigorous, high-throughput assessment of substrate release under a wide variety of thermal treatment conditions, the lack of advective flow and spatial control of system temperature make assessment of substrate transport and consumption difficult. Furthermore, the magnitude of VFAs release (up to 23±1 $\mu molC/g_{solid}$ from solids representative of aquifer materials with <0.01 – 2.86 wt% OC) was substantial enough to warrant continued investigation to determine whether thermally-released VFAs could stimulate microbial reductive dechlorination of chlorinated ethenes.

In this chapter, a series of 1-D column flow studies was completed using two of the solid materials tested in the ampule batch studies: Webster soil (1.97 wt% OC) and Hudson soil (1.14 wt% OC). The primary objective of the Webster soil column study was to assess the transport and subsequent downgradient availability of electron donors and fermentable precursors following stepwise heating (+10 °C/3.3 PVs) of upgradient Webster soil from 22 – 82 °C. A matrix of four Hudson soil column studies was completed to assess whether these thermally-released electron donors and fermentable precursors were sufficient to promote the growth and activity of KB-1®, a PCE-to-ethene dechlorinating microbial consortium, in systems otherwise lacking an external electron donor source (e.g., lactate). Aqueous concentrations of VFAs, chlorinated ethenes, and ethene were monitored throughout the experiments to determine whether thermal treatment could provide native and amended microorganisms with sufficient reducing equivalents to drive complete dechlorination of PCE to ethene.

4.3 Materials and methods

4.3.1 Materials

PCE (≥99%), trichloroethene (TCE; ≥99.5%), *cis*-1,2-dichloroethene (*cis*-DCE; ≥97%), and ethene gas (≥99.5%) used in column experiments and gas chromatography (GC) standards were obtained from Sigma-Aldrich (St. Louis,

MO). Vinyl chloride gas (VC; 99%) was obtained from SynQuest Laboratories (Alachua, FL). Ion chromatography (IC) standards were prepared using sodium acetate (≥99%; EMD Millipore, Burlington, MA), sodium butyrate (≥98%; Alfa Aesar, Haverhill, MA), sodium formate (≥99%; Sigma-Aldrich), and sodium propionate (≥99%; Sigma-Aldrich). Ultra-high purity gases used during experiment preparation and analyses were obtained from Airgas (Radnor, PA). All aqueous solutions were prepared using 18.2 MΩ deionized (DI) water (EMD Millipore).

4.3.2 System design and preparation – Webster soil column

An initial column experiment designed to assess electron donor availability downgradient of a heated soil zone was completed using a horizontally-oriented borosilicate glass chromatography column (90 cm *l* × 5 cm *ID*; Ace Glass, Vineland, NJ). The upgradient 30 cm was packed with non-sterile Webster soil (30-mesh; Ames, IA), a silty clay loam with 1.97 wt% OC content.[100] The first 20 cm of this upgradient segment made up the heated zone and contained approximately 500 g of soil. The PV of the heated zone was approximately 175 mL. Subsequent mentions of PV in the Webster soil column study are with respect to this number. The downgradient 60 cm of the column was packed with steam-sterilized Federal Fine Ottawa sand (U.S. Silica, Frederick, MD), a 30 – 140 mesh quartz sand with <0.01 wt% TOC content. Upper and lower sides of the downgradient zone were each equipped with six evenly distributed sampling ports and fixed stainless-steel

needles to facilitate sampling and temperature monitoring (Figure 4-1). Needles installed in the upper ports were used to collect gas-phase samples and did not penetrate the sand. Needles installed in the lower ports extended 2.5 cm beyond the inner wall of the column to the axial center of the Federal Fine Ottawa sand pack and were used to collect aqueous-phase samples. Ports were sealed with Teflon Mininert syringe valves (Valco Instruments, Houston, TX) between sampling events.

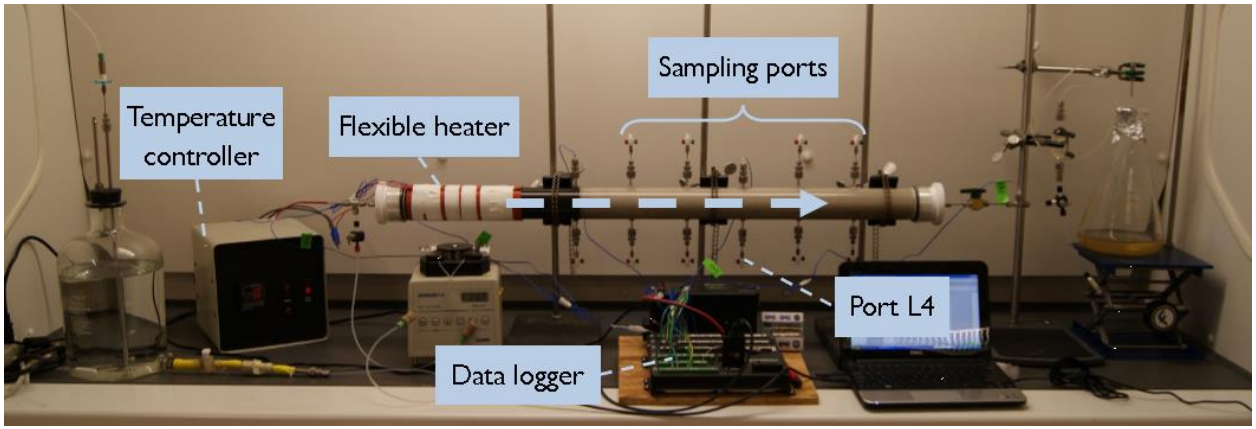

Figure 4-1: Experimental system setup of 90 cm thermal column experiment designed to assess electron donor availability and mobility downgradient of a thermal treatment zone.

4.3.3 Operation and sampling – Webster soil column

A sterile, Argon-sparged solution containing 24 mM calcium chloride (72 mM ionic strength) was pumped through the column at a pore water velocity of v = 25 cm/day (Q ≈ 0.125 mL/min) for the duration of the experiment using a Rainin Dynamax RP-1 peristaltic pump (Mettler-Toledo; Columbus, OH). The system was initially operated at ambient temperature (approximately 22 °C), then heating began after 3.3 PVs using a flexible silicone heater (Omega Engineering, Stamford, CT) wrapped around the column and covered with an insulating sleeve to minimize heat loss. A Watlow Series 965 feedback controller (Watlow Electric Manufacturing, St. Louis, MO) was used to regulate temperature, which was steady within the set value ±0.5 °C. Temperatures were continuously measured at multiple points throughout the system using Type K thermocouples (VWR, Radnor, PA) and were recorded to a CR1000 data logger (Campbell Scientific, Logan, UT). Unless otherwise specified, all temperature values reported herein were measured using a thermocouple located at the axial center of the Webster soil, 10 cm from the influent endplate. Temperature was increased in a stepwise manner between 3.3 and 21.4 PVs until reaching a high of 82.7 °C, which was maintained for 6.2 PVs. Temperature was then returned to ambient over the next 16.3 PVs and remained there until the end of the experiment.

Aqueous effluent samples were collected approximately once per PV from a 20 mL, custom glass sampling bulb (G. Finkenbeiner, Waltham, MA) that was used to maintain anoxia in the effluent samples. After collection, effluent samples were immediately analyzed for oxidation-reduction potential (ORP) and pH. Aqueous port samples (0.5 mL) were collected from ports L2 – L6 with similar frequency, though clogging in ports L2 and L3 with Webster soil particles prevented sampling during the latter half of the experiment. All aqueous samples were analyzed using an IC to identify and quantify VFAs released during heating of the Webster soil. Gas samples were collected from port U2 when gas accumulation was sufficient for analysis. Using a GC equipped with a thermal conductivity detector (TCD), samples of at least 3 mL were analyzed for hydrogen (H_2) and methane (CH_4), two compounds commonly produced and consumed by microorganisms in anaerobic environments.

4.3.4 System design and preparation – Hudson soil columns

Four additional flow experiments (A, B, C, and D) were completed, each consisting of a stainless-steel column (15 cm *l* × 5.7 cm *ID*) and a glass chromatography column (15 cm *l* × 5.7 cm *ID*; Kimble-Chase, Vineland, NJ) equipped with three sampling ports and Teflon endplates. Following steam-sterilization, columns were packed in 1 cm increments. The stainless-steel column was packed with dry, 30 mesh (ASTM E-11) Hudson soil (60 – 104 cm depth, Allegany County, NY), a silty

clay with a post-sieving OC content of 1.14 wt%. Hudson soil was chosen as the solid phase for these experiments because it better represents a likely aquifer material (i.e., collected at 60 – 104 cm depth, at or just below the water table) compared to a topsoil like Webster soil, but still demonstrated strong VFAs release during 180 d, 90 °C incubation (Chapter 3). The glass chromatography column was packed with steam-sterilized, 30 – 40 mesh Federal Fine Ottawa sand (U.S. Silica, Frederick, MD), a quartz sand containing <0.01 wt% OC. Packed columns were purged with filter-sterilized carbon dioxide (CO_2) to facilitate complete saturation, then saturated with a sterile, synthetic groundwater solution containing 1 mM sulfide as reductant. Preparation of the synthetic groundwater solution is described in Section 5.3.3. The aqueous PV of each Federal Fine Ottawa sand column was determined by analyzing breakthrough curves from non-reactive bromide tracer tests ($[Br^-]$ = 10 mM, flow rate = 3 mL/min) using the Code for Estimating Equilibrium Transport Parameters from Miscible Displacement Experiments (CFITM).[109]

Following column packing and saturation, each experimental system was assembled per the diagram in Figure 4-2, with the Hudson (stainless-steel) column and Federal Fine Ottawa sand (glass) column connected in series.

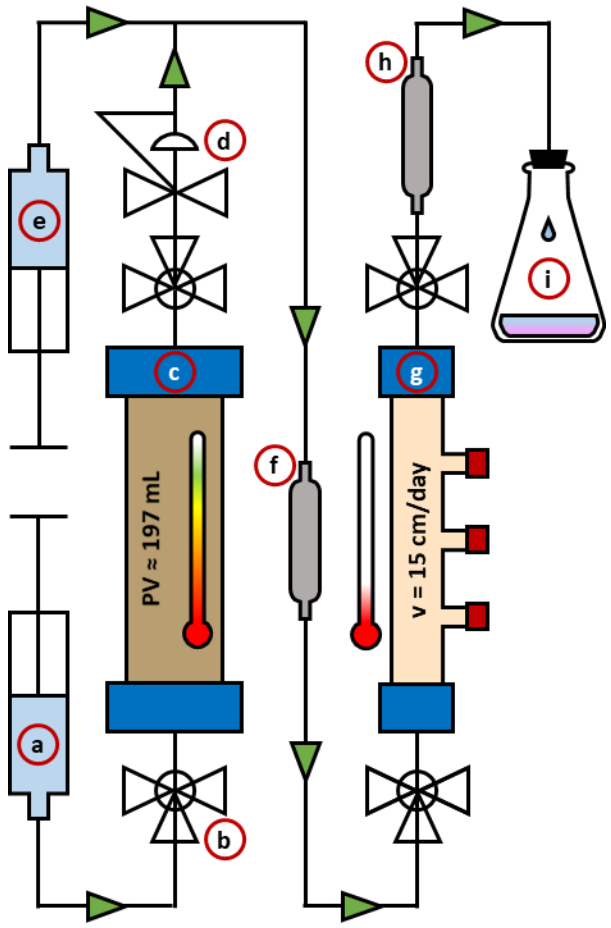

Figure 4-2. System diagram including: a) Nexus 6000 syringe pump (primary flow); b) three-way valve; c) stainless-steel column packed with Hudson soil; d) back-pressure regulator; e) Fusion 200 syringe pump (secondary flow); f) midpoint sampling reservoir; g) borosilicate glass chromatography column packed with Federal Fine Ottawa sand; h) effluent sampling reservoir; i) effluent waste.

Primary system flow (Q_P = 0.018 mL/min) was driven using a Nexus 6000 syringe pump (Chemyx, Holliston, MA) connected to the Hudson column inlet (Figure 4-2a). The Hudson column was wrapped in copper tape (3M, Maplewood, MN) and housed in an Isotemp Premium Lab Oven (Thermo Fisher) to facilitate uniform heating, and temperature was continuously measured and recorded using Type K thermocouples (VWR, Radnor, PA) connected to a CR1000 data logger (Campbell Scientific, Logan, UT). A back-pressure regulator (Swagelok, Solon, OH) was located immediately downgradient of the Hudson column to prevent gas formation in the tubing (Figure 4-2d). Secondary flow (Q_S = 0.002 mL/min) was driven using a Fusion 200 syringe pump (Figure 4-2e) (Chemyx) connected downgradient of the back-pressure regulator. System midpoint (Figure 4-2f) and effluent (Figure 4-2h) sampling reservoirs were located immediately upgradient and downgradient, respectively, of the Federal Fine Ottawa sand column (Figure 4-2g).

4.3.5 Operation and sampling – Hudson soil columns

Although the experimental setup was similar for each of the four flow systems, operational parameters varied depending upon experimental goals. Systems A and B were operated in parallel, followed by Systems C and D, also in parallel.

Table 4-1. Summary of Hudson soil columns experimental system design and operational parameters.

	PCE delivery method	KB-1 present *(Y/N)*	FFOS PV *(mL)*	Hudson soil temperature *(°C)*		Q *(µL/min)*		[PCE] *(µM)*		[S_{2-}] *(mM)*	
				i	f	P	S	P	S	P	S
A	Thermal desorption	Yes	32.7	21	96	19.8	0.2	563 (0 – 6.1 PV) 0 (6.1 – 47 PV)	0	1	100
B	Thermal desorption	No	32.4	21	96	19.8	0.2	563 (0 – 6.1 PV) 0 (6.1 – 47 PV)	0	1	100
C	Secondary flow	Yes	31.1	21	21	18.0	2.0	0	100 → 700	1	10
D	Secondary flow	No	31.5	21	21	18.0	2.0	0	100 → 700	1	10

FFOS = Federal Fine Ottawa sand, i = initial, f = final, P = primary flow, S = secondary flow

Each of the Hudson columns in Systems A and B were initially loaded with approximately 135 μmol PCE by injecting 241 mL of synthetic groundwater containing 563±58 μM PCE via the primary syringe pump (Q_P = 0.07 mL/min). This initial loading with PCE was completed so that subsequent heating of the Systems A and B Hudson columns would lead to thermal desorption of PCE, similar to that at an ISTT site. Flow through both systems was then paused and 30 mL of the KB-1 culture was manually injected into the System A Federal Fine Ottawa sand column via the influent, effluent, and three aqueous sampling ports (6 mL each). After 24 hours, primary and secondary flows were set to Q_P = 0.0198 mL/min and Q_S = 0.0002 mL/min, respectively, and the temperature of the oven housing the Hudson columns was set to 28 °C. Both primary and secondary flow solutions consisted of clean (i.e., PCE-free) synthetic groundwater, but the secondary flow solution also contained 100 mM sulfide to ensure that reducing conditions (1 mM sulfide) were maintained after results from preliminary experiments suggested that little, if any, sulfide remains in the aqueous phase after passing through the Hudson soil column. The resulting total flow (Q_T = 0.02 mL/min) through each Federal Fine Ottawa sand column corresponded to a pore water velocity (v_T) of approximately 15 cm/d, or 1 PV/d. Hudson column temperature was subsequently increased by approximately +2 °C/PV, causing desorption of PCE to the aqueous phase, where it was subject to advective transport downgradient. Heating continued until each Hudson column reached a maximum

temperature of 96 °C. Federal Fine Ottawa sand column temperature was maintained at 21±1 °C for the experiment duration.

Unlike Systems A and B, the Hudson columns in Systems C and D were unheated, so gradual thermal desorption of PCE from the Hudson soil could not be used as the PCE delivery mechanism to the downgradient Federal Fine Ottawa sand columns. Thus, PCE was introduced to Systems C and D downgradient of each Hudson column via the secondary syringe pump. The primary flow (Q_P = 0.018 mL/min) solution consisted of clean synthetic groundwater. The secondary flow (Q_S = 0.002 mL/min) solution consisted of synthetic groundwater with 10 mM sulfide (target 1 mM in column aqueous phase) and 100 – 700 μM PCE. The PCE concentration was increased over the experiment duration to imitate the gradual thermal desorption employed in Systems A and B.

Samples were collected approximately every 3 PVs from the system midpoint and effluent sampling reservoirs to determine pH, ORP, and concentrations of chlorinated ethenes, ethene, and VFAs. Aqueous port samples (1 mL) were also collected periodically to determine aqueous abundances of *Dhc* and reductive dehalogenase (RDase) genes.

4.3.6 Analytical methods

Volatile fatty acids

VFAs were measured using a Thermo Fisher ICS-2100 IC according to the method described in Section 3.3.6.

Permanent gases

Permanent gases were measured using a Hewlett-Packard model 6890 GC equipped with a TCD according to the method described in Section 3.3.6.

Chlorinated ethenes

Chlorinated ethenes and ethene were measured using an Agilent 7890B GC (Agilent, Santa Clara, CA) equipped with a Teledyne Tekmar HT3 Headspace Analyzer (Teledyne Technologies, Thousand Oaks, CA) and a flame ionization detector (FID). A 1 mL aqueous sample was loaded into a 20 mL headspace vial, which was then capped, allowed to equilibrate for 30 minutes at 70 °C, and pressurized to 10 psi. A 1 mL gas sample from the vial was then carried via a 110 °C transfer line to the GC inlet, which was operated at 200 °C in splitless mode, and onto an Agilent DB-624 capillary column with 320 µm mean outer diameter and 60 m length. The GC oven was held at an initial temperature of 60 °C for 4 minutes, followed by a +25 °C/min ramp to 200 °C, which was maintained for 2 minutes until the end of the run. Helium was used as the carrier gas at a flow rate of 3 mL/min, respectively. The FID was operated at 300 °C with air and H_2 flows

of 400 and 30 mL/min, respectively. Helium flowing at 30 mL/min served as the makeup gas. PCE, TCE, and *cis*-DCE calibration standards were prepared by diluting a concentrated stock solution (5,000 – 10,000 µg/mL) of each compound dissolved in methanol. VC and ethene calibration standards were prepared by injecting a known volume of each gas into a sealed 160 mL culture bottle containing 100 mL of 18.2 MΩ water and allowing them to equilibrate overnight. The method detection limit for each chlorinated ethene and ethene was approximately 1 µM.

4.4 Results

4.4.1 VFAs release during thermal treatment of Webster soil in a 90 cm, 1-D column study

The 90 cm Webster soil column experiment was completed to assess electron donor availability downgradient of a heated soil zone in a continuously flowing system. After heating of the upgradient Webster soil began (27 – 38 °C), concentrations of VFAs detected in previous Webster soil batch studies (formate, acetate, propionate, and butyrate) remained below 30 µM for 10 PVs (Figure 4-3, 0 – 10 PVs) in downgradient port and effluent samples. However, once the temperature of the Webster soil zone exceeded 50 °C, pronounced increases in concentrations of acetate (1.7 mM as C) and propionate (0.6 mM as C) were detected in aqueous samples collected from downgradient Port L2 (Figure 4-3, 11 – 12 PVs). These

sharp increases in VFAs concentrations propagated in the direction of flow and were evident to varying extents in aqueous samples collected from Port L3 (Figure 4-4), Port L4 (Figure 4-5), Port L5 (Figure 4-6), Port L6 (Figure 4-7), and the column effluent (Figure 4-8). Subsequent stepwise increases in the temperature of the upgradient Webster soil (+10 °C/3.3 PVs) led to similar increases in downgradient VFAs concentrations. In samples collected from Port L4, for example, each subsequent temperature increase was associated with an increase in total VFAs concentration of 1.5 – 1.6 mM as carbon (Figure 4-5, 15 – 24 PVs). However, each increase in VFAs concentrations was followed by an immediate (e.g., acetate) or gradual (e.g., propionate) decline of up to 1.3 mM total VFAs as carbon (Figure 4-5, 19 – 22 PVs) until the temperature was increased again. Acetate was the most abundant VFA detected in aqueous port and effluent samples, with a maximum concentration of 3.3 mM (as carbon) observed immediately after the upgradient Webster soil temperature was increased to 72 °C (Figure 4-3, 17 PVs). The final increase in VFAs concentrations occurred at 24 PVs, approximately 3 PVs after the temperature of the upgradient Webster soil was increased to 82 °C (Figure 4-5, 21 – 24 PVs). This increase was associated with the highest concentration of total VFAs (4.6 mM as carbon) measured during the experiment, as well as the highest concentration of butyrate (0.3 mM as carbon). The stepwise decrease in upgradient temperature (-10 °C/3.3 PVs) back to the 22 °C ambient temperature did not promote any further releases of VFAs, and concentrations of individual and total VFAs decreased to pre-heating levels (approximately 30 µM

or less) in all subsequent port and effluent samples until experiment termination at 52 PVs.

Over the course of the entire experiment, acetate represented 68 – 74% (as carbon) of overall total VFAs detected in Ports L2 – L6 (Table 4-2). Propionate was the second most abundant VFA, accounting for 25 – 29% (as carbon) of the overall totals in Ports L2 – L6. Formate and butyrate were detected only at low concentrations throughout the experiment (0 – 3% of overall total VFAs as carbon).

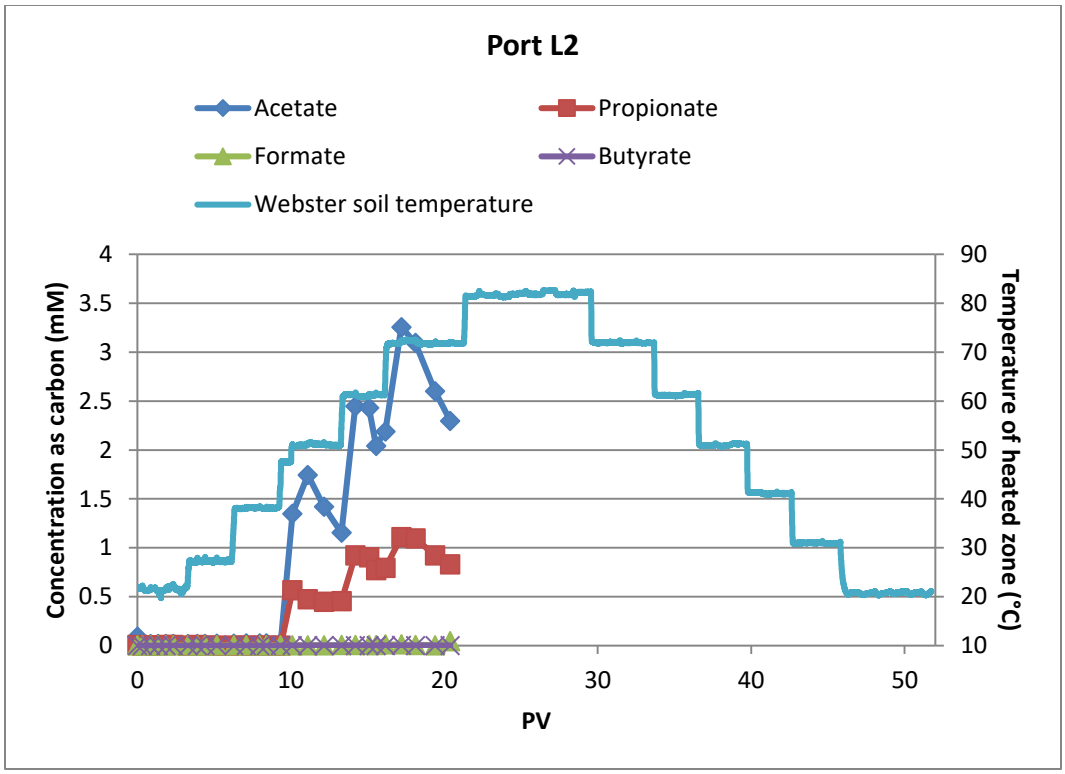

Figure 4-3: Temperature profile of upgradient heated Webster soil zone and resulting concentrations of VFAs in aqueous samples collected from Port L2 of the 90 cm Webster soil thermal column. VFAs data are unavailable beyond 21 PVs due to clogging of Port L2.

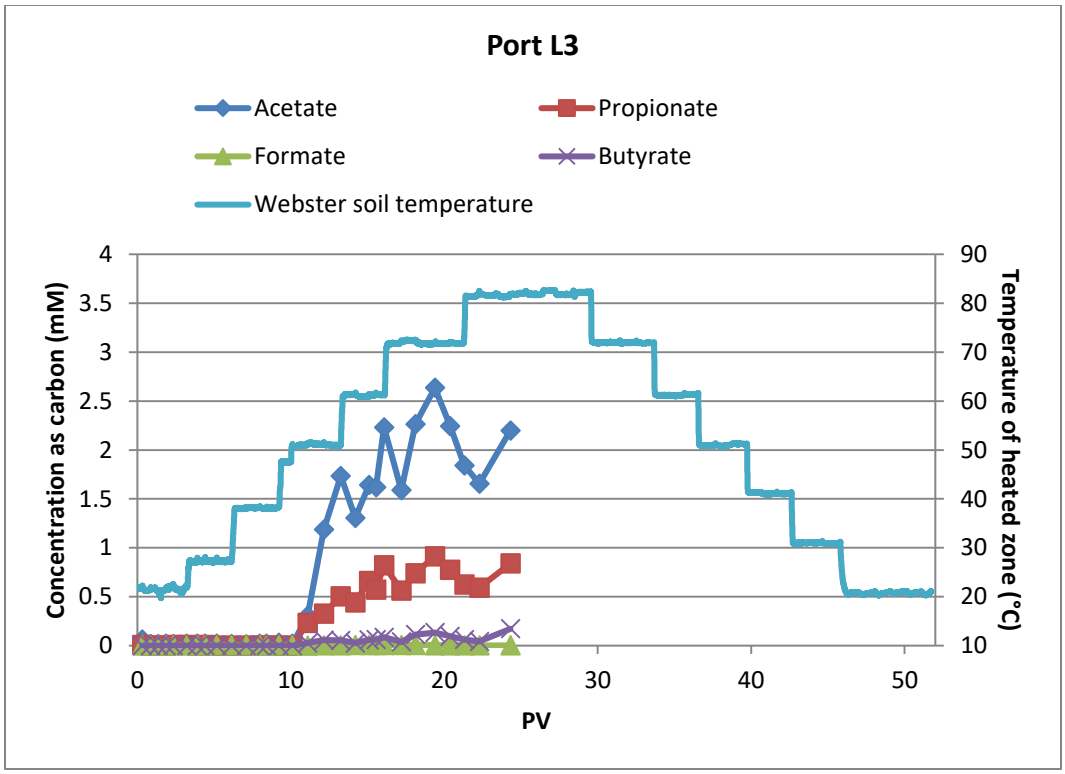

Figure 4-4: Temperature profile of upgradient heated Webster soil zone and resulting concentrations of VFAs in aqueous samples collected from Port L3 of the 90 cm Webster soil thermal column. VFAs data are unavailable beyond 24 PVs due to clogging of Port L3.

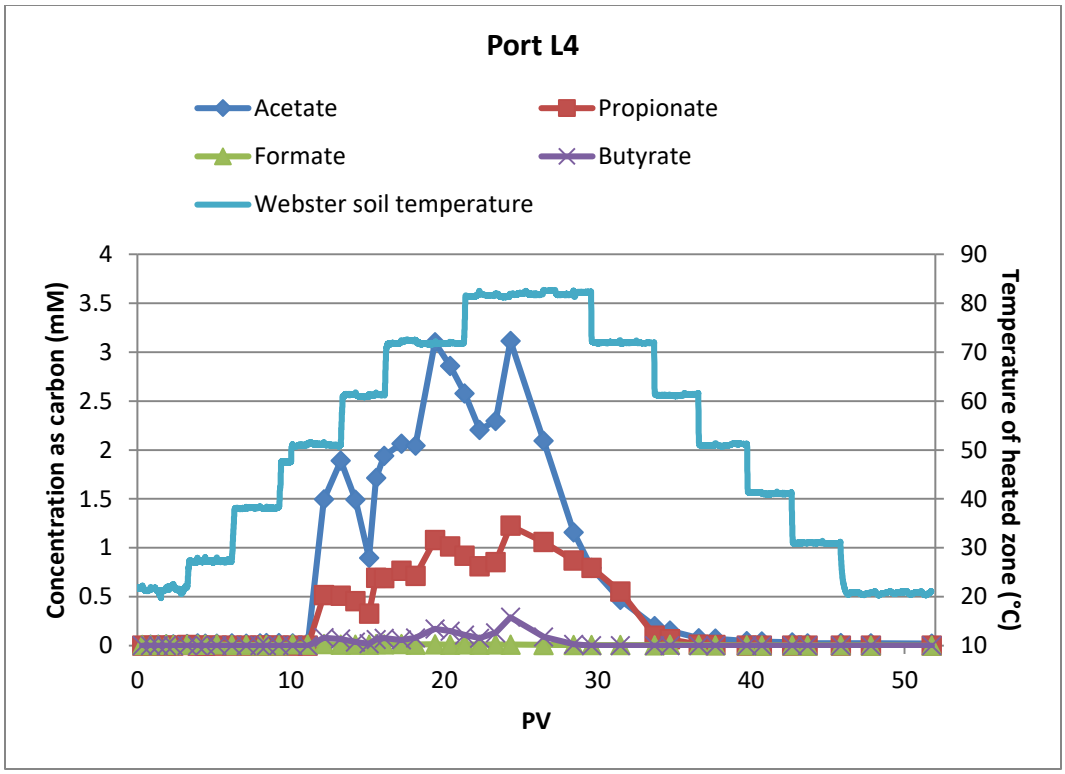

Figure 4-5: Temperature profile of upgradient heated Webster soil zone and resulting concentrations of VFAs in aqueous samples collected from Port L4 of the 90 cm Webster soil thermal column.

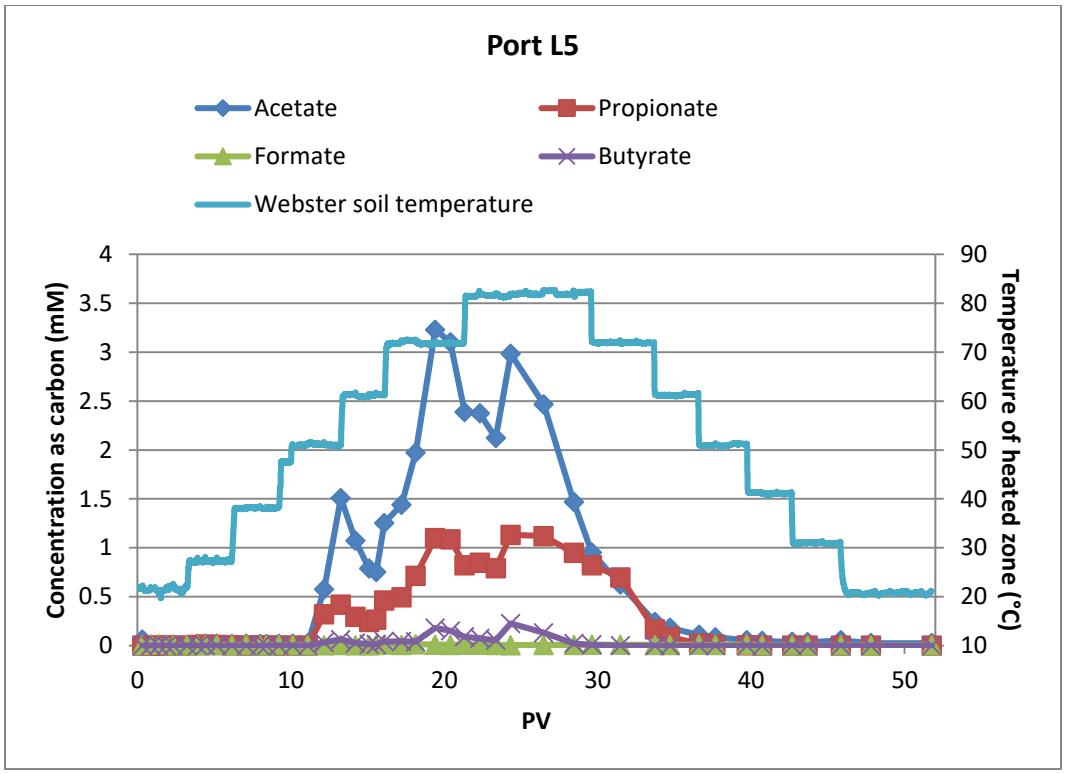

Figure 4-6: Temperature profile of upgradient heated Webster soil zone and resulting concentrations of VFAs in aqueous samples collected from Port L5 of the 90 cm Webster soil thermal column.

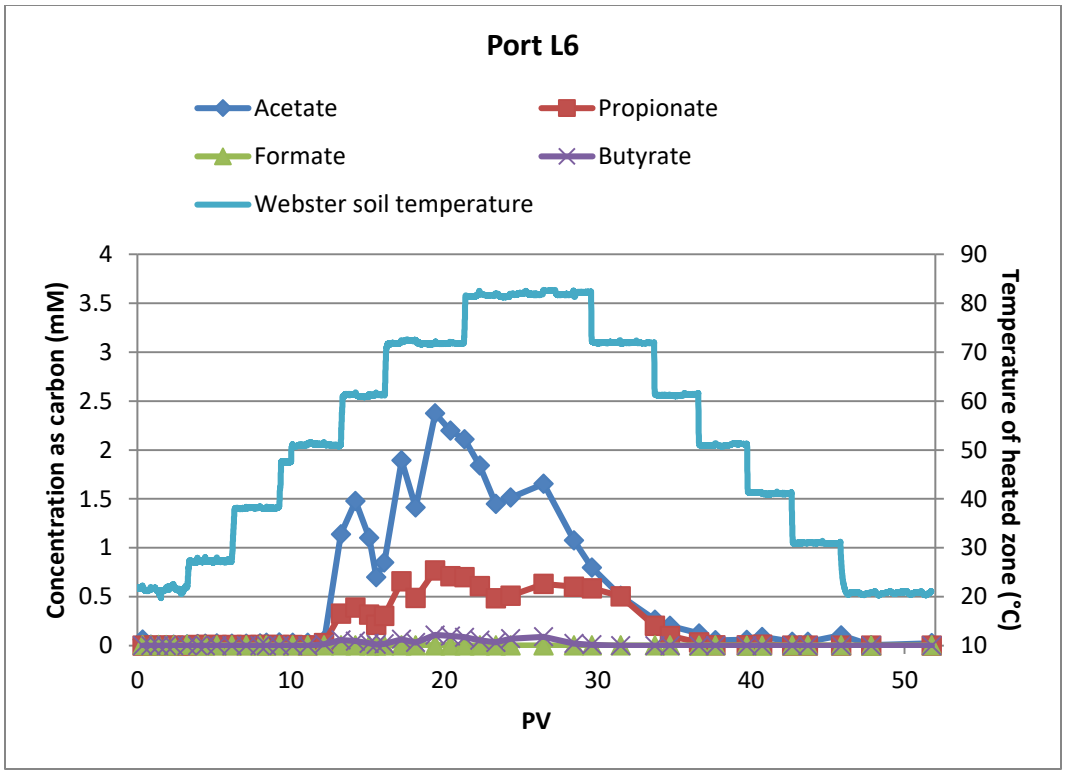

Figure 4-7: Temperature profile of upgradient heated Webster soil zone and resulting concentrations of VFAs in aqueous samples collected from Port L6 of the 90 cm Webster soil thermal column.

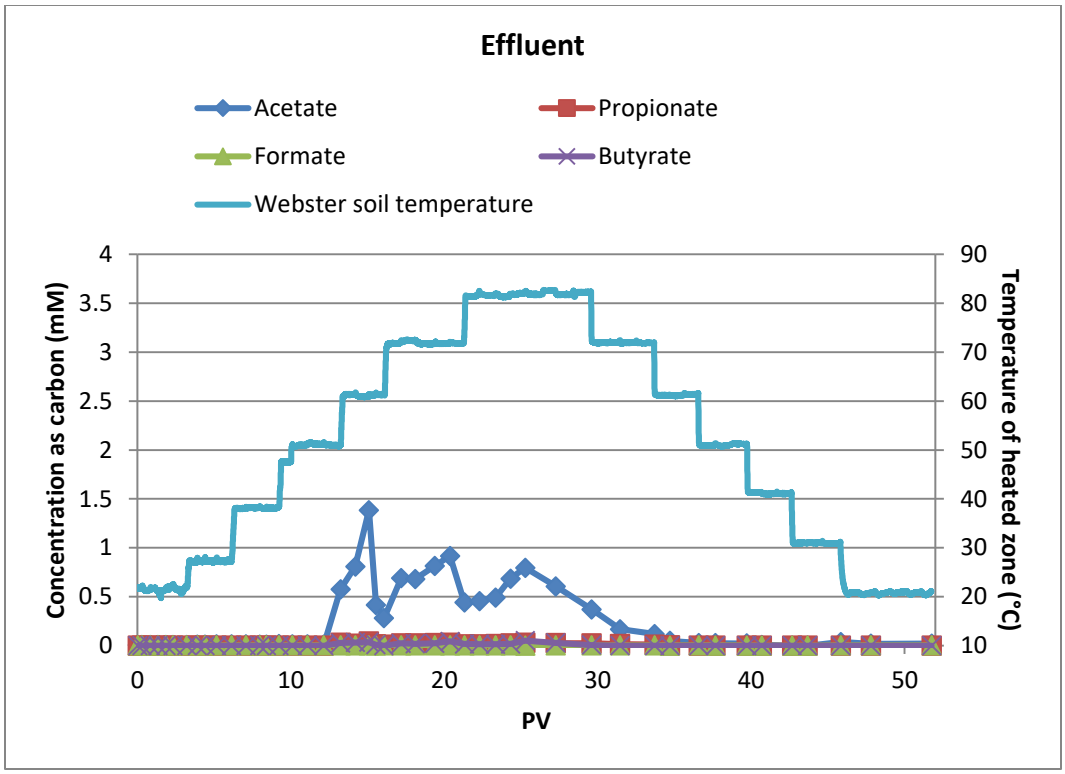

Figure 4-8: Temperature profile of upgradient heated Webster soil zone and resulting concentrations of VFAs in aqueous samples collected the effluent of the 90 cm Webster soil thermal column.

Table 4-2: Individual VFAs detected in Ports L2 – L3 and effluent samples as percentage (% as carbon) of total overall VFAs detected.

	Port L2	Port L3	Port L4	Port L5	Port L6	Effluent
Formate	0	0	1	1	0	1
Acetate	74	72	68	68	70	93
Propionate	26	25	29	29	27	4
Butyrate	0	3	3	3	2	3
Sum	100	100	100	100	100	100

In addition to VFAs, H_2 and CH_4 were detected in samples collected from a gas phase that developed in the vicinity of Port U2 within 1 PV after the final temperature increase to 82 °C. The initial gas sample contained 0.10 vol% H_2 and 14.0 vol% CH_4 (Figure 4-9, 22 PVs). The concentration of H_2 decreased rapidly to 0.01 vol% and did not exceed that value again before 42 PVs, when collection of gas samples from Port U2 was no longer possible. CH_4 production continued, however, reaching a maximum concentration of 68.4 vol% after 36 PVs and a final concentration of 58.7 vol% after 42 PVs (Figure 4-9, 36 – 42 PVs), consistent with methanogenic activity observed in Webster soil batch studies (Chapter 3). The final decline in CH_4 concentration and disappearance of the gas phase coincided with the return of VFAs concentrations to below the 30 μM baseline observed during the initial 10 PVs of the experiment (Figure 4-5, 36 – 42 PVs).

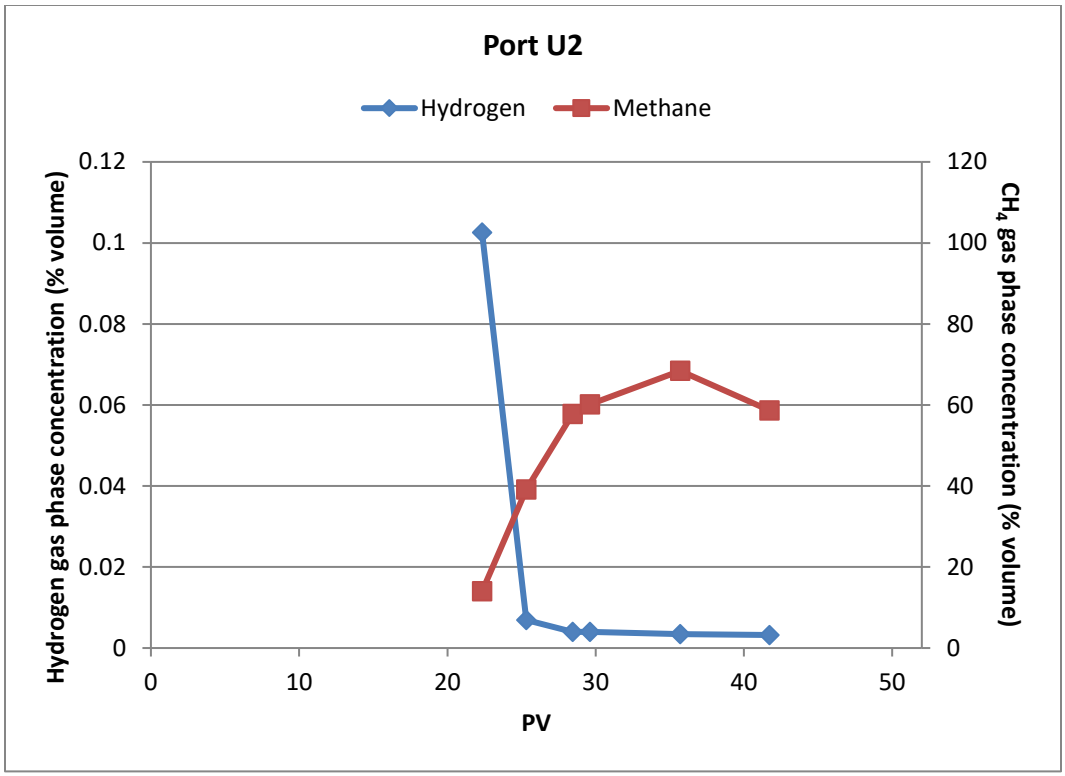

Figure 4-9: Concentrations of H_2 and CH_4 in gas samples collected from Port U2 of the 90 cm Webster soil thermal column. Note that gas samples were not collected with regular frequency until a gas phase formed in the column upon temperature increase of the upgradient Webster soil to 82 °C.

4.4.2 Hudson soil column, System A: Heating with bioaugmentation

Unlike the 90 cm Webster soil column study, the series of four Hudson soil column studies incorporated a contaminant (Systems A – D) and dechlorinating bacteria (Systems A and C) to determine whether thermally-released electron donor sources (e.g., VFAs) were capable of supporting microbial reductive dechlorination of chlorinated ethenes. System A consisted of a Hudson soil column initially loaded with approximately 135 µmol PCE, and a downgradient Federal Fine Ottawa sand column inoculated with the PCE-to-ethene dechlorinating KB-1® culture. The inoculating culture contained 4.2±0.6 × 10^8 *Dhc* 16S rRNA gene copies/mL, 8.9±2.6 × 10^8 *vcrA* gene copies/mL, and 3.9±0.7 × 10^6 *bvcA* gene copies/mL. Subtracting cells that were immediately washed out during inoculation, initial aqueous abundances of *Dhc* 16S rRNA, *vcrA*, and *bvcA* in the Federal Fine Ottawa sand column were 2.3±0.5 × 10^8, 5.8±2.6 × 10^8, and 2.1±0.6 × 10^8 gene copies/mL, respectively. The *tceA* gene was not detected in the System A inoculating culture nor any subsequent aqueous- or solid-phase samples. The inoculating culture also contained 49±2 µM ethene, but chlorinated ethenes were not detected.

Following bioaugmentation of the Federal Fine Ottawa sand column with the KB-1® culture and initiation of the Hudson column heating regime (+2 °C/PV), concentrations of VFAs at the System A midpoint (between the Hudson soil and Federal Fine Ottawa sand columns, Figure 4-2f) remained below the 1 µM detection limit until the Hudson column temperature reached 43 °C (Figure 4-10,

14 PVs). At that point, formate (0.1 mM as C), acetate (2.8 mM as C), propionate (1.5 mM as C), butyrate (1.0 mM as C), and isovalerate (0.8 mM as C) were detected. Subsequent aqueous samples contained VFAs at similar relative ratios (i.e., acetate > propionate > butyrate and isovalerate > formate). Following initial detection, total VFAs concentration in the System A midpoint declined to a minimum of 3.0 mM as C, but then steadily increased to a maximum of 10.6 mM as C as the Hudson column temperature rose from 43 to 78 °C (Figure 4-10, 19 – 30 PVs). All subsequent concentrations of total VFAs at the System A midpoint were between 4.7 and 7.8 mM as C, despite continued increases in the Hudson column temperature from 78 to 96 °C (Figure 4-10, 30 – 45 PVs). At the experiment conclusion, the overall total of VFAs measured in the System A midpoint sampling bulb was 6.6 mmol (as carbon), of which acetate accounted for 59%, propionate accounted for 25%, butyrate and isovalerate accounted for 7% each, and formate accounted for 2%.

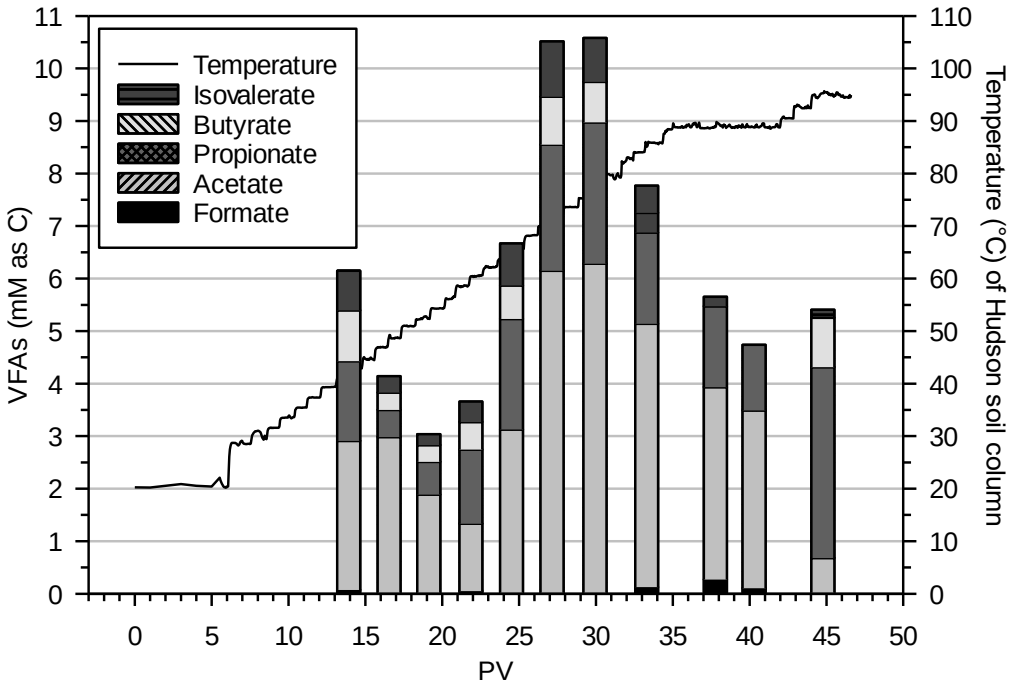

Figure 4-10: Temperature profile of the Hudson soil column and concentrations of VFAs measured in aqueous samples collected from the System A (heated with bioaugmentation) midpoint.

Unlike VFAs, chlorinated ethenes were detected in System A midpoint aqueous samples immediately after heating began. PCE and TCE reached maximum concentrations of 45±1 and 54±1 μM (Figure 4-11, 11 PVs), respectively, before giving way to *cis*-DCE (79±6 μM) after 14 PVs. The concentration of *cis*-DCE at the System A midpoint reached a maximum of 162±3 μM after 17 PVs, corresponding to a Hudson column temperature of 49 °C, and accounting for 95 mol% of PCE and its daughter products at that point. Total System A midpoint chlorinated ethene concentrations declined over the remaining 30 PVs of the experiment (Figure 4-11, 17 – 47 PVs), but *cis*-DCE remained the most abundant PCE daughter product, accounting for 75% of overall chlorinated ethene mass.

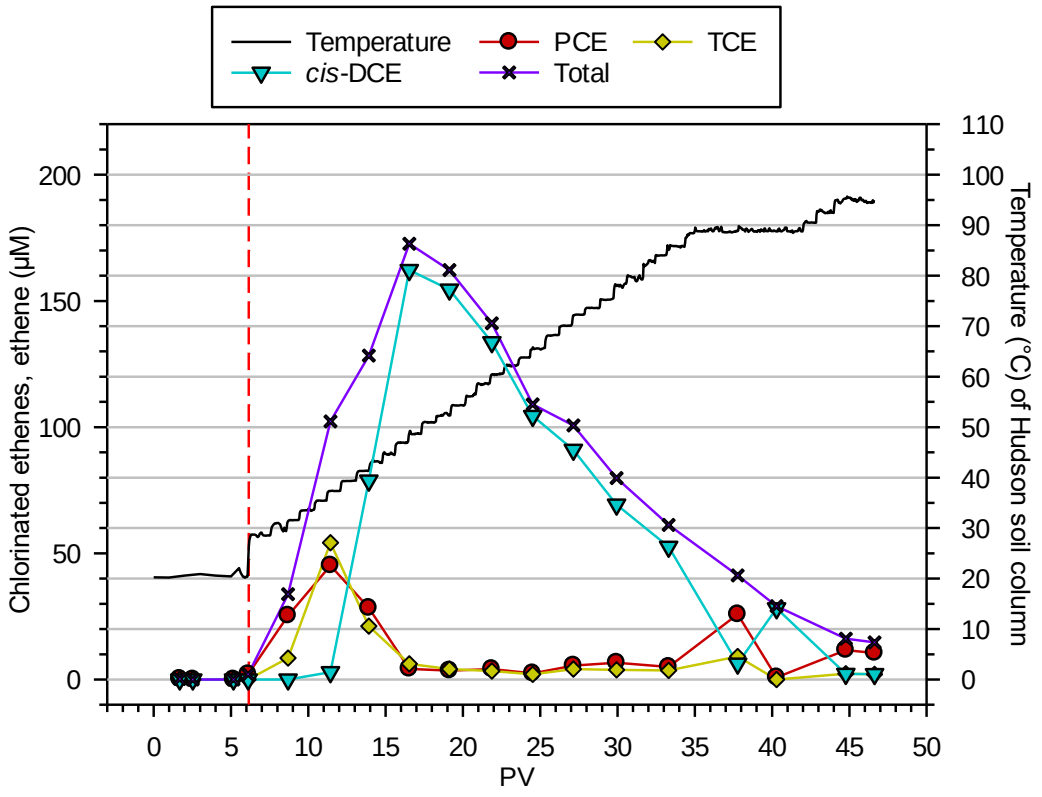

Figure 4-11: Temperature profile of the Hudson soil column and concentrations of chlorinated ethenes measured in aqueous samples collected from the System A (heated with bioaugmentation) midpoint. Dashed vertical red line indicates bioaugmentation of the Federal Fine Ottawa sand column A with KB-1®.

Concentrations of VFAs in the System A effluent were similar to those in midpoint samples. Total VFAs concentrations were lowest (2.7 mM as C) after 21 PVs and highest (9.7 mM as C) after 31 PVs (Figure 4-12). Overall, the total mass of VFAs detected in the System A effluent was 6.2 mmol as carbon, of which acetate accounted for 63%, followed by propionate (22%), butyrate and isovalerate (7% each), and formate (1%). Total overall VFAs mass was 6% lower (as C) in System A effluent samples than in midpoint samples.

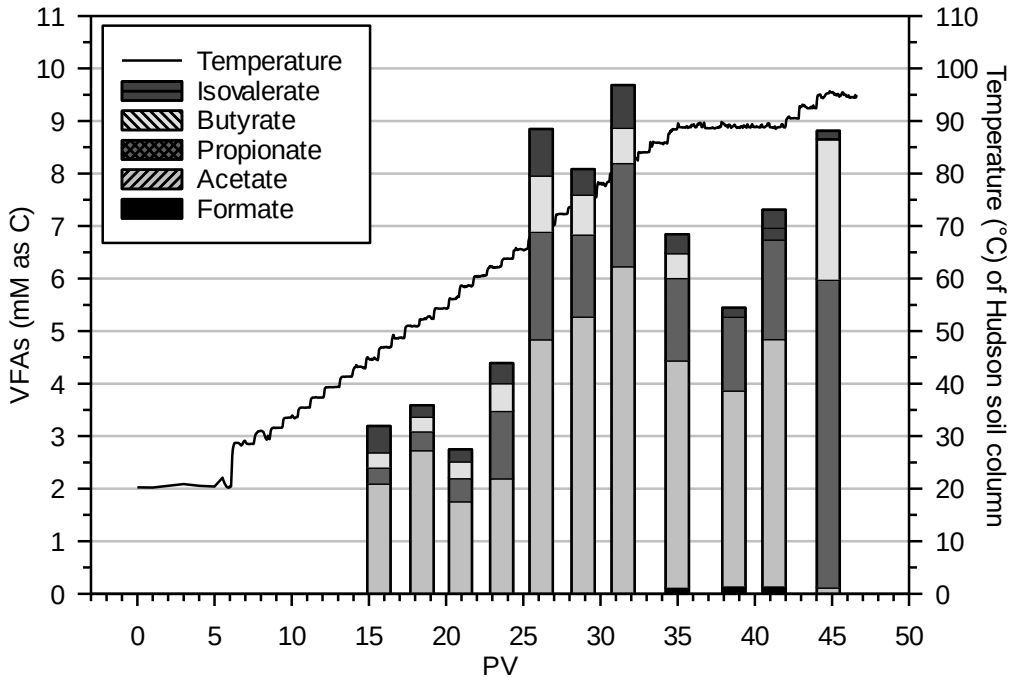

Figure 4-12: Temperature profile of the Hudson soil column and concentrations of VFAs measured in aqueous samples collected from the System A (heated with bioaugmentation) effluent.

The initial post-bioaugmentation sample of the System A effluent contained 38±1 μM of ethene (Figure 4-13, 8 PVs), which accounted for 100 mol% of PCE daughter product mass at that point and likely reflected the mass introduced to the Federal Fine Ottawa sand column with the KB-1® culture. However, sustained dechlorination to VC and ethene was evident as the Hudson column temperature was increased, providing a continued source of bioavailable substrates. The greatest total concentration of PCE and its daughter products was 157±4 μM (Figure 4-13, 18 PVs), consisting of 58 mol% *cis*-DCE, 23 mol% VC, and 18 mol% ethene, and corresponding to a Hudson column temperature of 53 °C. At that point, PCE and PCE daughter products measured in the effluent accounted for a cumulative total of 26 mol% of PCE initially loaded to the Hudson soil column. Concentrations of total chlorinated ethenes and ethene declined in subsequent effluent samples as the Hudson column temperature was raised by +2 °C/PV to 96 °C and the sorbed PCE mass was gradually depleted (Figure 4-13, 18 – 47 PVs). During this period, effluent VC and ethene concentrations declined from 36±1 and 29±1 μM, respectively, to below the 1 μM detection limit for those compounds (Figure 4-13, 18 – 29 PVs). Although VC concentrations remained below the detection limit, the final 16 PVs of the experiment were characterized by a decrease in *cis*-DCE effluent concentrations and a resurgence of ethene formation (Figure 4-13, 31 – 47 PVs). Ethene surpassed *cis*-DCE as the primary PCE degradation product after 39 PVs and accounted for 47 – 60 mol% of total products in all subsequent effluent samples. Ethene accounted for a cumulative 23 mol% of effluent product mass over

the duration of the experiment. The overall mass balance of chlorinated ethenes and ethene in System A (heated and bioaugmented) was 106%.

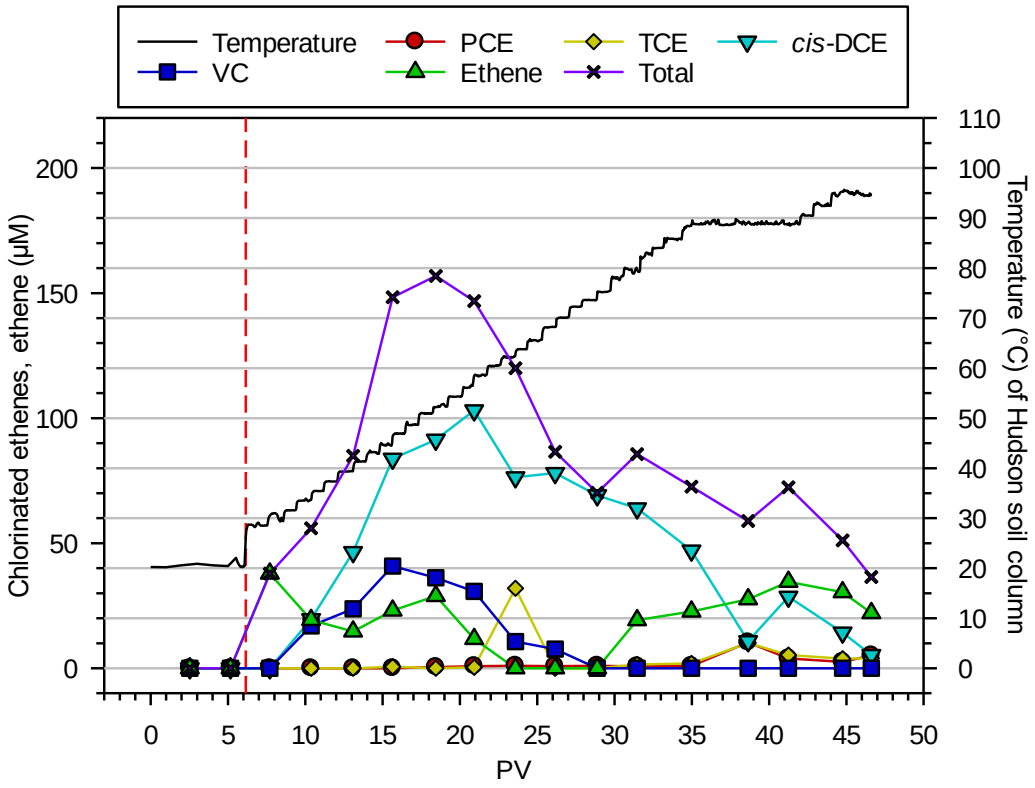

Figure 4-13: Temperature profile of the Hudson soil column and concentrations of chlorinated ethenes and ethene measured in aqueous samples collected from the System A (heated with bioaugmentation) effluent. Dashed vertical red line indicates bioaugmentation of the Federal Fine Ottawa sand column A with KB-1®.

Abundances of the *Dhc* 16S rRNA, *vcrA*, and *bvcA* genes were approximately two orders of magnitude lower in initial aqueous port samples (Figure 4-14, PV = 11) than immediately post-bioaugmentation (i.e., cells retained during column inoculation), with maximum abundances of $8.2\pm1.1 \times 10^6$, $1.5\pm0.4 \times 10^7$, and $1.1\pm0.0 \times 10^5$ gene copies/mL, respectively (Figure 4-14 , PV = 11). Aqueous abundances of each gene remained steady or declined over the course of the experiment. At experiment termination, final aqueous abundances were $2.1\pm0.2 \times 10^5 – 3.9\pm1.0 \times 10^5$ *Dhc* 16S rRNA gene copies/mL, $1.3\pm0.3 \times 10^5 – 7.0\pm0.2 \times 10^5$ *vcrA* gene copies/mL, and $3.1\pm0.4 \times 10^4 – 4.9\pm0.3 \times 10^4$ *bvcA* gene copies/mL (Figure 4-14, PV = 48).

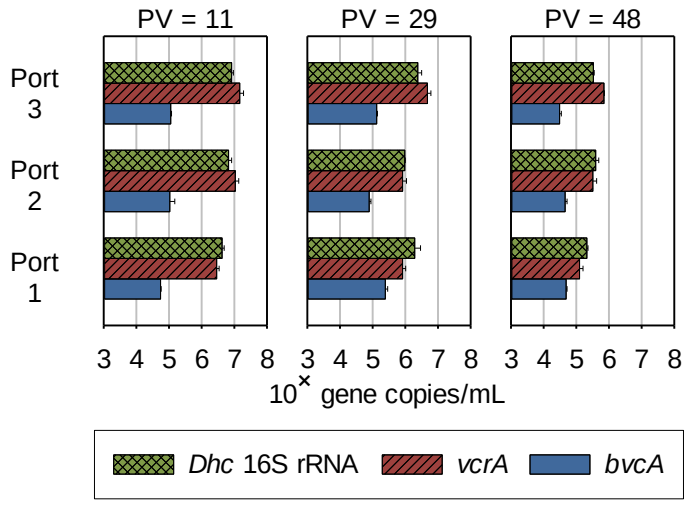

Figure 4-14: *Dhc* 16S rRNA and RDase gene abundances in aqueous port samples collected from Federal Fine Ottawa sand column A.

4.4.3 Hudson soil column, System B: Heating without bioaugmentation

System B consisted of a Hudson soil column initially loaded with approximately 135 µmol PCE, and a downgradient, non-bioaugmented Federal Fine Ottawa sand column. Abundances of the *Dhc* 16S rRNA, *vcrA*, and *bvcA* genes were below the detection limit in System B over the course of the experiment, confirming that no *Dhc* strains were present at any time during the experiment.

Similar to System A, VFAs were not detected in System B midpoint aqueous samples until the System B Hudson column temperature reached 43 °C, when the total VFAs concentration was 5.0 mM as carbon (Figure 4-15, 14 PVs). Relative concentrations of each VFA were also similar to System A midpoint samples, but butyrate (11% as carbon) and isovalerate (9% as carbon) were more highly represented in System B midpoint samples, while acetate was slightly less prevalent (54% as carbon). However, after reaching a maximum concentration of 9.7 mM as carbon, total VFAs at the System B midpoint fell sharply to 0.2 mM as carbon, remaining below that concentration for the duration of the experiment (Figure 4-15, 27 – 47 PVs).

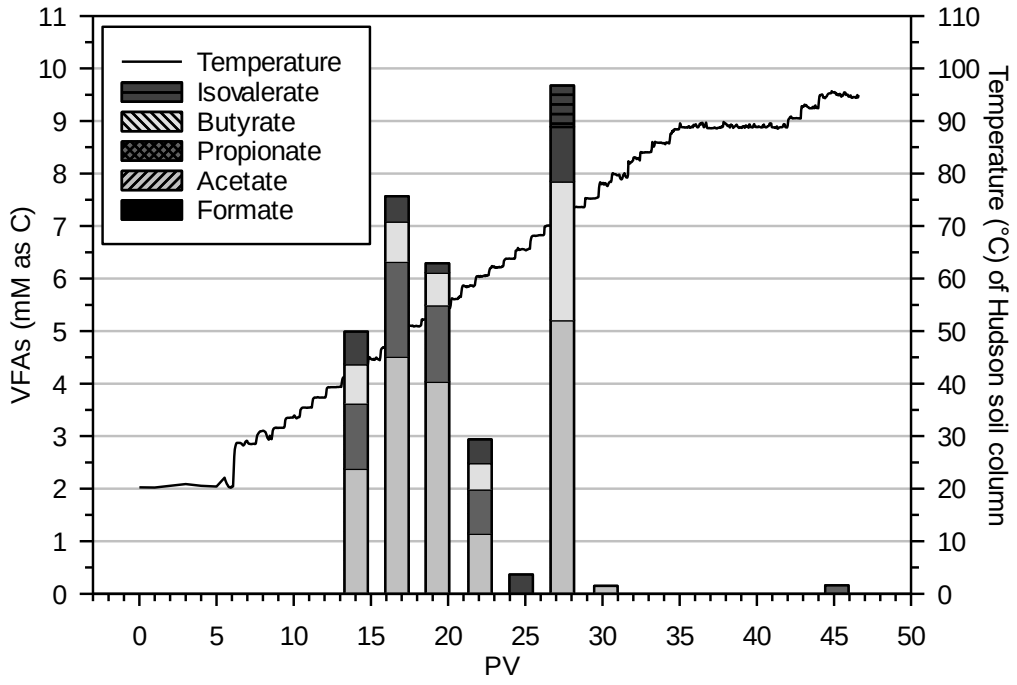

Figure 4-15: Temperature profile of the Hudson soil column and concentrations of VFAs measured in aqueous samples collected from the System B (heated without bioaugmentation) midpoint.

Chlorinated ethenes were detected at the System B midpoint during the first sampling event and throughout the experiment. TCE was initially the dominant compound, peaking at 93±4 µM (Figure 4-16, 14 PVs) before being surpassed by PCE (Figure 4-16, 22 PVs), which itself reached a maximum of 125±3 µM and remained the primary chlorinated ethene in System B midpoint samples until experiment termination. PCE and TCE accounted for 63 and 37 mol% of total detected chlorinated ethenes, respectively. Unlike in System A, no *cis*-DCE was detected at the System B midpoint. These results were consistent with those from Hudson soil microcosm studies (data not shown), wherein microorganisms native to the Hudson soil were capable of reducing PCE to TCE at 40, 50, and 60 °C, but not at 25 °C.

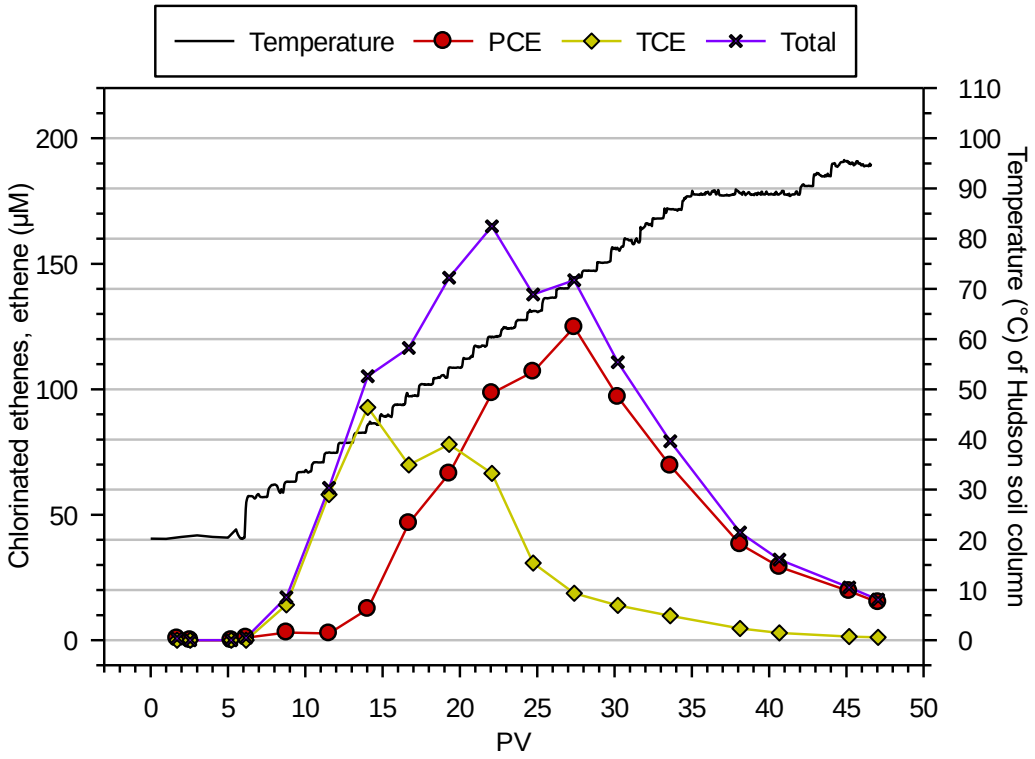

Figure 4-16: Temperature profile of the Hudson soil column and concentrations of chlorinated ethenes and ethene measured in aqueous samples collected from the System B (heated without bioaugmentation) midpoint.

Concentrations of VFAs and chlorinated ethenes detected in the System B effluent samples mirrored those in midpoint samples. VFAs were present in System B effluent samples between 13 and 29 PVs (Figure 4-17), after which concentrations remained below 0.2 mM as C for the experiment duration. Overall mass distribution of VFAs (as carbon) was similar to System B midpoint samples (52% acetate, 26% propionate, 12% butyrate, 10% isovalerate, 0% formate). Similarly, the breakthrough profiles of chlorinated ethenes in the System B effluent were nearly identical to midpoint concentrations, with no indication that further dechlorination beyond TCE had taken place within the non-bioaugmented Federal Fine Ottawa sand column (Figure 4-18). PCE and TCE accounted for 61 and 39 mol%, respectively, of total chlorinated ethenes detected in the System B effluent. The overall mass balance of chlorinated ethenes in System B (heated and non-bioaugmented) was 80%.

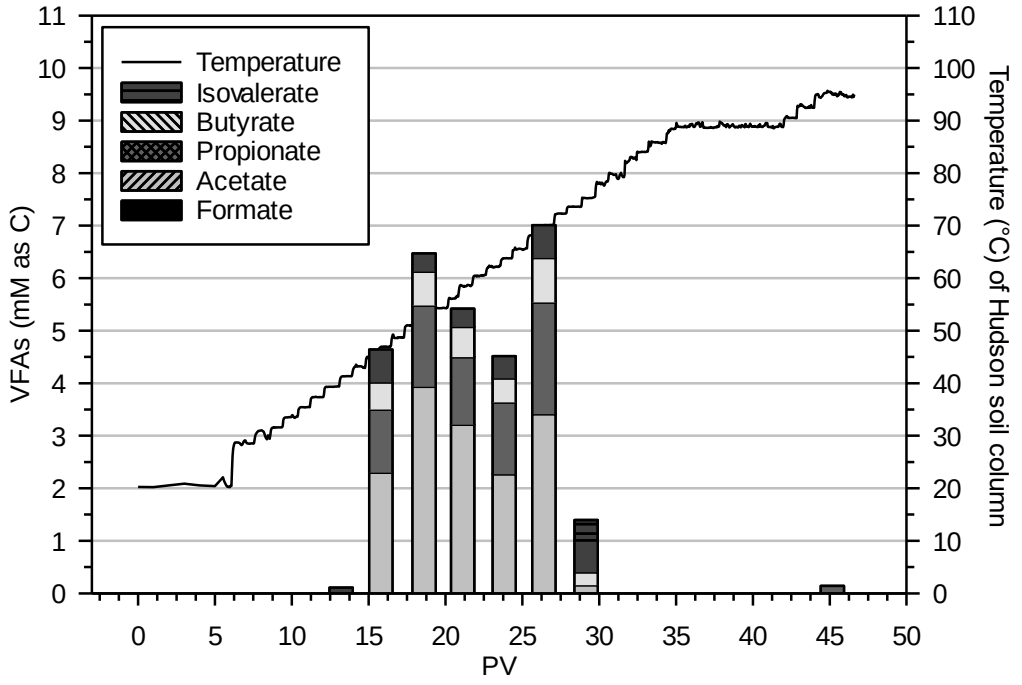

Figure 4-17: Temperature profile of the Hudson soil column and concentrations of VFAs measured in aqueous samples collected from the System B (heated without bioaugmentation) effluent.

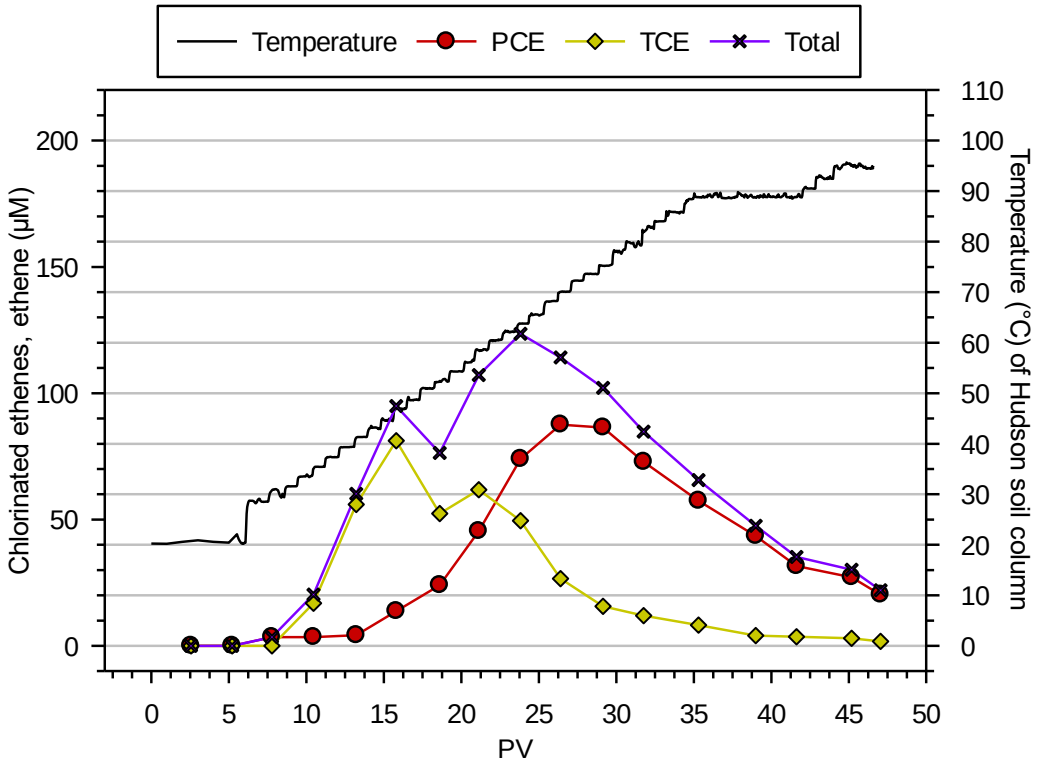

Figure 4-18: Temperature profile of the Hudson soil column and concentrations of chlorinated ethenes measured in aqueous samples collected from the System B (heated without bioaugmentation) effluent.

4.4.4 Hudson soil columns, System C: Bioaugmentation without heating and System D: Unheated, non-bioaugmented control

System C consisted of an unheated Hudson soil column, and a downgradient Federal Fine Ottawa sand column inoculated with the PCE-to-ethene dechlorinating KB-1® culture. The inoculating culture contained $6.7\pm1.2 \times 10^7$ *Dhc* 16S rRNA gene copies/mL, $7.1\pm0.7 \times 10^7$ *vcrA* gene copies/mL, and $3.8\pm0.5 \times 10^6$ *bvcA* gene copies/mL. Subtracting cells that were immediately washed out during inoculation, initial aqueous abundances of *Dhc* 16S rRNA, *vcrA*, and *bvcA* retained in the Federal Fine Ottawa sand column were $6.3\pm1.2 \times 10^7$, $6.7\pm0.7 \times 10^7$, and $3.5\pm0.5 \times 10^6$ gene copies/mL, respectively. The *tceA* gene was not detected in the System C inoculating culture nor any subsequent samples. The inoculating culture contained 14±1 µM ethene and no chlorinated ethenes. System D was identical to System C, but the downgradient Federal Fine Ottawa sand column was not bioaugmented with the KB-1® culture. Abundances of the *Dhc* 16S rRNA, *vcrA*, and *bvcA* genes were below the detection limit in aqueous port samples collected throughout the experiment in System D, confirming that no *Dhc* strains were present at any time during the experiment.

No VFAs were detected in midpoint or effluent samples at any time during operation of Systems C and D, consistent with the lack of heating of the upgradient Hudson soil columns. PCE was detected in aqueous midpoint samples at gradually increasing concentrations of 6 – 59 µM (Figure 4-19) and 10 – 66 µM (Figure 4-20)

in Systems C and D, respectively, consistent with efforts to mimic the thermal desorption of PCE from the Hudson soil in Systems A and B.

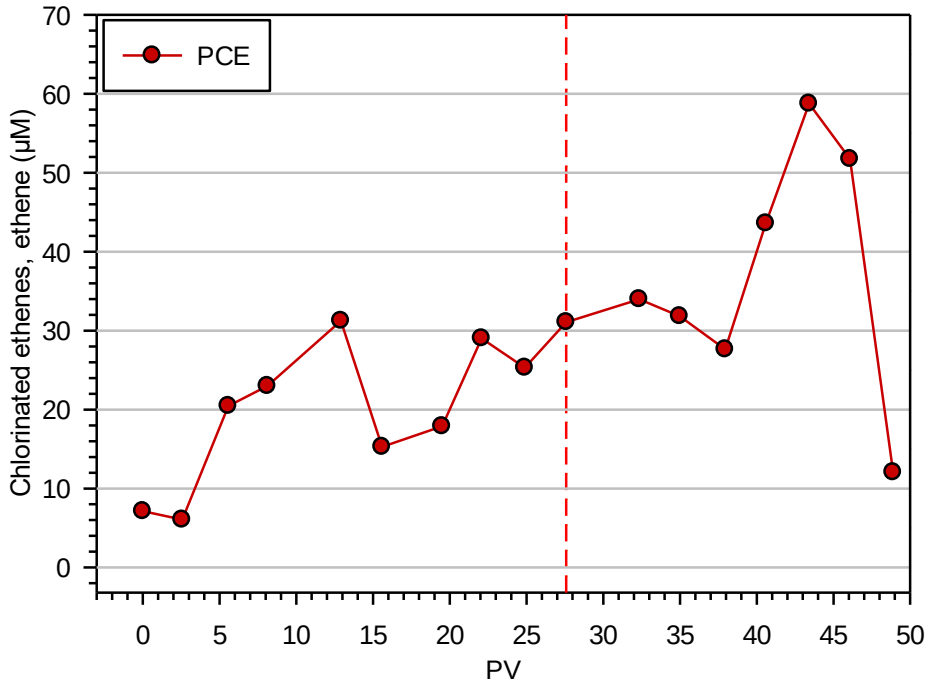

Figure 4-19: Concentrations of chlorinated ethenes measured in aqueous samples collected from the System C (unheated with bioaugmentation) midpoint. Dashed vertical red line indicates bioaugmentation of the Federal Fine Ottawa sand column C with KB-1®.

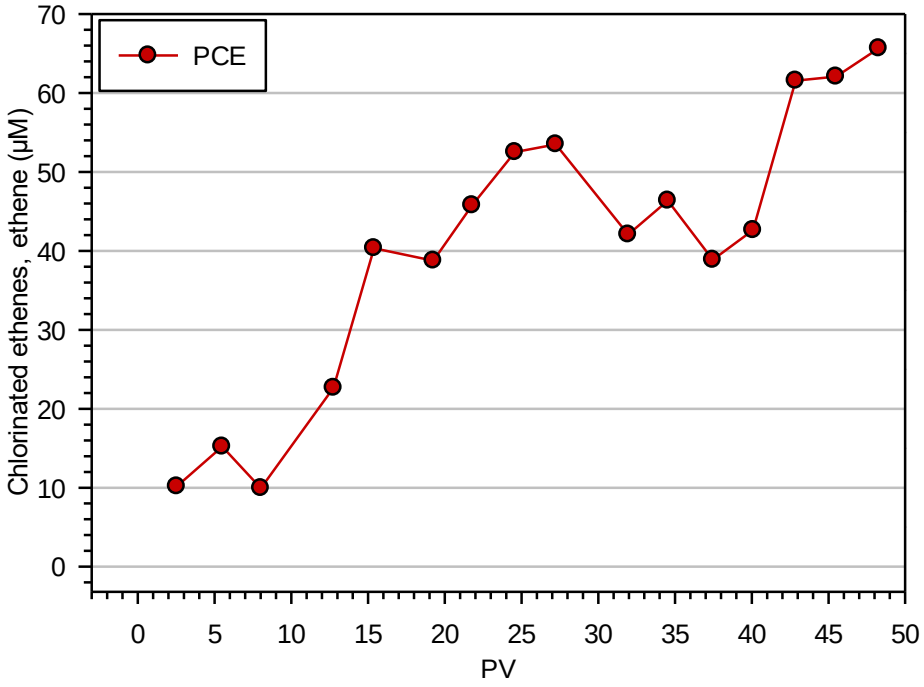

Figure 4-20: Concentrations of chlorinated ethenes measured in aqueous samples collected from the System D (unheated without bioaugmentation) midpoint.

Chlorinated ethenes were immediately detected in the System C effluent following bioaugmentation of the Federal Fine Ottawa sand column as PCE (1±0 µM), cis-DCE (14±0 µM), VC (8±0 µM), and ethene (9±0 µM) (Figure 4-21, 32 PVs). *Cis*-DCE was the primary degradation product over the remainder of the experiment, accounting for 44 – 63 mol% of total chlorinated ethenes, followed by VC (27 – 36 mol%). Ethene was detected in all post-bioaugmentation effluent samples, but accounted for only 14 mol% of total chlorinated ethenes and ethene mass detected in the System C effluent (Figure 4-21, 27 – 49 PVs). The overall mass balance of chlorinated ethenes and ethene System C (unheated and bioaugmented) was 97% (98% post-bioaugmentation). Only PCE was detected in the System D effluent, with no evidence that any dechlorination took place (Figure 4-22). The overall mass balance of PCE in System D (unheated and non-bioaugmented) was 76%.

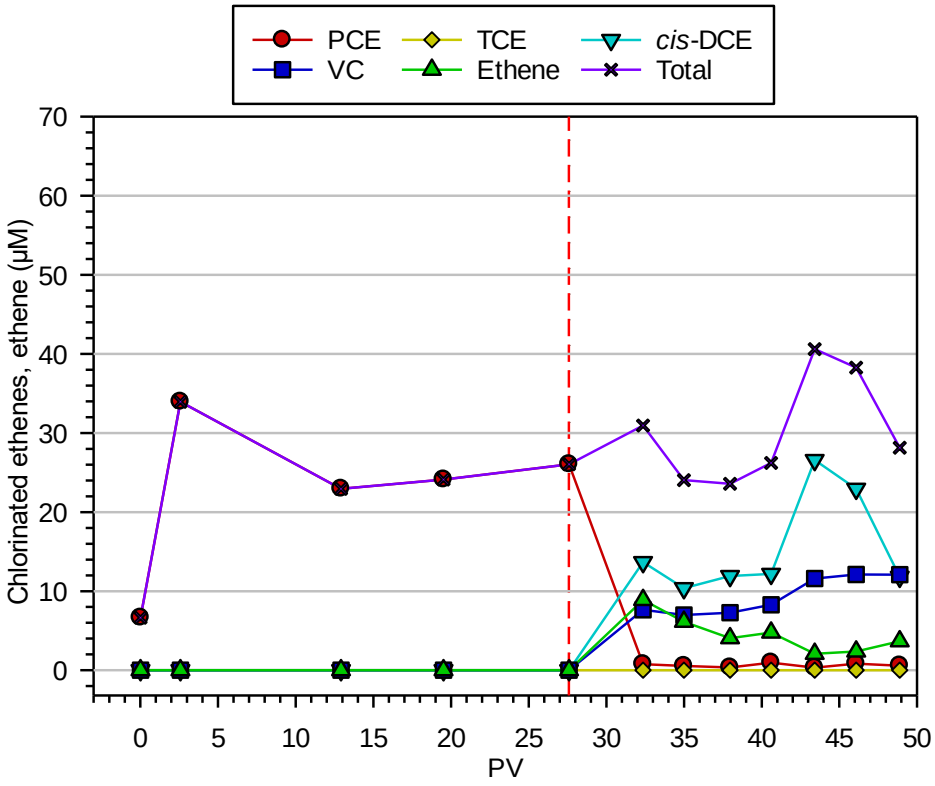

Figure 4-21: Concentrations of chlorinated ethenes and ethene measured in aqueous samples collected from the System C (unheated with bioaugmentation) effluent. Dashed vertical red line indicates bioaugmentation of the Federal Fine Ottawa sand column C with KB-1®.

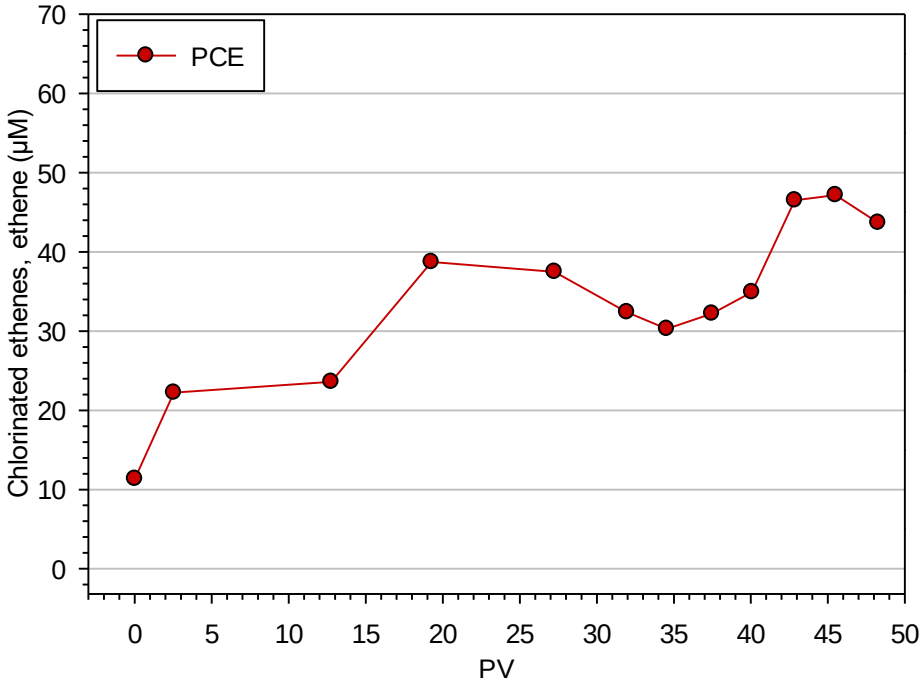

Figure 4-22: Concentrations of chlorinated ethenes measured in aqueous samples collected from the System D (unheated without bioaugmentation) effluent.

In initial aqueous port samples collected from Federal Fine Ottawa sand column C, the *Dhc* 16S rRNA gene was present at $1.7\pm0.4 \times 10^6$ – $3.7\pm0.5 \times 10^6$ gene copies/mL, the *vcrA* gene was present at $2.1\pm0.3 \times 10^6$ – $3.8\pm1.0 \times 10^6$ gene copies/mL, and the *bvcA* gene was present at $8.5\pm0.4 \times 10^4$ – $1.8\pm0.2 \times 10^4$ gene copies/mL (Figure 4-23, PV = 39). These gene abundances remained consistent throughout the experiment. Upon experiment termination, average abundances of the *Dhc* 16S rRNA and *vcrA* genes had increased by less than one order of magnitude, while average abundance of the *bvcA* gene had increased by 1.1 orders of magnitude.

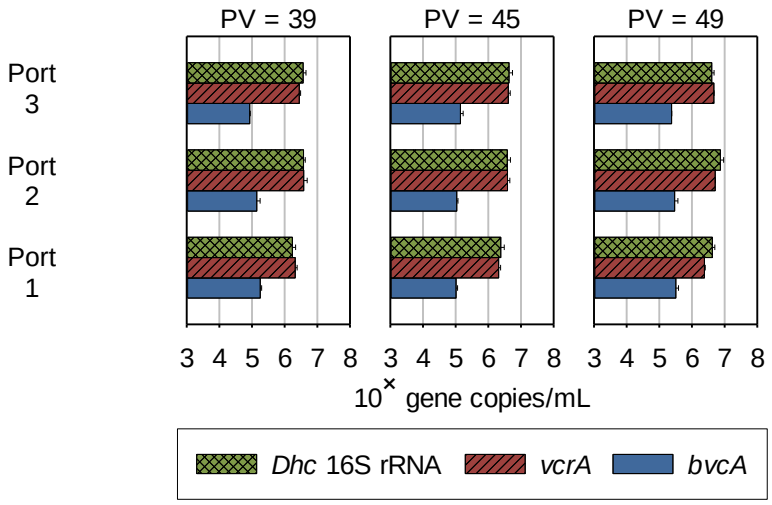

Figure 4-23: *Dhc* 16S rRNA and RDase gene abundances in aqueous port samples collected from Federal Fine Ottawa sand column C.

4.5 Discussion

4.5.1 Impacts of heating regime on VFAs release

Results from the Webster soil column experiment and the four Hudson soil column experiments confirmed findings from previous studies described in Chapter 3, but also revealed phenomena that were not readily apparent from the ampule batch studies. The same four VFAs (i.e., formate, acetate, propionate, butyrate) were consistently released from the solid phase to the aqueous phase regardless of solid type or system scale, but column study results also suggested that heating regime may impact the rate, and thus longevity, of VFAs release. The stepwise heating regime employed during the Webster soil column study (+10 °C/3.3 PVs) caused rapid increases in downgradient VFAs concentrations with each temperature increase. These increases in VFAs concentrations were followed by rapid decreases as the VFAs were transported downgradient and consumed by microorganisms native to the Webster soil, demonstrated by the formation and rapid consumption of H_2, CH_4 gas formation (68.4 vol%, Figure 4-9), and decrease in total VFAs mass with increasing distance from the upgradient heated zone (Figure 4-24).

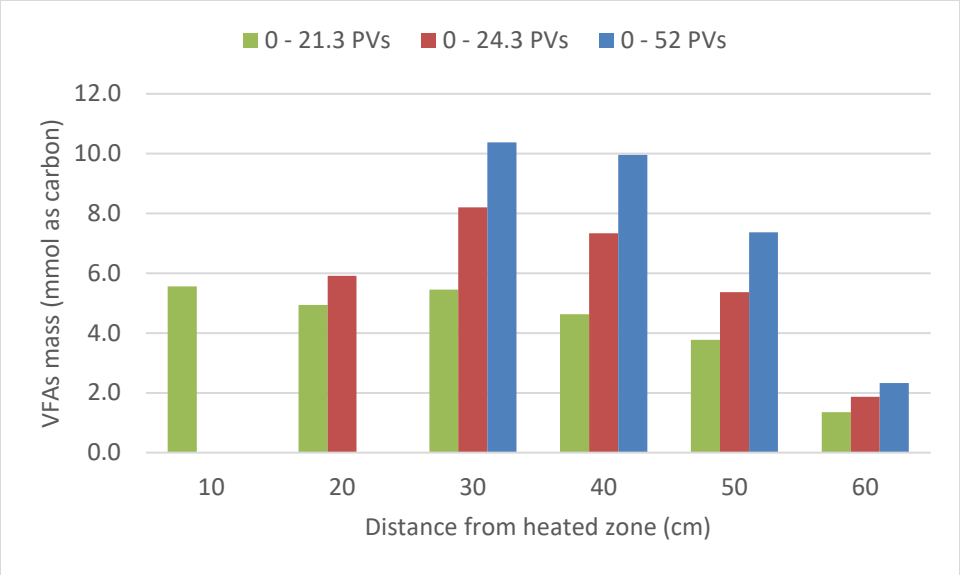

Figure 4-24: Total overall VFAs mass (as carbon) detected in aqueous port and effluent samples with increasing distance downgradient from the upgradient heated Webster soil zone.

These heat-induced spikes in VFAs concentrations indicate that release from the Webster solid phase occurred rapidly once a threshold temperature was reached. Despite the gradual heating regime (+2 °C/PV) employed during the Hudson column studies, results from those studies also support this argument: VFAs concentrations remained below the detection limit for the duration of the unheated Hudson soil column experiments (Systems C and D) and were not detected in Systems A and B until the Hudson soil temperature reached 43 °C. By comparison, the temperature in the heated zone of the Webster soil column had to reach 51 °C before a detectable pulse of VFAs was released, and subsequent releases of VFAs at a set temperature were minor in comparison to the initial pulse. For example, following heating of the Webster soil zone to 82 °C and the resulting peak in total VFAs concentration (4.6 mM as carbon; Figure 4-5, 21 – 24 PVs), only 34% (as carbon) of that VFAs mass was still detectable in Port L4 samples after 4 PVs. After 10 PVs, 96% (as carbon) of the VFAs mass had been consumed or transported downgradient. This finding is consistent with results from ampule batch studies (Chapter 3), where increased incubation time was associated with greater release of VFAs, but the majority of VFAs released for a given set of incubation conditions was typically accounted for during the initial sampling event (Figure 3-1, Figure 3-2, Figure 3-3, Figure 3-4).

Interestingly, results from the Hudson column studies also indicate that a gradual heating regime (+2 °C/PV) does not necessarily lead to more consistent

downgradient VFAs concentrations compared a stepwise heating regime. For example, VFAs concentrations in midpoint samples collected from the Systems A and B Hudson column studies declined steadily following the initial pulse observed at 43 °C (Figure 4-10, 14 – 19 PVs and Figure 4-12, 17 – 25 PVs), despite consistent increases in the upgradient Hudson soil temperature. In both systems, however, VFAs concentrations rebounded upon heating to 70 °C. These and the findings from the Webster soil column study indicate that the majority of VFAs releases occur within certain temperature ranges that may vary with soil type. This is consistent with results from ampule batch experiments, which demonstrated a positive, but non-linear, relationship between incubation temperature and total VFAs release.

4.5.2 Utilization of thermally-released substrates by dechlorinating bacteria

Results from the Hudson soil column studies demonstrate that thermally-released substrates can support the sustained MRD of chlorinated ethenes. Assuming complete oxidation of thermally-released VFAs (

Table 2-2), the 6% difference in VFAs mass (as carbon) between the System A midpoint and effluent would have provided the KB-1® culture with up to 1,650 µmol reducing equivalents. In System A (heated and bioaugmented), KB-1® in the downgradient Federal Fine Ottawa sand column dechlorinated 16 µmol PCE, 11 µmol TCE, and 81 µmol cis-DCE (Figure 4-11) to 2 µmol PCE, 5 µmol TCE, 66 µmol *cis*-DCE, 14 µmol VC, and 26 µmol non-toxic ethene over the duration of the experiment (Figure 4-13). Given that the MRD process consumes two reducing equivalents per dechlorination step (Figure 2-4), such dechlorination would have required 199 µmol of reducing equivalents, approximately 12% of the 1,650 µmol reducing equivalents available as VFAs. At least 129 µmol of the 199 µmol reducing equivalents (65%) required for dechlorination were consumed by *Dhc* during the reduction of *cis*-DCE to VC and ethene. By comparison, dechlorination activity in System C (unheated and bioaugmented) consumed 94 reducing equivalents. Although dechlorination still occurred in the downgradient Federal Fine Ottawa sand column, only 22 µmol of reducing equivalents consumption (23%) was attributable to *cis*-DCE and VC reduction. The greater consumption of reducing equivalents by *Dhc* in the heated system (System A) compared to the unheated system (System C) suggests that thermal treatment can not only help to sustain MRD activity, but may specifically benefit *Dhc* and, thus, VC and ethene production.

4.5.3 Biological VFAs production from complex thermally-released organic compounds

In System B (heated and non-bioaugmented), the limited dechlorination of PCE to TCE by microorganisms native to the Hudson soil accounted for less than 1% of the 906 µmol (as carbon) of VFAs-associated reducing equivalents consumed between the midpoint and effluent. Because System B was heated but not bioaugmented, the relative lack of dechlorination compared to System A could easily be attributed to a low abundance of dechlorinating microorganisms. However, low substrate availability may also help to explain the lack of dechlorination activity. Despite having an identical heating regime to System A (+2 °C/PV) and evidence that PCE-to-TCE dechlorinating bacteria were present (i.e., production of TCE), total VFAs concentrations (as carbon) were nearly 100% lower during the 80 – 96 °C phase of System B (Figure 4-15, 31 – 49 PVs) compared to System A (Figure 4-10, 31 – 49 PVs). Given that the experimental systems were otherwise identical, these findings suggest that bioaugmentation with KB-1® improved the net availability of VFAs, presumably due to the activity of fermenting microorganisms in the culture that were not native to the Hudson soil. Although this finding is seemingly in conflict with results of ampule batch studies, which in most cases demonstrated statistically similar ($p < 0.05$) release of VFAs in ampules with or without 2 mM $HgCl_2$ as a microbial inhibitor (Section 3.4.2, Figure 3-2), it is plausible that the spatial discretization of the heated and unheated zones in the

column experiment systems may have allowed for the additional, microbiologically-catalyzed production of VFAs.

As discussed in Chapter 3, a maximum of 4.8% of DOC in ampule aqueous phases post-incubation was attributable to VFAs, so a minimum of 95.2% of DOC was associated with other, more complex organic compounds. While hydrolytic degradation alone was not sufficient to break these compounds down to detectable VFAs during ampule incubation, bacteria or archaea native to the ampule solid phases would likely have been able to do so had they not also undergone extended, high-temperature incubation.[108] In the Webster and Hudson column studies, however, native and amended microorganisms would have had the opportunity to degrade these more complex molecules once they were transported downgradient.

Although measurement of VFAs only provides data on net concentrations and does little to elucidate individual sources and sinks within a system, collective interpretation of experimental results indicates that VFAs production in the Webster and Hudson column studies was not isolated to hydrolysis in the heated zone, but also continued downgradient due to microbial activity. Multiple lines of evidence support this argument, most notably that overall VFAs release at a given temperature was consistently greater in column studies than in ampule batch studies. For example, the greatest total VFAs release at temperatures up to 60 °C in the Webster soil column was 35 μmolC/g_{solid} (Figure 4-3, 0 – 16 PVs), nearly

double the value of corresponding Webster soil ampule experiments (18 $\mu molC/g_{solid}$) (Figure 3-1k,

Table 3-3). The difference in net VFAs release between batch and column studies was also more pronounced at higher temperatures, presumably due to the higher availability of complex DOC and the more severe temperature suppression of microbial activity during batch studies. The greatest total VFAs release in 90 °C Webster soil ampules was 23 μmolC/g_{solid} (Figure 3-1l,

Table 3-3), compared to overall release of 102 μmolC/g_{solid} in the Webster column study (Figure 4-5), during which the peak temperature was only 82 °C, but microorganisms native to the Webster soil were able to colonize the downgradient unheated zone. Similarly, total VFAs release during the 21 – 90 °C phase of the System A Hudson column study (150 μmolC/g_{solid}) (Figure 4-10, 0 – 42 PVs) was one order of magnitude greater than after 180 d, 90 °C ampule incubation (15 μmolC/g_{solid}) in the batch study (Figure 3-5,

Table 3-9).

It is possible that the greater VFAs release observed during the column studies was a result of differences in system scale and parametric complexity relative to the ampule batch studies (e.g., diffusive versus advective transport, spatially homogeneous versus heterogeneous temperature zones). For example, despite the low pore water velocities (v = 15 – 25 cm/d) employed during the column studies, substantially greater mixing would have occurred in the Webster and Hudson soil columns than in the ampule batch studies, which were not agitated during incubation. More mixing in the column studies may have increased interaction between reactants, thus helping to drive the hydrolysis reactions and increase product yield (i.e., VFAs). Similarly, VFAs in the column systems were subject to continuous advective transport downgradient, whereas the lack of advective transport in the ampule batch studies led to accumulation of hydrolysis products (i.e., VFAs) in the aqueous phase. This accumulation could potentially have reduced the energetic driving force of the hydrolysis reactions, thus limiting VFAs formation that may otherwise have occurred. However, while increased mixing and advective flow likely explains some of the increased VFAs mass in the column studies, data collected at differential spatial locations during the column studies further supports the argument that additional, microbiologically-catalyzed VFAs production occurred downgradient of the heated zones. Most notably, spatial increases in total VFAs mass were observed during the 78 – 96 °C phase of the

System A Hudson column study: total VFAs mass (as carbon) increased by 47% between the midpoint (Figure 4-10, 31 – 45 PVs) and effluent (Figure 4-11, 31 – 45 PVs).

During the same 78 – 96 °C period of the System A Hudson column study, the relative complexity of VFAs also increased between the midpoint (Figure 4-10, 31 – 45 PVs) and effluent (Figure 4-11, 31 – 45 PVs). In midpoint samples, 28% of VFAs mass (as carbon) was associated with propionate, butyrate, or isovalerate, compared to 33% in effluent samples. However, reactions that consume low molecular weight VFAs (e.g., formate, acetate) and produce higher molecular weight VFAs (e.g., propionate, butyrate, isovalerate) are energetically unfavorable in an anaerobic environment such as the downgradient Federal Fine Ottawa sand columns. For example, conversion of acetate to propionate (i.e., $acetate^- + HCO_3^- + 3H_2 + H^+ \rightarrow propionate^- + 3H_2O$) under conditions relevant to an anaerobic system is associated with a change in Gibbs free energy ($\Delta G'_c$) of $\Delta G'_c$ = +57.8 – +93.9 kJ/reaction ().

Table 3-1). Thus, it follows that the increased concentrations of propionate, butyrate, and isovalerate resulted from microbiologically-catalyzed degradation of complex DOC liberated during heating. This also helps to reconcile the detection of low concentrations (< 1.1 mmolC) of isovalerate throughout the Hudson column studies (Figure 4-10, Figure 4-12, Figure 4-15, Figure 4-17) with the lack of isovalerate detected during ampule incubation studies.

4.5.4 Implications for chlorinated solvent remediation

Findings from the Webster and Hudson soil column studies build upon those of the ampule batch studies and argue for the continued research and development of combined ISTT and MRD systems for the cleanup of chlorinated solvents. These studies demonstrate that thermally-released organic compounds are able to provide native and amended dechlorinating bacteria with the necessary substrates to drive MRD of PCE to *cis*-DCE, VC, and non-toxic ethene, which may reduce time and cost associated with amendment (i.e., lactate) delivery. Remediation professionals interested in taking full advantage of thermally-released substrates will also benefit from the knowledge that substrate release and system temperature do not maintain a linear relationship, and that certain temperature zones may be more highly associated with substrate release. Understanding of these solid-specific temperature thresholds will allow practitioners to cater the subsurface heating regime to maximize substrate longevity and minimize waste (i.e., advective flux outside of

the treatment zone before they can be used by target microorganisms). Finally, preliminary evidence that complex organic compounds released during thermal treatment can continue to provide a source of VFAs downgradient of the heated zone may allow for adaptation of coupled ISTT and ISB technologies to larger, more dilute contaminant plumes, rather than only the highly concentrated source zones for which ISTT technologies are typically reserved.

5. Impacts of low-temperature thermal treatment on a PCE-to-ethene dechlorinating consortium

5.1 Abstract

Coupling *in situ* thermal treatment (ISTT) with microbial reductive dechlorination (MRD) could enhance contaminant degradation and reduce cleanup costs compared to conventional standalone remediation technologies. Impacts of low-temperature ISTT on *Dehalococcoides mccartyi* (*Dhc*), a critical species in the anaerobic degradation of *cis*-1,2-dichloroethene (*cis*-DCE) and vinyl chloride (VC) to non-toxic ethene, were assessed in continuous flow 1-D sand columns. Dissolved tetrachloroethene (PCE; 258±46 μM) was introduced to identical columns bioaugmented with the PCE-to-ethene dechlorinating consortium KB-1®. Initial column temperatures represented a typical aquifer (15 °C) or a site undergoing low-temperature ISTT (35 °C), and were subsequently increased to determine the maximum temperature permissive of MRD. PCE in the 15 °C column was transformed primarily to *cis*-DCE (159±2 μM), which was further degraded to VC (164±3 μM) and ethene (30±0 μM) within 17 pore volumes (PVs) after the temperature was increased to 35 °C. Ethene constituted >50% of effluent degradation products in both columns after approximately 73 – 74 PVs at 35 °C, regardless of the initial temperature. Temperature increase of the column initially at 35 °C resulted in continued VC and ethene production until *Dhc* activity ceased

at approximately 43 °C. The abundance of the *vcrA* reductive dehalogenase (RDase) gene exceeded that of the *bvcA* gene by 1 – 2.5 orders of magnitude at 15 °C, but this relationship reversed at temperatures >35 °C. These findings imply that reported batch reactor results underestimate *Dhc* activity at elevated temperatures, and that VC-dechlorinating *Dhc* strains respond differently to temperature increases.

5.2 Introduction and background

The coupling of ISTT and microbial reductive dechlorination (MRD) has been proposed to improve remediation performance at sites contaminated with chlorinated solvents.[3-5] The average groundwater temperature in the United States ranges from 3 °C in parts of Maine and Minnesota to 25 °C in southern Florida and Texas,[20] but the key dechlorinating bacteria involved in reductive dechlorination of chlorinated solvents are mesophilic, with optimal growth temperatures ranging from 22 to 38 °C.[13, 17-19, 21] A narrower optimal range of 25 to 30 °C has been identified for neutrophilic, strictly hydrogenotrophic *Dhc* strains, which are keystone bacteria for the reduction of *cis*-DCE and VC to non-toxic ethene.[13] Use of ISTT to close this gap between ambient groundwater and optimal temperatures for MRD could substantially impact *in situ* dechlorination rates. A batch culture study using the PCE-to-ethene dechlorinating consortium Bio-Dechlor INOCULUM (BDI) demonstrated *Dhc* activity at 40 °C, but sustained MRD

activity required temperatures not exceeding 35 °C,[17] emphasizing the potential negative impacts of heating on the MRD process.

MRD has been studied extensively in static batch incubations, but system scale (i.e., presence of porous medium and dynamic flow conditions) has been shown to influence microbial activity, in some cases impacting microbial tolerance to environmental stressors. In a study designed to compare MRD in continuous flow versus batch reactor systems, *Dhc* dechlorination rates in columns exceeded those in batch reactors by more than 200 fold,[89] highlighting the potential for flow conditions to substantially affect microbial activity. Similarly, the PCE- and TCE-dechlorinating bacterium *Dehalobacter restrictus* strain PER-K23 did not grow in batch reactors maintained at 10 °C,[21] despite reaching PCE transformation rates of 3.7 µM/h in a continuous flow column operated at the same temperature.[110] Contaminant toxicity has also been shown to vary with system scale and microbial diversity. For example, despite batch study results demonstrating that four pure cultures (*Sulfurospirillum multivorans*, *Desulfuromonas michiganensis* strain BB1, *Geobacter lovleyi* strain SZ, *Desulfitobacterium* sp. strain Viet1) were unable to dechlorinate PCE when concentrations exceeded 540 µM,[111, 112] reduction of PCE near the aqueous solubility ($C_{sat,PCE} \approx 1{,}200$ µM) has been reported in column,[113] aquifer cell,[114] and field pilot[115] studies. The causes of these apparent discrepancies are unclear, but geochemical conditions such as dissolved oxygen,[112] temperature,[10, 17, 44, 116] pH,[117] contaminant concentration gradients[112, 118-120], or

biofilms/microenvironments[121, 122] can have strain-specific impacts, leading to variability in microbial growth and dechlorination activity.

Dhc strains involved in the reductive dechlorination of chlorinated ethenes each possess a single copy of the *Dhc* 16S rRNA gene and a single copy of one of the RDase genes implicated in *cis*-DCE or VC reduction: strains 195 and FL2 possess the *tceA* gene (TCE → DCEs → VC), strains VS and GT possess the *vcrA* gene (*cis*-DCE → VC → ethene), and strain BAV1 possesses the *bvcA* gene (DCEs → VC → ethene).[13] The *vcrA* and *bvcA* genes are often targeted in groundwater via quantitative real-time polymerase chain reaction (qPCR) analysis because of their association with ethene formation.[73, 123-125] A few studies observed that *Dhc* strains harboring the *vcrA* and *bvcA* genes appear to have different responses to geochemical conditions.[74, 117, 120] For example, shifts in the relative abundance of *Dhc* strains occurred during ISTT at a site in Fort Lewis, WA, wherein heating from ambient temperature (~12 °C) to 33 °C caused a relative increase of the *bvcA* gene versus the *vcrA* gene.[10]

During ISTT, temperatures of 80 – 110 °C are commonly targeted for the treatment zone to volatilize and recover gaseous organic contaminants.[47] Laboratory-scale microcosm studies showed that these conditions led to viability loss of bacteria capable of MRD;[17, 18] however, MRD activity could be retained or even increased in peripheral and down-gradient zones where temperatures were lower, but still

elevated relative to ambient groundwater. Alternatively, ISTT could be specifically designed to moderately increase groundwater temperatures with the goal of stimulating MRD. This strategy has substantially lower energy requirements than conventional ISTT and eliminates the need for costly gas-phase extraction and above-ground treatment systems. [5, 10] Although a promising remedial strategy, the potential benefits of coupling low-temperature ISTT with MRD have received little quantitative attention, particularly with respect to the simultaneous effects of variable temperature and flow through porous medium.[10, 44] Given the impacts of system scale and geochemical conditions on microbial activity, the results of batch studies are not immediately transferrable to *in situ* conditions. Thus, the objectives of this study were to: a) assess the impacts of low-temperature thermal treatment on the extent of MRD of PCE and its chlorinated daughter products, and b) determine the impacts of increasing temperature on strain-specific growth and activity of *Dhc* in continuous flow, 1-D column systems. Dissolved PCE was continuously introduced to columns bioaugmented with a PCE-to-ethene dechlorinating consortium, and the columns were chilled or heated to represent groundwater temperatures at an unheated site or a site undergoing low-temperature ISTT, respectively. Monitoring of chlorinated ethenes and ethene concentrations, as well as the abundance and distribution of *Dhc* 16S rRNA and RDase genes, demonstrated the benefits of low-temperature ISTT.

5.3 Materials and methods

5.3.1 Materials

PCE (≥99%) and sodium lactate (60% w/w syrup) used in the column experiments were obtained from Sigma-Aldrich (St. Louis, MO). Gas chromatography (GC) standards were prepared with PCE, TCE (≥99.5%; Sigma-Aldrich), *cis*-DCE (97%; Sigma-Aldrich), VC gas (VC; 99%; SynQuest Laboratories, Alachua, FL), and ethene gas (≥99.5%; Sigma-Aldrich). Ion chromatography (IC) standards were prepared with the sodium lactate syrup and the sodium salts of acetate (≥99%; EMD Millipore, Burlington, MA); butyrate (≥98%; Alfa Aesar, Haverhill, MA); formate (≥99%; Sigma-Aldrich); and propionate (≥99%; Sigma-Aldrich). All other chemicals were of reagent grade or higher purity. Unless specified otherwise, gases used for medium preparation, column operation, and analyses were of ultra-high purity and obtained from Airgas (Radnor, PA). Aqueous solutions were prepared using 18.2 MΩ deionized (DI) water (EMD Millipore).

5.3.2 Column design and preparation

Low-temperature thermal treatment experiments were performed using borosilicate glass chromatography columns (15 cm *l* × 2.5 cm *ID*; Kimble-Chase, Vineland, NJ) equipped with Teflon endplates. Each column was customized with three evenly spaced glass sampling ports sealed with rubber septa, with Port 1 nearest the column influent. All components of the experimental setup were steam-sterilized

for 30 min at 121 °C prior to use. The columns were packed in 1 cm increments with dry Federal Fine Ottawa sand (30 – 140 mesh; U.S. Silica, Frederick, MD), a quartz sand with mean grain size of 0.32 mm, permeability of 4.2×10^{-11} m^2, and total organic carbon (OC) content of <0.01 wt%.[126] Packed columns were purged with filter-sterilized carbon dioxide (CO_2) gas and saturated with a sterile synthetic groundwater solution (see below). Non-reactive bromide tracer tests ($[Br^-]$ = 10 mM, flow rate (Q) = 0.02 mL/min) were completed prior to and following each column experiment to determine initial porosity (n) and aqueous PV.

5.3.3 Synthetic groundwater preparation and delivery

Reduced, synthetic groundwater was prepared by making the following modifications to the synthetic basal salt medium used to grow *Dhc* cultures:[127] the trace element concentrations were reduced by 90%; the sodium sulfide nonahydrate concentration was increased from 0.2 to 1 mM; vitamins were eliminated; and the target pH was adjusted to 7.1±0.1. Lactate (5 mM) was added in stoichiometric excess to serve as both the electron donor and carbon source. Synthetic groundwater was prepared in 1,600 mL batches, evenly dispensed into each of three 1,000 mL glass bottles (Chemglass, Vineland, NJ) under an 80% nitrogen/20% CO_2 (v/v) headspace. Neat PCE (300 µL) was added to one bottle to serve as a PCE-saturated stock solution, then each bottle was sealed with a rubber stopper and sterilized by autoclave at 121 °C for 30 min. The concentration of the PCE-saturated stock was then verified by GC and the column influent solution was prepared by diluting the

PCE-saturated stock in a sterile, 100 mL gastight syringe (SGE Analytical Science, Victoria, AU). Synthetic groundwater was used as diluent to reach a PCE concentration of 258±46 µM. Column influent was delivered via a PHD 2000 syringe pump (Harvard Apparatus, Holliston, MA) and syringes were refilled approximately every 3 PVs.

5.3.4 Column bioaugmentation, operation, and sampling

Two identical columns, hereinafter referred to as A_{i15} ($n_{A,initial}$ = 0.40 cm^3/cm^3, $PV_{A,initial}$ = 30.3 mL) and B_{i35} ($n_{B,initial}$ = 0.40 cm^3/cm^3, $PV_{B,initial}$ = 30.3 mL), were operated similarly and in parallel, except with respect to temperature (Figure 6-1). A third column experiment, $C_{control}$ ($n_{C,initial}$ = 0.41 cm^3/cm^3, $PV_{C,initial}$ = 31.4 mL), was performed to verify that no abiotic contaminant degradation occurred in the absence of the KB-1® consortium (SiREM, Ontario, CA). A recirculating water bath (Thermo Fisher, Waltham, MA) was used to chill Column A_{i15} and associated influent tubing (1.6 mm *OD*; Kimble-Chase) to an initial temperature of 15 °C, while a second recirculating water bath (VWR, Radnor, PA) was used to heat Column B_{i35} and associated influent tubing to an initial temperature of 35 °C. Columns were thoroughly wrapped with polyethylene pipe insulation (2.5 cm wall thickness; Grainger, Lake Forest, IL) to ensure that the target temperatures were not impacted by ambient laboratory conditions. A Type K thermocouple (VWR) was used approximately every 3 PVs to independently verify column temperatures and the accuracy of the water baths' digital temperature controllers. Synthetic

groundwater was introduced to Columns A_{i15} and B_{i35} at an initial pore water velocity of 15 cm/d (Q = 0.020 mL/min or 1 PV/d) for 17 PVs to establish reduced conditions and stable concentrations of dissolved PCE and lactate. Flow was then paused and 6 mL of the KB-1® consortium was injected via each column influent, sampling ports 1 – 3, and effluent, for a total of 30 mL per column. KB-1® is a widely used, methanogenic, PCE-to-ethene dechlorinating consortium predominantly comprised of *Acetobacterium* sp., *Geobacter* sp., and multiple *Dhc* strains harboring the *vcrA*, *bvcA*, and *tceA* RDase genes.[54, 128, 129] Column flow was resumed after a 48-hour flow interruption to facilitate cellular attachment. For simplicity in all subsequent text and figures, this resumption of flow was considered PV = 0.

The experiment was completed in four phases: in Phase I, Columns A_{i15} and B_{i35} were held at their initial temperatures (15 and 35 °C, respectively), to allow for direct comparison of dechlorination activity at a typical ambient groundwater temperature versus an elevated temperature that might be targeted during low-temperature ISTT; in Phase II, Column A_{i15} was heated from 15 to 35 °C (+2 °C/PV) to assess dechlorination activity in a system initially at ambient groundwater temperature that later underwent low-temperature ISTT; in Phases III and IV, Column B_{i35} was heated from 35 °C (+0.5 – 1 °C/PV) to determine the maximum temperatures permissive of *Dhc* and overall MRD activity, respectively, in a continuous flow system. Effluent samples were collected every 2 – 3 PVs

throughout the experiment to determine concentrations of chlorinated ethenes, ethene, and organic acids, pH, and oxidation-reduction potential (ORP). Influent and effluent system components (e.g., syringes, tubing, valves) were periodically flushed with isopropanol and sterile synthetic groundwater to prevent microbial growth outside of the temperature-controlled, sand-packed columns. Port samples were collected at least once during each phase to determine aqueous abundances of the *Dhc* 16S rRNA, *tceA*, *bvcA*, and *vcrA* genes. Additional port samples were collected periodically to determine the spatial distribution of PCE and its daughter products. Columns were destructively sampled after the experiment to determine solid-phase abundances of the *Dhc* by enumerating 16S rRNA and RDase genes with qPCR.

5.3.5 Abiotic control column operation and sampling

Column $C_{control}$ was completed as an abiotic control to determine whether contaminant degradation would occur in the absence of the KB-1® culture. System preparation and operation were as described for Columns A_{i15} and B_{i35}, except that biological samples were not collected and the heating rate was accelerated. The initial Column $C_{control}$ PV was 30.2 mL and the average concentration of PCE in the influent synthetic groundwater solution was 221±13 µM. Column $C_{control}$ was initially operated at ambient laboratory temperature (21 °C) until influent and effluent PCE concentrations were similar. The temperature was then increased by +10 °C at intervals of 3 – 5 PVs until reaching a final temperature of 74 °C.

5.3.6 Analytical methods

Chlorinated ethenes and ethene

Chlorinated ethenes and ethene in aqueous samples were measured using an Agilent 7890B GC equipped with a headspace autosampler and flame ionization detector (FID) according to the method described in Section 4.3.6.

Organic acids

Lactate and other organic acids (i.e., formate, acetate, propionate, butyrate) were measured according to the method described in Section 3.3.6 ("*Volatile fatty acids*").

Sample preparation and DNA extraction of aqueous samples

Aqueous samples (1 mL) collected from column ports for qPCR analysis were immediately placed in a sterile 1.8 mL microcentrifuge tube and centrifuged at 15,000 rpm (21,230 × *g*) for 15 minutes at ambient temperature. The supernatant was then discarded and cell pellets were stored at -20 °C until DNA extraction using the QIAGEN QIAamp DNA Mini Kit (Qiagen, Venlo, NL). Extractions were completed per the protocol provided by QIAGEN for Gram-positive bacteria, as recommended by the manufacturer to ensure efficient cell lysis. DNA was collected in 600 µL of Buffer AE and stored at -20 °C until qPCR analysis.

Sample preparation and DNA extraction of solid samples

Upon experiment termination, columns were destructively sampled to allow for determination of solid-phase abundances of the *Dhc* 16S rRNA and RDase genes. Columns were divided into 11 segments (Figure 5-1) then each segment (6 – 18 g) was transferred to a sterile 15 mL centrifuge tube using a flame-sterilized stainless steel spatula.

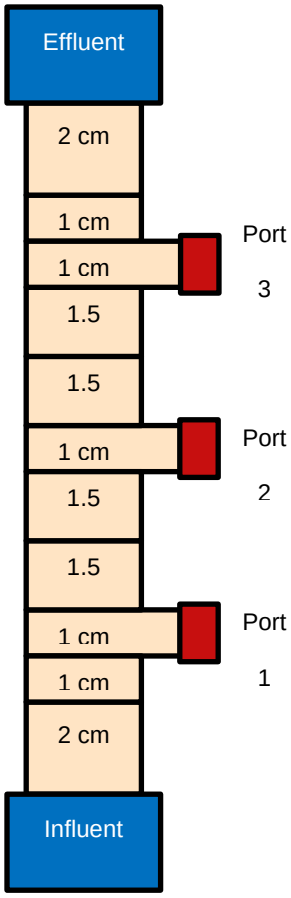

Figure 5-1: Column diagram with 11 segments delineated for solid-phase dissection and DNA extraction. Segment 1 was nearest the column influent and segment 11 was nearest the column effluent. Ports 1, 2, and 3 were immediately adjacent to solid-phase segments 3, 6, and 9.

Samples were homogenized, then approximately 2 g of each wet sample was placed in an aluminum dish and dried at 110 °C overnight to determine the water content. Bacterial DNA was extracted from approximately 0.25 g of each wet solid sample using the PowerSoil DNA Isolation Kit (MO BIO, West Carlsbad, CA), per the provided protocol. DNA was collected in 100 µL of solution C6 and stored at -20 °C.

Gene copy abundance

Dhc 16S rRNA and RDase gene abundances were determined by qPCR analysis using a StepOnePlus Real-Time PCR System (Applied Biosystems, Foster City, CA). Analyses targeting the *Dhc* 16S rRNA, *tceA*, *bvcA*, and *vcrA* genes were completed in triplicate according to an established TaqMan-based qPCR protocol.[130] Primers and probes used in qPCR analyses were obtained from IDT Technologies (Coralville, IA) or Thermo Fisher. TaqMan Universal PCR Master Mix was obtained from Applied Biosystems. Standards were prepared by using a Qubit 2.0 Fluorometer (Thermo Fisher) to determine the concentration of plasmid DNA containing a single copy of each target gene, then diluting the plasmid DNA to 1 ng/µL and performing 10:1 serial dilutions in molecular biology-grade water (Thermo Fisher). The linear range of each standard curve was approximately 10^2 – 10^8 gene copies/mL.

5.4 Results and discussion

5.4.1 Inoculum characterization and bioaugmentation

The KB-1® culture used to bioaugment Columns A_{i15} and B_{i35} contained 1.4±0.2 × 10^7 *Dhc* 16S rRNA gene copies/mL, 1.4±0.0 × 10^7 *vcrA* gene copies/mL, and 4.5±1.1 × 10^4 *bvcA* gene copies/mL. The culture also contained 77±1 µM ethene, but no chlorinated ethenes. Accounting for cells immediately washed out during bioaugmentation, the initial aqueous *Dhc* 16S rRNA gene abundance was 9.7±2.2 × 10^6 gene copies/mL in Column A_{i15} and 1.2±0.2 × 10^7 gene copies/mL in Column B_{i35}. More than 99% of *Dhc* cells retained in each column immediately following bioaugmentation possessed the *vcrA* gene, while only 0.3% possessed the *bvcA* gene. The *tceA* gene was not detected in the inoculum nor in any of the samples collected throughout the experiment, consistent with previous studies demonstrating low relative abundance compared to the *vcrA* and *bvcA* genes.[129]

Influent and effluent pH values in both columns were 7.1±0.1 and 7.0±0.2, respectively, for the experiment duration and ORP remained below -100 mV. Within 17 PVs post-bioaugmentation, effluent lactate concentrations decreased from 5.2 to 1.8 mM and 5.3 to 0.2 mM in Columns A_{i15} and B_{i35}, respectively. However, lactate fermentation products, acetate (0.2 – 3.8 mM) and propionate (2.7 – 4.9 mM), were consistently detected, indicating that availability of carbon and

fermentable organic substrates were not limiting MRD during the experiment (Table 5-1).

Table 5-1: Column A_{i15} and B_{i35} effluent lactate, propionate, and acetate concentrations.

	Column A_{i15} (mM)			Column B_{i35} (mM)		
PV	Lactate	Propionate	Acetate	Lactate	Propionate	Acetate
0	5.2	nd	nd	5.3	nd	nd
17	1.8	4.1	3.2	0.2	4.9	3.8
48	nd	3.5	3.7	nd	3.9	3.1
92	nd	3.2	2.7	nd	3.1	0.3
119	nd	3.4	2.7	nd	3.4	3.1
174	nd	2.7	0.2	0.2	3.3	2.9

nd = not detected.

5.4.2 Effects of heating on dechlorination

Phase I of the experiment assessed dechlorination activity (PCE_{IN} = 258±46 µM) at a typical ambient groundwater temperature (Column A_{i15}) versus a moderately elevated temperature (Column B_{i35}). Within the first 20 PVs following bioaugmentation, PCE and TCE in the effluent of Column A_{i15} was degraded primarily to *cis*-DCE (127±0 µM), with lower levels of VC (41±1 µM) and ethene (14±0 µM) (Figure 5-2, 0 – 20 PVs).

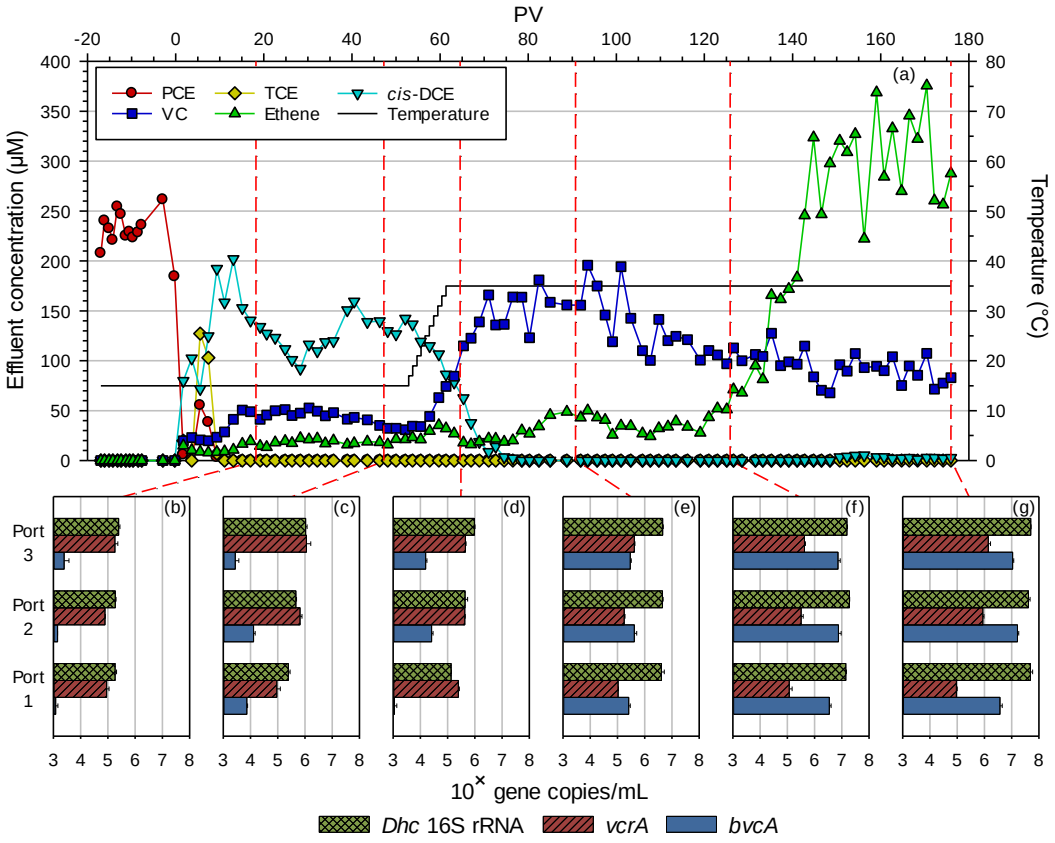

Figure 5-2: Column A_{i15} effluent concentration of PCE and daughter products (a). Bioaugmentation occurred at PV = 0. Dashed vertical lines link *Dhc* 16S rRNA and RDase gene abundances (b – g) in aqueous port samples to corresponding column PV. Error bars represent one standard deviation.

In contrast, PCE and TCE were not detected above the 1 μM detection limit in the effluent of Column B_{i35} post-bioaugmentation, and *cis*-DCE (132±13 μM) initially detected in the Column B_{i35} effluent was rapidly degraded to VC (163±3 μM) and ethene (63±0 μM) within the same period (Figure 5-3a, 0 – 20 PVs). These results indicate that a 20 °C temperature difference substantially impacts the extent of dechlorination between otherwise equivalent continuous flow systems with comparable initial abundances of *Dhc* cells.

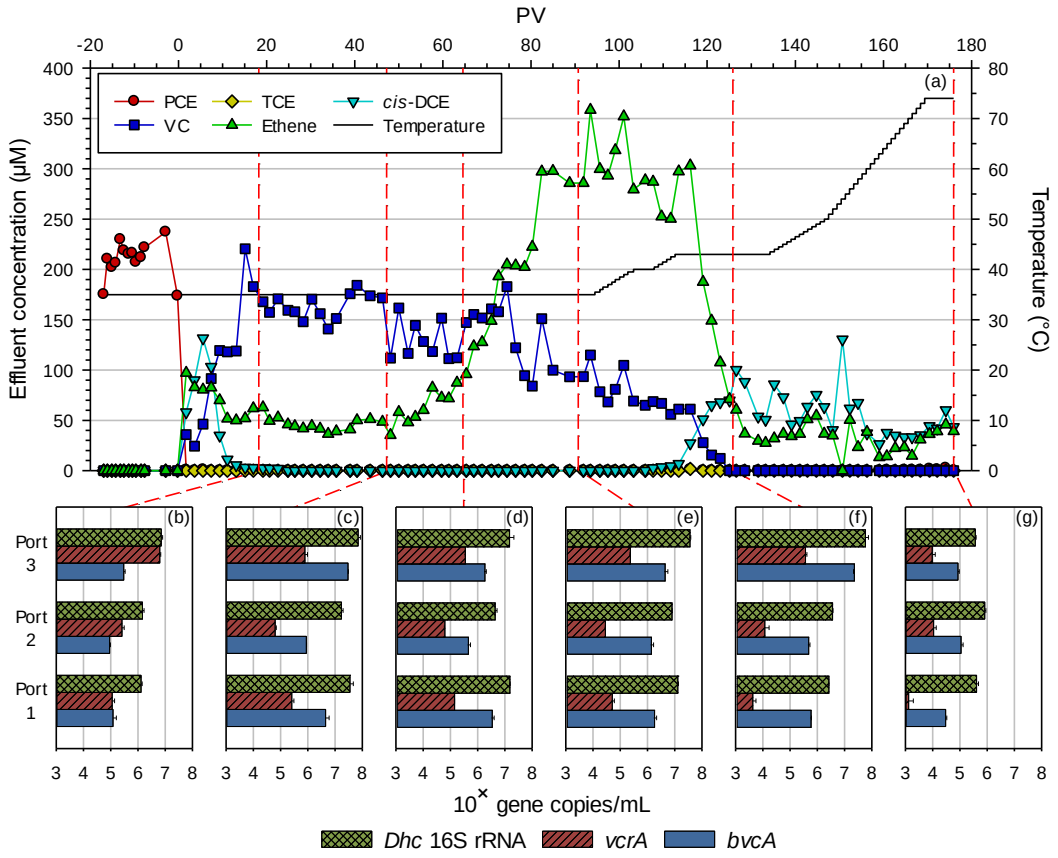

Figure 5-3: Column B_{i35} effluent concentration of PCE and daughter products (a). Bioaugmentation occurred at PV = 0. Dashed vertical lines link *Dhc* 16S rRNA and RDase gene abundances (b – g) in aqueous port samples to corresponding column PV. Error bars represent one standard deviation.

During Phase II, *cis*-DCE concentration in the Column A_{i15} effluent decreased from 142±2 to 86±1 µM as the system was heated from 15 to 35 °C (Figure 5-2a, 52 – 61 PVs), then fell below the 1 µM detection limit over the next 17 PVs at 35 °C (Figure 5-2a, 61 – 78 PVs). Effluent VC concentration rose from 31±0 to 74±1 µM over the duration of the temperature increase (Figure 5-2a, 52 – 61 PVs). This shift in dechlorination products was likely due to the increased activity of existing *Dhc* in response to the temperature increase, as evidenced by the rapid decline in *cis*-DCE despite consistent aqueous *Dhc* 16S rRNA gene abundances prior to ($2.4\pm0.4 \times 10^5$ – $1.0\pm0.1 \times 10^6$ gene copies/mL; Figure 5-2c) and immediately following ($1.3\pm0.0 \times 10^5$ – $9.6\pm0.4 \times 10^5$ gene copies/mL; Figure 5-2d) the temperature increase. However, the elevated temperature also prompted the growth of new *Dhc* cells implicated in *cis*-DCE degradation (Figure 5-2b-e), contributing to the continued decrease in *cis*-DCE concentrations after the 35 °C target was reached. The same 15-to-35 °C temperature increase that prompted rapid *cis*-DCE degradation had no immediately apparent impact on VC-to-ethene dechlorination, potentially due to inhibition by the *cis*-DCE itself.[79-81, 131] After Column A_{i15} had been at 35 °C for approximately 60 PVs, the effluent ethene concentration began to rise (Figure 5-2a, 121 PVs) and surpassed VC as the primary (>50%) dechlorination product after 74 PVs at 35 °C (Figure 5-2a, 135 PVs). This phenomenon of rapid *cis*-DCE degradation with delayed ethene formation also occurred in Column B_{i35}, with effluent ethene concentration surpassing VC concentration only after Column B_{i35} had been at 35 °C for 73 PVs (Figure 5-3a, 73 PVs). The consistent duration

of the lag period between complete *cis*-DCE reduction and rapid ethene formation suggests that the abundances of *Dhc* strains primarily responsible for VC reduction at 35 °C were initially insufficient in both columns (see *vcrA* and *bvcA* qPCR results below) or that high *cis*-DCE concentrations limited their activity.[79-81] Furthermore, the similar duration of the lag period (74 and 73 PVs in Columns A_{i15} and Column B_{i35}, respectively) suggests that the outcome of thermally enhanced MRD is not inherently linked to the order in which the remedies are applied (i.e., ISTT following bioaugmentation versus bioaugmentation following ISTT).

Concentrations of VC in both columns continued to decline during the periods of rapid ethene formation, but these reductions in VC mass accounted for only 18.2 and 18.4% of the increased ethene mass in Columns A_{i15} (Figure 5-2a, 121 – 165 PVs) and B_{i35} (Figure 5-3a, 50 – 94 PVs), respectively. These mass balance discrepancies resulted from equilibration between the aqueous phase and a gas phase that slowly developed in each column during their respective 35 °C phases. The discontinuity of each gas phase precluded direct sampling, but analyses of aqueous port samples collected from Column A_{i15} revealed that ethene accumulated in the column at 35 °C (Figure 5-5b), temporarily delaying ethene elution and inflating subsequent effluent concentrations.

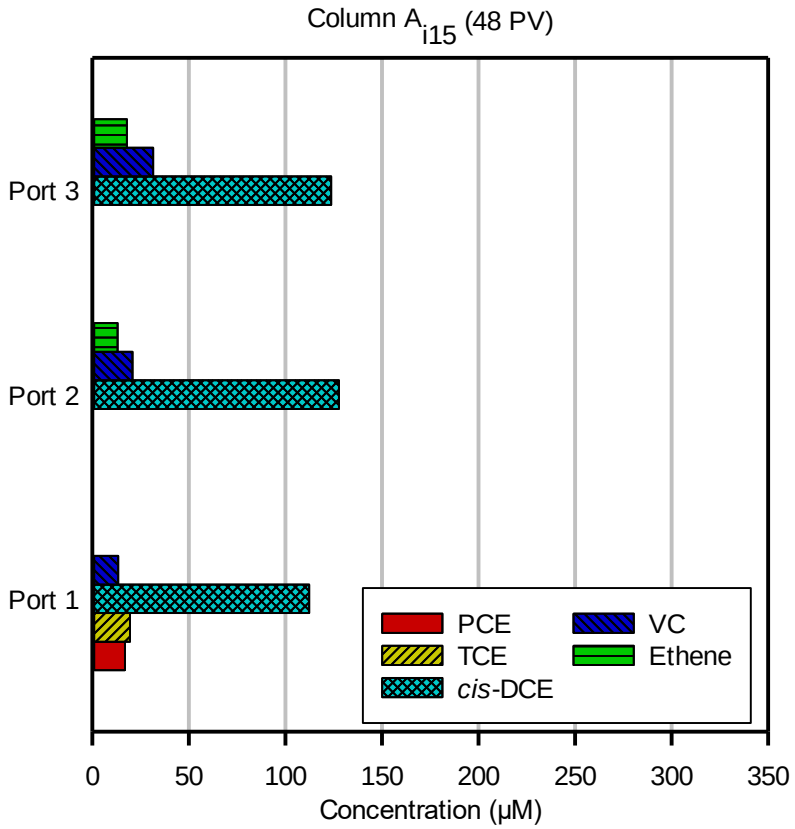

Figure 5-4: Concentrations of PCE and its daughter products in Column A_{i15} aqueous port samples collected prior to temperature (15 °C, 48 PVs).

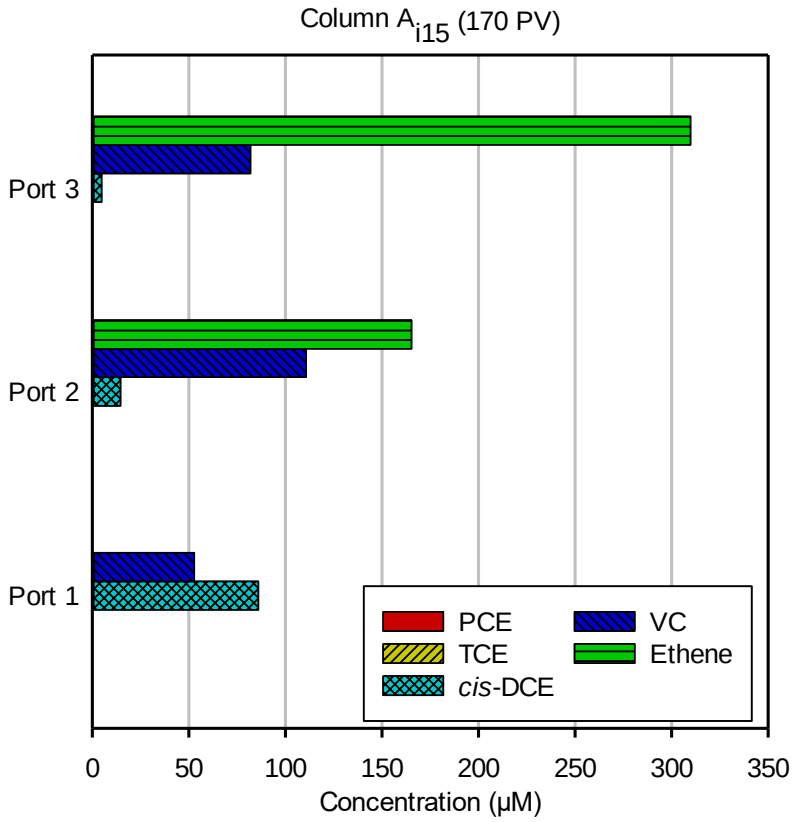

Figure 5-5: Concentrations of PCE daughter products in Column A_{i15} aqueous port samples collected following the temperature increase (35 °C, 170 PVs).

This hypothesis was supported by results of post-experiment tracer tests, which revealed markedly lower mobile porosities ($n_{A,final}$ = 0.33 cm^3/cm^3, $n_{B,final}$ = 0.30 cm^3/cm^3) compared to initial column conditions ($n_{A,initial}$ = 0.40 cm^3/cm^3, $n_{B,initial}$ = 0.40 cm^3/cm^3).

5.4.3 Maximum temperatures permissive of dechlorination activity

In order to assess whether the optimal (25 – 30 °C)[13] and maximum temperature (35 – 40 °C)[17] ranges determined for *Dhc* in batch reactors are applicable to a continuous flow system (Phase III), Column B_{i35} was gradually heated from 35 °C. During this period of gradual heating, the effluent concentration of VC continued to decrease from 115±3 to 61±1 µM (Figure 5-3a, 95 – 114 PVs); ethene concentration remained high (>250 µM) and *cis*-DCE remained below detection, indicating continued *Dhc* activity. Heating was paused at 40 °C when low concentrations (2 – 3 µM) of *cis*-DCE were again detected in effluent samples (Figure 5-3a, 103 – 108 PVs), but resumed upon confirmation that VC (68±2 µM) and ethene (285±5 µM) concentrations remained steady. However, once the temperature of Column B_{i35} reached 43 °C, effluent VC and ethene concentrations declined sharply and *cis*-DCE concentrations rebounded to 100±1 µM within 14 PVs (Figure 5-3a, 113 – 127 PVs), suggesting that a maximum temperature permissive of *Dhc* activity had been reached.

Phase IV, like Phase III, was intended to determine a maximum temperature permissive of dechlorination activity in a continuous flow system, but with focus on PCE and TCE dechlorination (i.e., dechlorination by non-*Dhc* bacteria). Heating of Column B_{i35} was continued from 43 °C until reaching a final temperature of 74 °C (Figure 5-3a, 134 – 169 PVs). Unfortunately, the high temperatures led to increased gas formation and loss of contaminant mass that did not occur at the lower temperatures (15 – 43 °C), limiting further quantitative assessment of PCE and its daughter products. Losses were confirmed by results of aqueous port sample analyses of Column B_{i35} before (Figure 5-6) and after (Figure 5-7) heating, which demonstrate an overall decrease in the mass of PCE and its daughter products in the direction of flow at the higher temperature, and results from the abiotic control experiment, Column $C_{control}$.

No PCE daughter products were detected in the Column $C_{control}$ effluent throughout the experiment, and although the influent concentration of PCE consistently exceeded the effluent concentration by 10 – 25 µM, the influent and effluent concentrations remained similar for the first 22 PVs (a). This confirms that the PCE degradation observed in Columns A_{i15} and B_{i35} was not the result of abiotic processes, and thus could not explain the loss of contaminant mass observed in Column B_{i35} at temperatures exceeding 43 °C. However, once the Column $C_{control}$ temperature was increased to 74 °C, the difference between influent and effluent PCE concentrations increased to a high of 41 µM, indicating potential mass loss by

another unidentified mechanism. In an effort to reconcile this discrepancy, the septa covering Ports 1 – 3 of Column $C_{control}$ were pierced with a 25-gauge needle, as they would have been if biological samples were collected during the experiment. After the septa were pierced, effluent PCE concentrations declined from 202±2 µM to 54±1 µM over the next 14 PVs, despite influent PCE concentrations remaining steady at 229±8 µM. This loss of PCE mass in response to the piercing of the septa indicates that volatile loss of contaminant mass was occurring at temperatures approaching 74 °C. This is further supported by results of PCE analysis performed on Column $C_{control}$ port samples collected at 34 PVs, which demonstrate a decrease in PCE concentration in the direction of flow, from 167 µM in Port 1 to 87 µM in Port 3 (b).

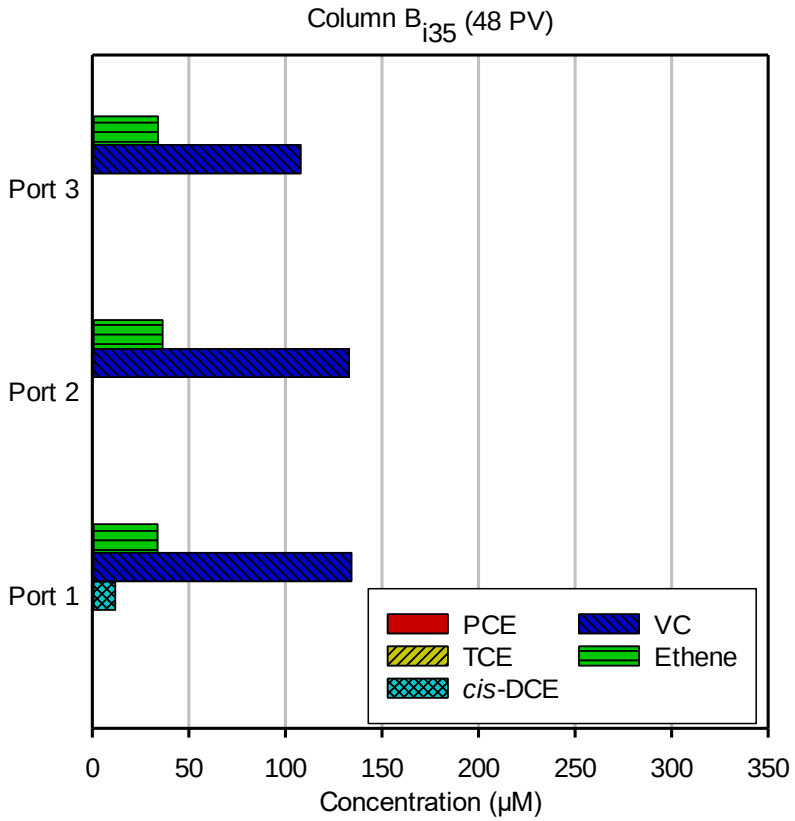

Figure 5-6: Concentrations of PCE daughter products in Column B_{i35} aqueous port samples collected prior to the temperature increase (35 °C, 48 PVs).

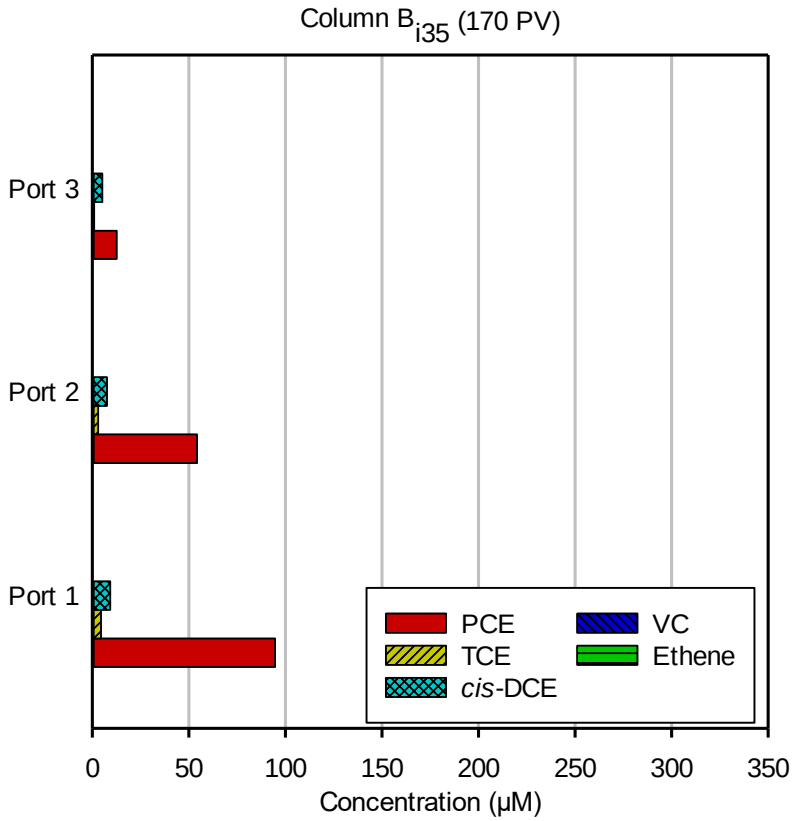

Figure 5-7: Concentrations of PCE daughter products in Column B_{i35} aqueous port samples collected following the temperature increase (74 °C, 170 PVs), demonstrating loss of contaminant mass in the direction of flow at high temperature.

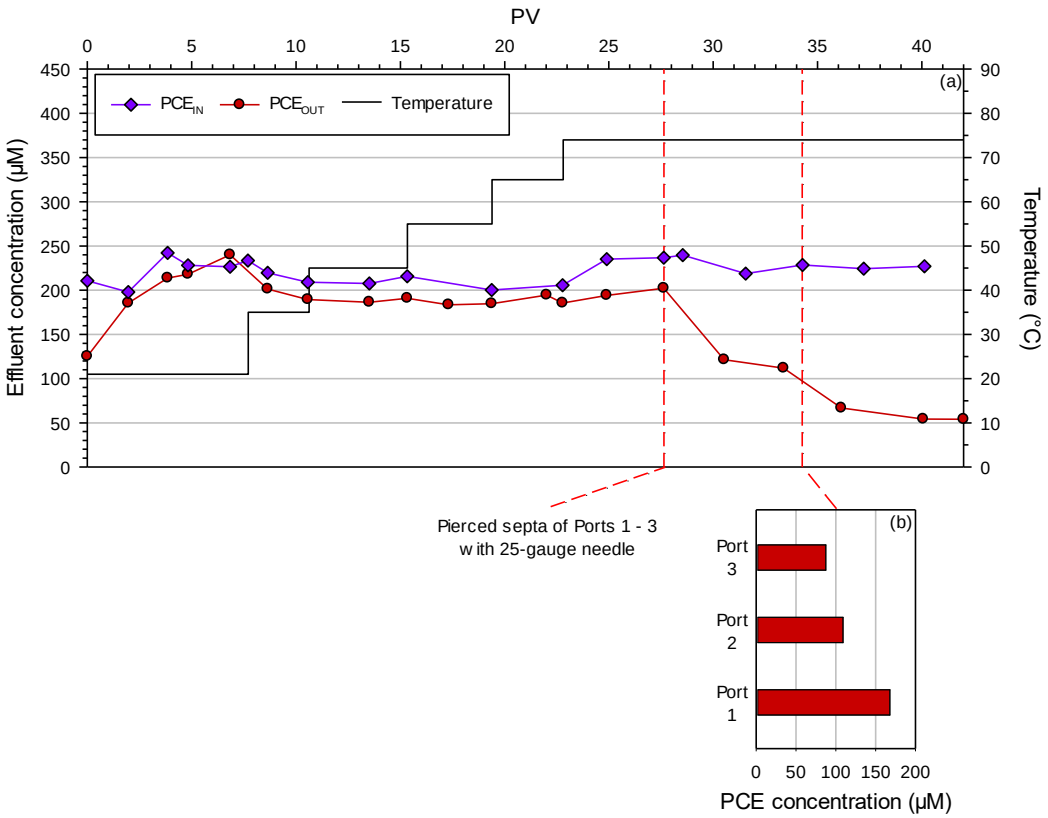

Figure 5-8: Column $C_{control}$ effluent concentration of PCE. First dashed vertical line designates column PV at which port septa were pierced with a 25-gauge needle. Second dashed vertical line links PCE concentrations in aqueous port samples to corresponding column PV.

The result was an overall mass balance of only 81% for Column B_{i35}, compared to 95% for Column A_{i15}. Despite these losses due to volatilization, low concentrations of *cis*-DCE persisted in the Column B_{i35} effluent, indicating that PCE-to-*cis*-DCE dechlorinating microbes remained active at temperatures exceeding 43 °C; however, lack of VC in effluent samples suggested that continued low concentrations of ethene were likely not indicative of continued *Dhc* activity, but instead resulted from the aqueous-gas equilibration discussed previously. These observations are consistent with the results of qPCR analysis of aqueous port samples, which demonstrate a steep decline in Column B_{i35} *Dhc* 16S rRNA and RDase gene abundances following heating from 43 °C (Figure 5-3f) to 74 °C (Figure 5-3g). The decline is illustrated in Port 3 samples, wherein the *Dhc* 16S rRNA gene abundance decreased from $5.5\pm2.1 \times 10^7$ to $3.7\pm0.3 \times 10^5$ gene copies/mL between 126 and 176 PVs (Figure 5-3f and Figure 5-3g). These results demonstrate that *Dhc* can retain metabolic activity at higher temperatures (35 – 43 °C) in continuous flow systems than previously reported for batch studies. Caution is warranted, however, as even slightly (i.e., 1 – 3 °C) exceeding the operational temperature range may cause near-immediate cessation of *Dhc* activity, rather than a gradual decline in dechlorination activity.

5.4.4 Impacts of temperature on *Dehalococcoides mccartyi* strains

Results of qPCR analyses performed on aqueous port samples (Figure 5-2b-g and Figure 5-3b-g) were consistent with dechlorination activity observed in Columns A_{i15} and B_{i35}. For example, aqueous samples collected from Port 3 (nearest effluent) of the chilled Column A_{i15} at 18 PVs post-bioaugmentation contained $2.5\pm0.3 \times 10^5$ *Dhc* 16S rRNA gene copies/mL (Figure 5-2b), compared to $7.1\pm0.9 \times 10^6$ gene copies/mL (Figure 5-3b) in corresponding samples collected from the warmer Column B_{i35}. Furthermore, although *Dhc* 16S rRNA gene abundance continued to increase in both columns from 18 – 47 PVs, the average abundance over Ports 1 – 3 increased only 3-fold in Column A_{i15} (Figure 5-2b and Figure 5-2c) compared to a 12-fold increase in Column B_{i35} (Figure 5-3b and Figure 5-3c). Following heating of Column A_{i15} from 15 to 35 °C (Figure 5-2a, 52 – 61 PVs), *Dhc* 16S rRNA gene abundance increased further, reaching a maximum of $5.0\pm0.2 \times 10^7$ gene copies/mL by the end of the experiment. This *Dhc* growth represents a 230-fold overall increase (Figure 5-2b and Figure 5-2g) and demonstrates the relationship between *Dhc* 16S rRNA gene abundance and system temperature.

The column study data also indicate that individual *Dhc* strains within the same culture (i.e., consortium KB-1®) responded differently to temperature changes. As noted previously, *Dhc* strains possessing the *vcrA* gene accounted for more than 99% of *Dhc* in the inoculum. This predominance of *vcrA* over *bvcA* was maintained throughout the entire 15 °C phase of Column A_{i15} and the beginning of the 35 °C

phase (Figure 5-2b-d). However, *vcrA* gene abundance remained static or declined during heating from 15 °C ($9.2\pm3.1 \times 10^4$ – $1.1\pm0.5 \times 10^6$ copies/mL) to 35 °C ($1.1\pm0.0 \times 10^5$ – $4.2\pm0.2 \times 10^5$ copies/mL), despite increases in *Dhc* 16S rRNA gene abundance at every sampling port between 47 and 92 PVs (Figure 5-2c and Figure 5-2e). Abundance of the *bvcA* gene increased from $2.8\pm0.9 \times 10^3$ – $1.3\pm0.2 \times 10^4$ copies/mL to $2.6\pm0.4 \times 10^5$ – $4.2\pm0.9 \times 10^5$ copies/mL during this period, indicating that growth of a *Dhc* strain carrying *bvcA* was positively impacted by the same temperature increase that limited growth of *Dhc* strains harboring the *vcrA* gene. Interestingly, effluent ethene concentration in Column A_{i15} exceeded VC concentration (Figure 5-2a, 121 PVs) only after *bvcA* gene abundance surpassed that of the *vcrA* gene (Figure 5-2f). Over the remainder of the experiment, *vcrA* gene abundance in Column A_{i15} slowly began to increase again, but still lagged behind *bvcA* gene abundance by an order of magnitude or greater (Figure 5-2f and Figure 5-2g). These strain-specific responses were also observed in Column B_{i35}: ethene became the primary (>50%) degradation product (Figure 5-3b, 73 PVs) after *bvcA* gene abundance exceeded *vcrA* gene abundance (Figure 5-3c and Figure 5-3d), and *bvcA* gene abundance (averaged over Ports 1 – 3) increased 3-fold during the 35-to-43 °C temperature increase (Figure 5-3a, 95 – 113 PVs) while average *vcrA* abundance remained unchanged (Figure 5-3e and Figure 5-3f). Destructive sampling and subsequent qPCR analysis revealed that 95 – 98% of *Dhc* 16S rRNA gene copies in Column A_{i15} (35 °C at experiment conclusion) were associated with the solid phase (Figure 5-9).

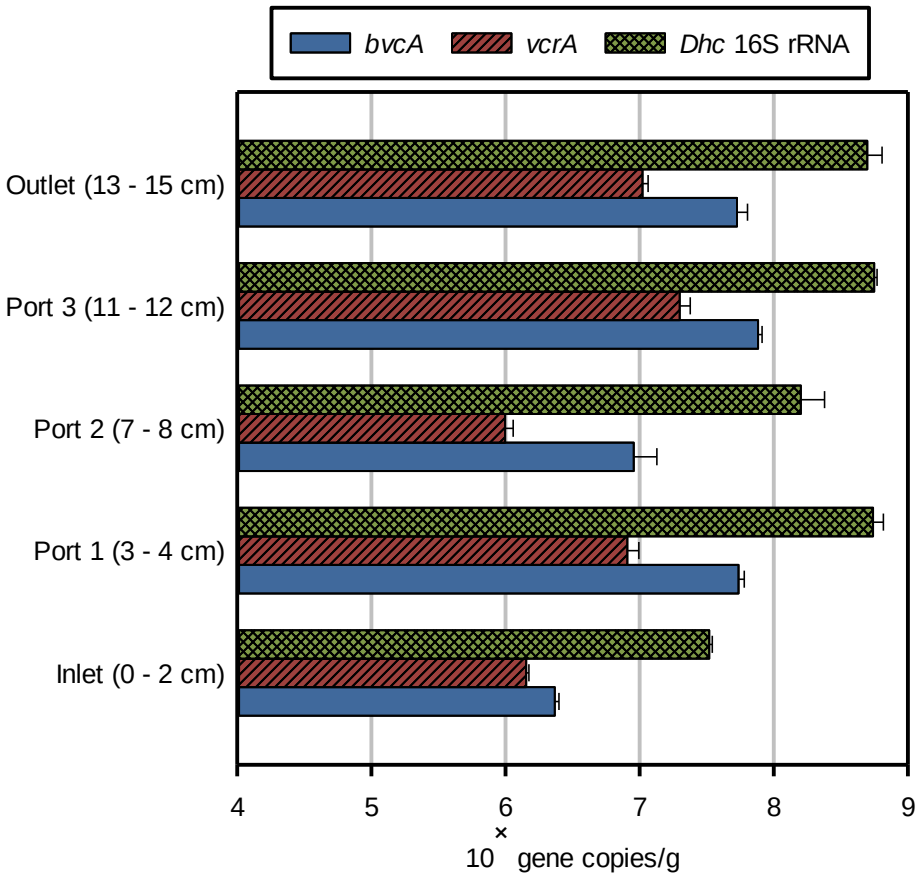

Figure 5-9: Solid-phase *Dhc* 16S rRNA and RDase gene abundances following dissection of Column A_{i15}. Error bars represent one standard deviation.

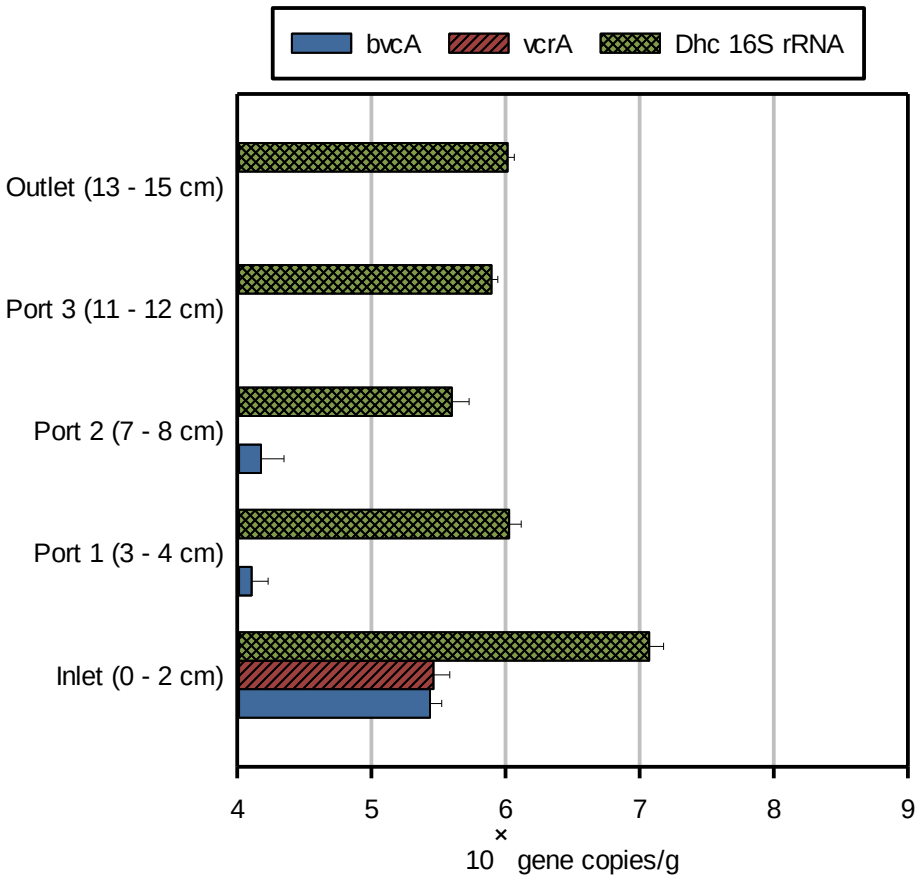

Figure 5-10: Solid-phase *Dhc* 16S rRNA and RDase gene abundances following dissection of Column B_{i35}. Error bars represent one standard deviation.

This finding is generally consistent with results of a previous study quantifying solid-phase attachment rates in a room temperature Federal Fine Ottawa sand column, wherein 73 – 89% of *Dhc* cells were attached to the solid phase upon experiment conclusion.[132] In the same study, a positive relationship was identified between extent of cellular attachment and dechlorination activity. Greater extents of cellular attachment (95 – 98%) and dechlorination in Column A_{i15} compared to the room temperature study support this relationship, and allude to a potentially complex link between system temperature, cellular attachment, and dechlorination activity. Furthermore, results of the Column A_{i15} qPCR analysis suggest that extent of *Dhc* attachment at 35 °C may be strain-specific. *Dhc* strains possessing the *bvcA* gene (averaged over Ports 1 – 3) were less likely to attach to the solid phase (87±18% attachment) than strains possessing the *vcrA* gene (94±9% attachment). Given the importance of *Dhc* 16S rRNA and RDase genes in assessing likely indicators of ethene formation (e.g., aqueous *Dhc* 16S rRNA abundance >0.05% of total bacteria, $>10^3$ gene copies/mL, ≈ *vcrA* + *bvcA* abundance), further study is warranted to ensure the continued, accurate interpretation of these biomarkers. If elevated temperatures result in greater *Dhc* attachment and activity, for instance, then ethene formation may remain likely despite a lower abundance of *Dhc* cells in the aqueous phase.

Dhc 16S rRNA and RDase gene abundances were predictably low in solid-phase samples collected 3 – 15 cm from the influent of Column B_{i35} (Figure 5-10), which

was held at 74 °C during the final stage of the experiment. The maximum total *Dhc* abundance was only 1.1±0.2 × 10^6 gene copies/g and RDase gene abundances were near or below the 1.0 × 10^4 gene copies/g detection limit for solid-phase samples. Solid-phase abundances of *Dhc* 16S rRNA genes (1.2±0.3 × 10^7 gene copies/g), *vcrA* (2.9±0.9 × 10^5 gene copies/g), and *bvcA* (2.7±0.6 × 10^5 gene copies/g) at the Column B_{i35} inlet remained elevated, but the lack of VC and ethene in port samples collected at the end of the experiment (Figure 5-7) indicated that these remaining cells were not active.

5.4.5 Implications for chlorinated solvent remediation

For more than a decade, the coupling of ISTT with MRD has been touted as an attractive remedial alternative that retains beneficial aspects of each parent technology, while minimizing disadvantageous aspects like high energy demand and prolonged time to cleanup. However, progression to rigorous field-scale application has been hindered by scarce and sometimes conflicting data, particularly with respect to the optimal and maximum temperatures permissive of *Dhc* activity. As with any new remedial approach, the coupling of ISTT with MRD entails some risk; a fine balance must be achieved to optimize contaminant degradation rates without causing inadvertent harm to the target microbial community. Results of these continuous flow studies provide additional insight to assist practitioners in maintaining this balance, most notably that sustained *Dhc* activity is achievable at temperatures (>35 °C) previously considered to be

inhibitory. Furthermore, the evidence that *bvcA*-harboring *Dhc* strains supersede *vcrA*-harboring strains as the key contributors to ethene production at elevated temperatures will allow for more effective biomarker selection and assessment of MRD performance. Collectively, results reaffirm the argument for the coupled implementation of ISTT and MRD technologies, and underscore the potential for substantial cost-savings and improved contaminant degradation rates.

6. Key findings, publications, and recommendations for future work

The research described herein is intended to elucidate the likely mechanisms by which in situ thermal treatment (ISTT) technologies may impact subsequent or simultaneous microbial reductive dechlorination (MRD) of chlorinated ethenes, thus improving the ability of remediation professionals and regulatory agencies to make informed technical decisions with respect to potential field-scale implementation of coupled in situ thermal and biological remedies. Key findings of this work and information about submitted or pending publications and presentations are described.

6.1 Key findings

6.1.1 Release of fermentable substrates and direct electron donors during thermal treatment of soils

i. Thermal treatment of 14 solid materials (quartz sand, aquifer material, natural soils, and humic and fulvic acid standards) led to the release of volatile fatty acids (VFAs) to the aqueous phase. Formate, acetate, propionate, and butyrate were consistently detected regardless of solid material or incubation conditions,

indicating that release of these compounds can be expected following heating of most natural porous media.

ii. Hydrogen (H_2) was detected in the gas phase following thermal treatment of each of nine solid materials, excluding Federal Fine Ottawa sand (<0.01 wt% OC) and the four sterile humic and fulvic acid standards, but accounted for <0.03% of reducing equivalents associated with VFAs. The greatest H_2 concentrations were measured following incubation under conditions conducive to fermentation (60 °C) and were significantly inhibited by the presence of 2 mM mercury II chloride ($HgCl_2$), indicating that H_2 was produced by microorganisms and should not be expected during ISTT unless microbial activity is maintained.

iii. The extent of VFAs release was in most cases positively associated with incubation temperature (30, 60, or 90 °C), incubation time (7 – 180 d), and the organic carbon (OC) content of the solid phase (<0.01 – 2.86 wt%). Total VFAs release represented 0.0 – 4.8 wt% of OC mass initially associated with the solid phase, regardless of whether native microbial activity was uninhibited, inhibited, or eliminated. Collectively, these findings indicate that hydrolytic

degradation of solid-phase organic matter was the dominant mechanism of VFAs release.

iv. Heating of solid materials representative of aquifer materials (<0.01 – 2.86 wt% OC) under conditions typical of ISTT (180 d at 90 °C) resulted in a strong linear correlation ($p < 0.0005$; adjusted $R^2 = 0.97$) between total VFAs release and solid-phase OC content. This suggests that the magnitude of substrate release from the solid phase during heating can be estimated based on known ISTT operational parameters and solid-phase properties that are routinely collected during initial site investigation and remedial planning stages.

v. The relationship between VFAs release and solid-phase OC content was not maintained during incubation of soils and humic and fulvic acid standards with exceptionally high OC content (46.90 – 63.81 wt%). This was due in part to the fact that the majority of OC comprising such solid materials must be associated with highly stable, carbon-dense functional groups (e.g., phenol) that are not susceptible to hydrolytic degradation under typical ISTT conditions. Thus, the correlation between total VFAs release

and solid-phase OC content should not be applied to estimate VFAs release during ISTT of high-OC solid materials.

6.1.2 Bioavailability and utilization of thermally-released substrates for the microbial reductive dechlorination of chlorinated ethenes

i. Thermal treatment of Webster soil under 1-D flow conditions led to the release of the same VFAs detected following ampule batch incubation (formate, acetate, propionate, and butyrate), and thermal treatment of Hudson soil under 1-D flow conditions also led to the release of isovalerate. Total VFAs releases under 1-D flow conditions were up to one order of magnitude greater than under corresponding conditions in batch studies, thus validating prior findings and supporting the role of ISTT as a potentially viable source of bioavailable substrates to support anaerobic microbial activity.

ii. The KB-1® microbial consortium dechlorinated tetrachloroethene (PCE), trichloroethene (TCE), and *cis*-1,2-dichloroethene (*cis*-DCE) to vinyl chloride (VC) and non-toxic ethene in a system lacking electron donor and carbon sources except for those released during heating of an upgradient Hudson soil column. Ethene accounted for up to 60 mol% of effluent dechlorination

products and 23 mol% overall, compared to only 14 mol% overall in an unheated system, thus demonstrating the capacity of ISTT to sustain MRD in a system otherwise lacking bioavailable substrates.

iii. In one case, the concentrations and relative complexity (i.e., average carbon content) of thermally-released VFAs were shown to increase during subsequent exposure to the KB-1® microbial consortium, while VFAs concentrations in an equivalent, but non-bioaugmented system declined to below the detection limit. These findings are preliminary, but suggest that microbial degradation of complex organic compounds liberated during ISTT may continue to provide a source of bioavailable VFAs downgradient of the heated zone.

6.1.3 Impacts of low-temperature thermal treatment on a PCE-to-ethene dechlorinating consortium

i. Low-temperature thermal treatment (35 °C) of a 1-D flow system bioaugmented with the KB-1® microbial consortium enhanced dechlorination of PCE, TCE, *cis*-DCE, and VC relative to an otherwise equivalent system designed to imitate ambient aquifer temperature (15 °C). Degradation of *cis*-DCE to VC by

Dehalococcoides mccartyi (*Dhc*) was most immediately affected, and an increase in temperature from 15 to 35 °C was associated with a rapid decline in *cis*-DCE concentrations and a surge in VC concentrations. This finding indicates that even slight increases in subsurface temperature (e.g., +20 °C) can have profound impacts on the activity of *Dhc*, potentially helping to alleviate the *cis*-DCE stall often encountered at sites undergoing MRD.

ii. Regardless of the initial system temperature, rapid ethene production occurred in each system after an extended lag period of approximately 73 – 74 pore volumes (PVs) at 35 °C. This finding suggests that the likelihood of achieving complete dechlorination to ethene in a coupled system is not affected by the order in which the low-temperature ISTT and MRD remedies are applied.

iii. Sustained dechlorination of PCE to non-toxic ethene was achieved at temperatures of up to 43 °C, or 13 – 18 °C greater than the optimal temperature range for *Dhc* activity based on the results of batch studies. This finding highlights the importance of system scale (i.e., batch vs. 1-D flow) during assessment of MRD activity, and indicates that dechlorinating bacteria, particularly *Dhc*, may

benefit from substantially greater subsurface temperatures than those previously understood to be inhibitory.

iv. The relative abundances of individual *Dhc* strains shifted with temperature, with strains possessing the *vcrA* gene dominating at 15 °C and strains possessing the *bvcA* gene dominating at 35 – 43 °C. This evidence that *bvcA*-harboring strains are primarily responsible for ethene formation at elevated temperatures will improve practitioners' ability to select appropriate biomarkers and evaluate MRD performance at low-temperature ISTT sites.

6.2 Publications and presentations

Three manuscripts based on this research have been submitted, prepared, or are currently in preparation for publication. Some content of this dissertation has been previously included in platform and poster presentations.

6.2.1 Publications

i. Marcet, T.F., N.L. Cápiro, Y. Yang, F.E. Löffler, and K.D. Pennell. "Utilization of thermally-released substrates by a PCE-to-ethene dechlorinating microbial consortium." *(manuscript in preparation)*

ii. Marcet, T.F., N.L. Cápiro, Y. Yang, F.E. Löffler, and K.D. Pennell. (2017) "Impacts of Low-Temperature Thermal Treatment on

Microbial Detoxification of Tetrachloroethene under Continuous Flow Conditions." *(manuscript complete, submission pending)*

iii. Marcet, T.M., N.L. Cápiro, L.A. Morris, S.M. Hassan, Y. Yang, F.E. Löffler and K.D. Pennell. (2017) "Release of fermentable substrates and direct electron donors during thermal treatment of soils." *Environmental Science & Technology (manuscript in review)*

6.2.2 Select presentations

i. Marcet, T.F., K.D. Pennell, N.L. Cápiro, F.E. Löffler, Y. Yang. "Impacts of Thermal Treatment on the Activity of a PCE-to-Ethene Dechlorinating Consortium (Invited Platform)." Association for Environmental Health and Sciences Foundation 32nd Annual International Conference on Soils, Sediments, Water, and Energy; Amherst, MA. October 2016.

ii. Marcet, T.F., K.D. Pennell, N.L. Cápiro, F.E. Löffler, Y. Yang. "Impacts of Thermal Treatment on the Activity of a PCE-to-Ethene Dechlorinating Consortium (Platform)." Battelle Tenth International Conference on Remediation of Chlorinated and Recalcitrant Compounds; Palm Springs, CA. May 2016.

iii. Marcet, T.F., Y. Yang, F.E. Löffler, N.L. Cápiro, and K.D. Pennell. "Coupling Thermal Treatment with Microbial Reductive Dechlorination for the Enhanced Remediation of Chlorinated Ethenes

(Poster).” Association for Environmental Health and Sciences Foundation 31st Annual International Conference on Soils, Sediments, Water, and Energy; Amherst, MA. October 2015.

iv. Marcet, T.F., Y. Yang, J. Costanza, N.L. Cápiro, F.E. Löffler, and K.D. Pennell. “Evaluating the Potential for Thermal Treatment of Soils to Supply Electron Donors to a PCE-to-Ethene Dechlorinating Consortium (Platform).” Battelle Ninth International Conference on Remediation of Chlorinated and Recalcitrant Compounds; Monterey, CA. May 2014.

v. Marcet, T.F., Y. Yang, J. Costanza, N.L. Cápiro, F.E. Löffler, and K.D. Pennell. “Quantification of Electron Donor Release During Thermal Treatment (Platform).” Battelle Second International Symposium on Bioremediation and Sustainable Environmental Technologies; Jacksonville, FL. June 2013.

6.3 Recommendations for future work

The experimental results detailed in Chapters 3, 4, and 5 help to improve understanding of the mechanisms by which ISTT may impact MRD, hopefully leading to more effective and efficient coupling at the field scale. However, additional studies should be completed to confirm and expand upon findings described herein.

In Chapters 3 and 4, VFAs were the primary analytical foci due to their importance in providing bioavailable substrates to dechlorinating microorganisms. However, results indicated that more than 95% of OC was associated with organic compounds other than VFAs. Thus, it would be beneficial to evaluate the release, bioavailability, and consumption of these other organic compounds, such as alcohols, during ISTT. Additionally, given the complex microbial communities that exist in most subsurface environments, it would be beneficial to design experimental systems in such a way that sources and sinks of potential substrates can be monitored, rather than monitoring only net accumulation. Similarly, the impact of microbiological analyses would be improved if the activity of native or amended communities was more highly emphasized, rather than continuing to use microbial abundance as a surrogate for microbial activity. Finally, while laboratory experimentation is critical to identify the mechanisms responsible for substrate release and consumption, computer modeling and simulation will be equally critical to maximize the applicability and impact of experimental results. Thus, future studies should incorporate robust computer modeling and simulation components so that relationships between contaminant and substrate concentrations, microbial abundances, advective and diffusive transport, and solid-phase properties (e.g., OC content) can be more thoroughly quantified and extrapolated.

In Chapter 5, column study results demonstrated that key dechlorinating bacteria may be substantially more robust under ISTT conditions than previously

understood. While it might be beneficial to complete similar laboratory-scale flow studies using additional porous media (e.g., soils with appreciable OC content), chemical conditions (e.g., pH, ORP, electron donor speciation and availability), and thermal treatment parameters, results also highlight the importance of system scale in governing experimental outcomes. Thus, future experimental designs should emphasize increased system scale (e.g., 3-D aquifer cell and field-scale pilot studies) over increased parametric complexity in 1-D column studies. Given the increasing popularity of ISTT in subsurface remediation, widespread interest among consulting firms and technology vendors in coupling ISTT and MRD technologies, and the reduced governmental funding available to study chlorinated ethene remediation, future research efforts should be built around academic-industry collaboration and field-scale pilot testing.

7. References

1. Superfund: National priorities list (npl); https://www.epa.gov/superfund/superfund-national-priorities-list-npl
2. Bakke, B.; Stewart, P. A.; Waters, M. A. Uses of and exposure to trichloroethylene in us industry: A systematic literature review. *J Occup Environ Hyg* **2007**, *4* (5), 375-390; DOI 10.1080/15459620701301763.
3. Christ, J. A.; Ramsburg, C. A.; Abriola, L. M.; Pennell, K. D.; Löffler, F. E. Coupling aggressive mass removal with microbial reductive dechlorination for remediation of DNAPL source zones: A review and assessment. *Environ Health Persp* **2005**, *113* (4), 465-477; DOI 10.1289/ehp.6932.
4. Stroo, H. F.; Leeson, A.; Marqusee, J. A.; Johnson, P. C.; Ward, C. H.; Kavanaugh, M. C.; Sale, T. C.; Newell, C. J.; Pennell, K. D.; Lebrón, C. A. Chlorinated ethene source remediation: Lessons learned. *Environ Sci Technol* **2012**, *46* (12), 6438-6447; DOI 10.1021/es204714w.
5. Beyke, G.; Fleming, D. In situ thermal remediation of DNAPL and LNAPL using electrical resistance heating. *Remed J* **2005**, *15* (3), 5-22; DOI 10.1002/rem.20047.
6. Ramsburg, C. A.; Abriola, L. M.; Pennell, K. D.; Löffler, F. E.; Gamache, M.; Amos, B. K.; Petrovskis, E. A. Stimulated microbial reductive dechlorination following surfactant treatment at the bachman road site. *Environ Sci Technol* **2004**, *38* (22), 5902-5914; DOI 10.1021/es049675i.
7. Rao, P. S. C.; Jawitz, J. W.; Enfield, C. G.; Falta, R. W.; Annable, M. D.; Wood, A. L. In *Technology integration for contaminated site remediation: Clean-up goals and performance criteria*, Groundwater quality, Sheffield, UK, 2001; Sheffield, UK, 2001; pp 571-578.
8. Davis, E. L., *How heat can enhance in-situ soil and aquifer remediation: Important chemical properties and guidance on choosing the appropriate technique*. USEPA: 1997.
9. Alvarez, P. J.; Illman, W. A., *Bioremediation and natural attenuation: process fundamentals and mathematical models*. John Wiley & Sons, Inc.: Hoboken, NJ, 2006.
10. Macbeth, T. W.; Truex, M.; Powell, T.; Michalsen, M. *Final report: Combining low-energy electrical resistance heating with biotic and abiotic reactions for treatment of chlorinated solvent DNAPL source areas*. Environmental Security Technology Certification Program: December 5, 2012.
11. Smith, L. M.; Price, S.; Stallard, M.; Laduzinsky, D. In *Combined thermal and enhanced reductive dechlorination remediation at a former dry cleaner source area*, Tenth International Conference on Remediation of Chlorinated and Recalcitrant Compounds, Palm Springs, CA, May 23, 2016, 2016; Palm Springs, CA, 2016.

12. Smith, N.; Macbeth, T. W.; Giaudrone, D.; Chichakli, R.; Cora, C.; Lynch, K.; Powell, T. In *Implementation and performance of thermally enhanced bioremediation for targeted DNAPL source treatment*, Tenth International Conference on Remediation of Chlorinated and Recalcitrant Compounds, Palm Springs, CA, 2016; Palm Springs, CA, 2016.
13. Löffler, F. E.; Yan, J.; Ritalahti, K. M.; Adrian, L.; Edwards, E. A.; Konstantinidis, K. T.; Mueller, J. A.; Fullerton, H.; Zinder, S. H.; Spormann, A. M. *Dehalococcoides mccartyi* gen. nov., sp nov., obligately organohalide-respiring anaerobic bacteria relevant to halogen cycling and bioremediation, belong to a novel bacterial class, *Dehalococcoidia* classis nov., order *Dehalococcoidales* ord. nov and family *Dehalococcoidaceae* fam. nov., within the phylum *Chloroflexi*. *Int J Syst Evol Microbiol* **2013**, *63*, 625-635; DOI 10.1099/ijs.0.034926-0.
14. Costanza, J.; Fletcher, K. E.; Löffler, F. E.; Pennell, K. D. Fate of TCE in heated Fort Lewis soil. *Environ Sci Technol* **2009**, *43* (3), 909-914; DOI 10.1021/es802508x.
15. Fletcher, K. E.; Costanza, J.; Pennell, K. D.; Löffler, F. E. Electron donor availability for microbial reductive processes following thermal treatment. *Water Res* **2011**, *45* (20), 6625-6636; DOI 10.1016/j.watres.2011.09.033.
16. Friis, A. K.; Albrechtsen, H. J.; Heron, G.; Bjerg, P. L. Redox processes and release of organic matter after thermal treatment of a TCE-contaminated aquifer. *Environ Sci Technol* **2005**, *39* (15), 5787-5795; DOI 10.1021/es048322g.
17. Fletcher, K. E.; Costanza, J.; Cruz-Garcia, C.; Ramaswamy, N. S.; Pennell, K. D.; Löffler, F. E. Effects of elevated temperature on *Dehalococcoides* dechlorination performance and DNA and RNA biomarker abundance. *Environ Sci Technol* **2011**, *45* (2), 712-718; DOI 10.1021/es1023477.
18. Friis, A. K.; Heimann, A. C.; Jakobsen, R.; Albrechtsen, H.-J.; Cox, E.; Bjerg, P. L. Temperature dependence of anaerobic TCE-dechlorination in a highly enriched *Dehalococcoides*-containing culture. *Water Res* **2007**, *41* (2), 355-364; DOI 10.1016/j.watres.2006.09.026.
19. Gerritse, J.; Renard, V.; Gomes, T. P.; Lawson, P. A.; Collins, M. D.; Gottschal, J. C. *Desulfitobacterium* sp. strain PCE1, an anaerobic bacterium that can grow by reductive dechlorination of tetrachloroethene or ortho-chlorinated phenols. *Arch Microbiol* **1996**, *165* (2), 132-140; DOI 10.1007/s002030050.
20. Average temperature of shallow ground water; https://www3.epa.gov/ceampubl/learn2model/part-two/onsite/ex/jne_henrys_map.html
21. Holliger, C.; Schraa, G.; Stams, A. J.; Zehnder, A. J. A highly purified enrichment culture couples the reductive dechlorination of tetrachloroethene to growth. *Appl Environ Microb* **1993**, *59* (9), 2991-2997; DOI

22. ATSDR *Toxicological profile for trichloroethylene*. United States Department of Health and Human Services: 1997.
23. USEPA, Toxicologial review of trichloroethylene. In 2011.
24. ATSDR *Toxicological profile for vinyl chloride*. United States Department of Health and Human Services: 2006.
25. NCI, Carcinogenesis bioassay of trichloroethylene. In U.S. Department of Health, E., and Welfare, Ed. National Institutes of Health: 1976.
26. Resource Conservation and Recovery Act. In United States, 1976.
27. Comprehensive Environmental Response, Compensation, and Liability Act. In United States, 1980.
28. Sale, T.; Newell, C.; Stroo, H.; Hinchee, R.; Johnson, P. *Frequently asked questions regarding management of chlorinated solvents in soils and groundwater*. DTIC Document: 2008.
29. Harr, J., *A Civil Action*. Random House: 1995.
30. ATSDR *Toxicological profile for 1,2-Dichloroethene*. United States Department of Health and Human Services: 1996.
31. ATSDR *Draft toxicological profile for tetrachloroethylene*. United States Department of Health and Human Services: 2014.
32. Goldman, S. M.; Quinlan, P. J.; Ross, G. W.; Marras, C.; Meng, C.; Bhudhikanok, G. S.; Comyns, K.; Korell, M.; Chade, A. R.; Kasten, M.; Priestley, B.; Chou, K. L.; Fernandez, H. H.; Cambi, F.; Langston, J. W.; Tanner, C. M. Solvent exposures and parkinson disease risk in twins. *Ann Neurol* **2012**, *71* (6), 776-784; DOI 10.1002/ana.22629.
33. Kavanaugh, M. C.; Suresh, P.; Rao, C. *The DNAPL remediation challenge: Is there a case for source depletion?* DTIC Document: 2003.
34. Mackay, D. M.; Cherry, J. A. Groundwater contamination - pump-and-treat remediation .2. *Environ Sci Technol* **1989**, *23* (6), 630-636; DOI 10.1021/es00064a001.
35. Stroo, H. F.; Unger, M.; Ward, C. H.; Kavanaugh, M. C.; Vogel, C.; Leeson, A.; Marqusee, J. A.; Smith, B. P. Remediating chlorinated solvent source zones. *Environ Sci Technol* **2003**, *37* (11), 224A-230A; DOI 10.1021/es032488k.
36. Chapman, S. W.; Parker, B. L. Plume persistence due to aquitard back diffusion following dense nonaqueous phase liquid source removal or isolation. *Water Res* **2005**, *41* (12); DOI 10.1029/2005wr004224.
37. Parker, B. L.; Chapman, S. W.; Guilbeault, M. A. Plume persistence caused by back diffusion from thin clay layers in a sand aquifer following TCE source-zone hydraulic isolation. *J Contam Hydrol* **2008**, *102* (1-2), 86-104; DOI 10.1016/j.jconhyd.2008.07.003.
38. McGuire, T. M.; McDade, J. M.; Newell, C. J. Performance of DNAPL source depletion technologies at 59 chlorinated solvent-impacted sites. *Ground Water Monit R* **2006**, *26* (1), 73-84; DOI 10.1111/j.1745-6592.2006.00054.x.

39. National primary drinking water regulations; https://www.epa.gov/ground-water-and-drinking-water/table-regulated-drinking-water-contaminants#Organic
40. Jackson, R. E. The evolution of DNAPL remediation practice. In *Chlorinated Solvent and DNAPL Remediation: Innovative Strategies for Subsurface Cleanup*; Henry, S. M., Warner, S. D., Eds.; 2003; Vol. 837, pp 21-35.
41. Ramakrishnan, V.; Ogram, A. V.; Lindner, A. S. Impacts of co-solvent flushing on microbial populations capable of degrading trichloroethylene. *Environ Health Persp* **2005**, *113* (1), 55-61; DOI 10.1289/ehp.6937.
42. Friis, A. K.; Albrechtsen, H. J.; Cox, E.; Bjerg, P. L. The need for bioaugmentation after thermal treatment of a TCE-contaminated aquifer: Laboratory experiments. *J Contam Hydrol* **2006**, *88* (3-4), 235-248; DOI 10.1016/j.jconhyd.2006.09.001.
43. Friis, A. K.; Heron, G.; Albrechtsen, H. J.; Udell, K. S.; Bjerg, P. L. Anaerobic dechlorination and redox activities after full-scale electrical resistance heating (ERH) of a TCE-contaminated aquifer. *J Contam Hydrol* **2006**, *88* (3-4), 219-234; DOI 10.1016/j.jconhyd.2006.07.001.
44. Truex, M.; Powell, T.; Lynch, K. In situ dechlorination of TCE during aquifer heating. *Ground Water Monit R* **2007**, *27* (2), 96-105; DOI 10.1111/j.1745-6592.2007.00141.x.
45. Jeffers, P. M.; Ward, L. M.; Woytowitch, L. M.; Wolfe, N. L. Homogeneous hydrolysis rate constants for selected chlorinated methanes, ethanes, ethenes, and propanes. *Environ Sci Technol* **1989**, *23* (8), 965-969; DOI 10.1021/es00066a006.
46. Suthersan, S.; Horst, J.; Klemmer, M.; Malone, D. Temperature-activated auto-decomposition reactions: an under-utilized in situ remediation solution. *Ground Water Monit Rem* **2012**, *32* (3), 34-40; DOI 10.1111/j.1745-6592.2012.01407.x.
47. Triplett Kingston, J. L.; Dahlen, P. R.; Johnson, P. C. State-of-the-practice review of in situ thermal technologies. *Ground Water Monit R* **2010**, *30* (4), 64-72; DOI 10.1111/j.1745-6592.2010.01305.x.
48. Löffler, F. E.; Edwards, E. A. Harnessing microbial activities for environmental cleanup. *Curr Opin Biotechnol* **2006**, *17* (3), 274-284; DOI 10.1016/j.copbio.2006.05.001.
49. Löffler, F. E.; Ritalahti, K. M.; Zinder, S. H. *Dehalococcoides* and reductive dechlorination of chlorinated solvents. In *Bioaugmentation for groundwater remediation*; Stroo, H. F., Leeson, A., Ward, C. H., Eds.; Springer: New York, 2013; Vol. 5, pp 39-88.
50. He, J. Z.; Sung, Y.; Krajmalnik-Brown, R.; Ritalahti, K. M.; Löffler, F. E. Isolation and characterization of *Dehalococcoides* sp strain FL2, a trichloroethene (TCE)- and 1,2-dichloroethene-respiring anaerobe. *Environ Microbiol* **2005**, *7* (9), 1442-1450; DOI 10.1111/j.1462-2920.2005.00830.x.

51. Krajmalnik-Brown, R.; Holscher, T.; Thomson, I. N.; Saunders, F. M.; Ritalahti, K. M.; Löffler, F. E. Genetic identification of a putative vinyl chloride reductase in *dehalococcoides* sp strain bav1. *Appl Environ Microb* **2004**, *70* (10), 6347-6351; DOI 10.1128/aem.70.10.6347-6351.2004.
52. Maymó-Gatell, X.; Anguish, T.; Zinder, S. H. Reductive dechlorination of chlorinated ethenes and 1, 2-dichloroethane by "*dehalococcoides ethenogenes*" 195. *Appl Environ Microb* **1999**, *65* (7), 3108-3113; DOI
53. Daprato, R. C.; Löffler, F. E.; Hughes, J. B. Comparative analysis of three tetrachloroethene to ethene halorespiring consortia suggests functional redundancy. *Environ Sci Technol* **2007**, *41* (7), 2261-2269; DOI 10.1021/es061544p.
54. Duhamel, M.; Edwards, E. A. Microbial composition of chlorinated ethene-degrading cultures dominated by *Dehalococcoides*. *FEMS Microbiol Ecol* **2006**, *58* (3), 538-549; DOI 10.1111/j.1574-6941.2006.00191.x.
55. Major, D. W.; McMaster, M. L.; Cox, E. E.; Edwards, E. A.; Dworatzek, S. M.; Hendrickson, E. R.; Starr, M. G.; Payne, J. A.; Buonamici, L. W. Field demonstration of successful bioaugmentation to achieve dechlorination of tetrachloroethene to ethene. *Environ Sci Technol* **2002**, *36* (23), 5106-5116; DOI 10.1021/es0255711.
56. Ritalahti, K. M.; Löffler, F. E.; Rasch, E. E.; Koenigsberg, S. S. Bioaugmentation for chlorinated ethene detoxification: bioaugmentation and molecular diagnostics in the bioremediation of chlorinated ethene-contaminated sites. *Ind Biotechnol* **2005**, *1* (2), 114-118; DOI 10.1089/ind.2005.1.114.
57. Vainberg, S.; Condee, C. W.; Steffan, R. J. Large-scale production of bacterial consortia for remediation of chlorinated solvent-contaminated groundwater. *J Ind Microbiol Biotechnol* **2009**, *36* (9), 1189-1197; DOI 10.1007/s10295-009-0600-5.
58. Holliger, C.; Hahn, D.; Harmsen, H.; Ludwig, W.; Schumacher, W.; Tindall, B.; Vazquez, F.; Weiss, N.; Zehnder, A. J. B. *Dehalobacter restrictus* gen. Nov. And sp. Nov., a strictly anaerobic bacterium that reductively dechlorinates tetra- and trichloroethene in an anaerobic respiration. *Arch Microbiol* **1998**, *169* (4), 313-321; DOI 10.1007/s002030050577.
59. Krumholz, L. R.; Sharp, R.; Fishbain, S. S. A freshwater anaerobe coupling acetate oxidation to tetrachloroethylene dehalogenation. *Appl Environ Microb* **1996**, *62* (11), 4108-4113; DOI
60. Luijten, M.; de Weert, J.; Smidt, H.; Boschker, H. T. S.; de Vos, W. M.; Schraa, G.; Stams, A. J. M. Description of *sulfurospirillum halorespirans* sp nov., an anaerobic, tetrachloroethene-respiring bacterium, and transfer of *dehalospirillum multivorans* to the genus *sulfurospirillum* as *sulfurospirillum multivorans* comb. Nov. *int J Syst Evol Microbiol* **2003**, *53*, 787-793; DOI 10.1099/ijs.0.02417-0.

61. Maymó-Gatell, X.; Chien, Y. T.; Gossett, J. M.; Zinder, S. H. Isolation of a bacterium that reductively dechlorinates tetrachloroethene to ethene. *Science* **1997**, *276* (5318), 1568-1571; DOI 10.1126/science.276.5318.1568.
62. Neumann, A.; Scholz-Muramatsu, H.; Diekert, G. Tetrachloroethene metabolism of *dehalospirillum multivorans*. *Arch Microbiol* **1994**, *162* (4), 295-301; DOI 10.1007/bf00301854.
63. Scholz-Muramatsu, H.; Neumann, A.; Messmer, M.; Moore, E.; Diekert, G. Isolation and characterization of *dehalospirillum multivorans* gen-nov, sp-nov, a tetrachloroethene-utilizing, strictly anaerobic bacterium. *Arch Microbiol* **1995**, *163* (1), 48-56; DOI 10.1007/bf00262203.
64. Sung, Y.; Fletcher, K. F.; Ritalaliti, K. M.; Apkarian, R. P.; Ramos-Hernandez, N.; Sanford, R. A.; Mesbah, N. M.; Löffler, F. E. *Geobacter lovleyi* sp. nov. strain SZ, a novel metal-reducing and tetrachloroethene-dechlorinating bacterium. *Appl Environ Microb* **2006**, *72* (4), 2775-2782; DOI 10.1128/aem.72.4.2775-2782.2006.
65. Sung, Y.; Ritalahti, K. M.; Sanford, R. A.; Urbance, J. W.; Flynn, S. J.; Tiedje, J. M.; Löffler, F. E. Characterization of two tetrachloroethene-reducing, acetate-oxidizing anaerobic bacteria and their description as *Desulfuromonas michiganensis* sp. nov. *Appl Environ Microb* **2003**, *69* (5), 2964-2974; DOI 10.1128/aem.69.5.2964-2974.
66. Suyama, A.; Yamashita, M.; Yoshino, S.; Furukawa, K. Molecular characterization of the pcea reductive dehalogenase of *desulfitobacterium* sp strain y51. *J Bacteriol* **2002**, *184* (13), 3419-3425; DOI 10.1128/jb.184.13.3419-3425.2002.
67. Marcet, T. F. Secondary impacts of in situ chlorinated solvent remediation due to metal sulfide precipitation and thermal treatment. Tufts University, 2014.
68. Sung, Y.; Ritalahti, K. M.; Apkarian, R. P.; Löffler, F. E. Quantitative PCR confirms purity of strain gt, a novel trichloroethene-to-ethene-respiring *dehalococcoides* isolate. *Appl Environ Microb* **2006**, *72* (3), 1980-1987; DOI 10.1128/aem.72.3.1980-1987.2006.
69. He, J. Z.; Ritalahti, K. M.; Aiello, M. R.; Löffler, F. E. Complete detoxification of vinyl chloride by an anaerobic enrichment culture and identification of the reductively dechlorinating population as a *dehalococcoides* species. *Appl Environ Microb* **2003**, *69* (2), 996-1003; DOI 10.1128/aem.69.2.996-1003.2003.
70. He, J. Z.; Sung, Y.; Dollhopf, M. E.; Fathepure, B. Z.; Tiedje, J. M.; Löffler, F. E. Acetate versus hydrogen as direct electron donors to stimulate the microbial reductive dechlorination process at chloroethene-contaminated sites. *Environ Sci Technol* **2002**, *36* (18), 3945-3952; DOI 10.1021/es025528d.
71. Cupples, A. M.; Spormann, A. M.; McCarty, P. L. Growth of a *dehalococcoides*-like microorganism on vinyl chloride and *cis*-

dichloroethene as electron acceptors as determined by competitive PCR. *Appl Environ Microb* **2003**, *69* (2), 953-959; DOI 10.1128/aem.69.2.953-959.2003.

72. Ritalahti, K. M.; Hatt, J. K.; Lugmayr, V.; Henn, K.; Petrovskis, E. A.; Ogles, D. M.; Davis, G. A.; Yeager, C. M.; Lebrón, C. A.; Löffler, F. E. Comparing on-site to off-site biomass collection for *Dehalococcoides* biomarker gene quantification to predict in situ chlorinated ethene detoxification potential. *Environ Sci Technol* **2010**, *44* (13), 5127-5133; DOI 10.1021/es100408r.
73. Scheutz, C.; Durant, N. D.; Dennis, P.; Hansen, M. H.; Jørgensen, T.; Jakobsen, R.; Cox, E. E.; Bjerg, P. L. Concurrent ethene generation and growth of *Dehalococcoides* containing vinyl chloride reductive dehalogenase genes during an enhanced reductive dechlorination field demonstration. *Environ Sci Technol* **2008**, *42* (24), 9302-9309; DOI 10.1021/es800764t.
74. van der Zaan, B.; Hannes, F.; Hoekstra, N.; Rijnaarts, H.; de Vos, W. M.; Smidt, H.; Gerritse, J. Correlation of *Dehalococcoides* 16S rRNA and chloroethene-reductive dehalogenase genes with geochemical conditions in chloroethene-contaminated groundwater. *Appl Environ Microb* **2010**, *76* (3), 843-850; DOI 10.1128/aem.01482-09.
75. McGuire, T. M.; Newell, C. J.; Looney, B. B.; Vangelas, K. M.; Sink, C. H. Historical analysis of monitored natural attenuation: A survey of 191 chlorinated solvent sites and 45 solvent plumes. *Remed J* **2004**, *15* (1), 99-112; DOI 10.1002/rem.20036.
76. Lendvay, J. M.; Löffler, F. E.; Dollhopf, M.; Aiello, M. R.; Daniels, G.; Fathepure, B. Z.; Gebhard, M.; Heine, R.; Helton, R.; Shi, J.; Krajmalnik-Brown, R.; Major, C. L.; Barcelona, M. J.; Petrovskis, E.; Hickey, R.; Tiedje, J. M.; Adriaens, P. Bioreactive barriers: A comparison of bioaugmentation and biostimulation for chlorinated solvent remediation. *Environ Sci Technol* **2003**, *37* (7), 1422-1431; DOI 10.1021/es025985u.
77. Widada, J.; Nojiri, H.; Omori, T. Recent developments in molecular techniques for identification and monitoring of xenobiotic-degrading bacteria and their catabolic genes in bioremediation. *Appl Microbiol Biotechnol* **2002**, *60* (1-2), 45-59; DOI 10.1007/s00253-002-1072-y.
78. McDade, J. M.; McGuire, T. M.; Newell, C. J. Analysis of DNAPL source-depletion costs at 36 field sites. *Remed J* **2005**, *15* (2), 9-18; DOI 10.1002/rem.20039.
79. Amos, B. K.; Suchomel, E. J.; Pennell, K. D.; Loffler, F. E. Spatial and temporal distributions of *Geobacter lovleyi* and *Dehalococcoides* spp. during bioenhanced PCE-NAPL dissolution. *Environ Sci Technol* **2009**, *43* (6), 1977-1985; DOI 10.1021/es8027692.
80. Azizian, M. F.; Behrens, S.; Sabalowsky, A.; Dolan, M. E.; Spormann, A. M.; Semprini, L. Continuous-flow column study of reductive dehalogenation of PCE upon bioaugmentation with the Evanite enrichment

culture. *J Contam Hydrol* **2008**, *100* (1), 11-21; DOI 10.1016/j.jconhyd.2008.04.006.
81. Yu, S.; Dolan, M. E.; Semprini, L. Kinetics and inhibition of reductive dechlorination of chlorinated ethylenes by two different mixed cultures. *Environ Sci Technol* **2005**, *39* (1), 195-205; DOI 10.1021/es0496773.
82. Krauter, P.; MacQueen, D.; Bishop, D. *Effects on subsurface electrical heating and steam injection on the indigenous microbial community*. 1995.
83. Yang, Y. R.; McCarty, P. L. Competition for hydrogen within a chlorinated solvent dehalogenating anaerobic mixed culture. *Environ Sci Technol* **1998**, *32* (22), 3591-3597; DOI 10.1021/es980363n.
84. Lovley, D. R. Minimum threshold for hydrogen metabolism in methanogenic bacteria. *Appl Environ Microb* **1985**, *49* (6), 1530-1531; DOI
85. Ritchie, J. D.; Perdue, E. M. Proton-binding study of standard and reference fulvic acids, humic acids, and natural organic matter. *Geochim Cosmochim Ac* **2003**, *67* (1), 85-96; DOI 10.1016/S0016-7037(02)01044-X.
86. Lu, X. Q.; Vassallo, A. M.; Johnson, W. D. Thermal stability of humic substances and their metal forms: An investigation using FTIR emission spectroscopy. *J Anal Appl Pyrol* **1997**, *43* (2), 103-113; DOI 10.1016/S0165-2370(97)00059-4.
87. Skhonde, M. P.; Herod, A. A.; van der Walt, T. J.; Tsatsi, W. L.; Mokoena, K. The effect of thermal treatment on the compositional structure of humic acids extracted from South African bituminous coal. *Int J Miner Process* **2006**, *81* (1), 51-57; DOI 10.1016/j.minpro.2006.07.001.
88. McCarty, P. L.; Chu, M.-Y.; Kitanidis, P. K. Electron donor and pH relationships for biologically enhanced dissolution of chlorinated solvent DNAPL in groundwater. *Eur J Soil Biol* **2007**, *43* (5-6), 276-282; DOI 10.1016/j.ejsobi.2007.03.004.
89. Schaefer, C. E.; Condee, C. W.; Vainberg, S.; Steffan, R. J. Bioaugmentation for chlorinated ethenes using *Dehalococcoides* sp.: Comparison between batch and column experiments. *Chemosphere* **2009**, *75* (2), 141-148; DOI 10.1016/j.chemosphere.2008.12.041.
90. Pennell, K. D.; Cápiro, N. L.; Walker, D. I. Surfactant and cosolvent flushing. In *Chlorinated solvent source zone remediation*; Kueper, B. H., Stroo, H. F., Vogel, C. M., Ward, C. H., Eds.; Springer Science & Business Media: New York, 2014; pp 353-394.
91. Boopathy, R. Factors limiting bioremediation technologies. *Bioresource Technol* **2000**, *74* (1), 63-67; DOI 10.1016/s0960-8524(99)00144-3.
92. Sale, T.; Parker, B.; Newell, C.; Devlin, J. *State-of-the-science review: Management of contaminants stored in low permeability zones*. ER-1740; Strategic Environmental Research and Development Program: October, 2013.
93. Stevenson, F. J., *Humus chemistry: Genesis, composition, reactions*. John Wiley & Sons: 1994.

94. Fennell, D. E.; Gossett, J. M.; Zinder, S. H. Comparison of butyric acid, ethanol, lactic acid, and propionic acid as hydrogen donors for the reductive dechlorination of tetrachloroethene. *Environ Sci Technol* **1997**, *31* (3), 918-926; DOI 10.1021/es960756r.
95. Kim, Y. J.; Lee, H. S.; Kim, E. S.; Bae, S. S.; Lim, J. K.; Matsumi, R.; Lebedinsky, A. V.; Sokolova, T. G.; Kozhevnikova, D. A.; Cha, S.-S.; Kim, S.-J.; Kwon, K. K.; Imanaka, T.; Atomi, H.; Bonch-Osmolovskaya, E. A.; Lee, J.-H.; Kang, S. G. Formate-driven growth coupled with H2 production. *Nature* **2010**, *467* (7313), 352-355; DOI 10.1038/nature09375.
96. Schink, B.; Friedrich, M. Energetics of syntrophic fatty acid oxidation. *FEMS Microbiol Rev* **1994**, *15* (2-3), 85-94; DOI 10.1111/j.1574-6976.1994.tb00127.x.
97. Bae, S. S.; Kim, T. W.; Lee, H. S.; Kwon, K. K.; Kim, Y. J.; Kim, M.-S.; Lee, J.-H.; Kang, S. G. H2 production from CO, formate or starch using the hyperthermophilic archaeon, *Thermococcusonnurineus*. *Biotechnol Lett* **2012**, *34* (1), 75-79; DOI 10.1007/s10529-011-0732-3
98. Smatlak, C. R.; Gossett, J. M.; Zinder, S. H. Comparative kinetics of hydrogen utilization for reductive dechlorination of tetrachloroethene and methanogenesis in an anaerobic enrichment culture. *Environ Sci Technol* **1996**, *30* (9), 2850-2858; DOI 10.1021/es9602455.
99. EPA superfund program: Groveland Wells, Groveland, MA; https://www.epa.gov/superfund/groveland
100. Wang, Y.; Li, Y.; Kim, H.; Walker, S. L.; Abriola, L. M.; Pennell, K. D. Transport and retention of fullerene nanoparticles in natural soils. *J Environ Qual* **2010**, *39* (6), 1925-1933; DOI 10.2134/jeq2009.0411.
101. Official soil series descriptions; https://www.soilseries.sc.egov.usda.gov/osdlist.aspx
102. International Humic Substances Society; http://www.humicsubstances.org/
103. Swift, R. S. Organic matter characterization. In *Methods of soil analysis part 3: Chemical methods*; Sparks, D. L., Page, A. L., Helmke, P. A., Loeppert, R. H., Eds.; Soil Science Society of America, American Society of Agronomy: Madison, WI, 1996; Vol. 5.
104. Jobbágy, E. G.; Jackson, R. B. The vertical distribution of soil organic carbon and its relation to climate and vegetation. *Ecol Appl* **2000**, *10* (2), 423-436; DOI 10.1890/1051-0761(2000)010[0423:TVDOSO]2.0.CO;2.
105. Nies, D. H. Microbial heavy-metal resistance. *Appl Microbiol Biot* **1999**, *51* (6), 730-750; DOI 10.1007/s002530051457.
106. Costanza, J. Degradation of tetrachloroethylene and trichloroethylene under thermal remediation conditions. Ph.D. Dissertation, Georgia Institute of Technology, Atlanta, GA, 2005.
107. Sander, R. Compilation of Henry's law constants (version 4.0) for water as solvent. *Atmos Chem Phys* **2015**, *15* (8), 4399-4981; DOI 10.5194/acp-15-4399-2015.

108. Wang, J.; Wan, W. Factors influencing fermentative hydrogen production: A review. *Int J Hydrogen Energ* **2009**, *34* (2), 799-811; DOI 10.1016/j.ijhydene.2008.11.015.
109. Van Genuchten, M. T., CFITM model: estimates of cde solute transport parameters (v, d) from analysis of column breakthrough data. In USDA Agricultural Research Service: 1980.
110. De Bruin, W. P.; Kotterman, M. J.; Posthumus, M. A.; Schraa, G.; Zehnder, A. Complete biological reductive transformation of tetrachloroethene to ethane. *Appl Environ Microb* **1992**, *58* (6), 1996-2000; DOI 10.1007/BF02431929.
111. Amos, B. K.; Christ, J. A.; Abriola, L. M.; Pennell, K. D.; Löffler, F. E. Experimental evaluation and mathematical modeling of microbially enhanced tetrachloroethene (PCE) dissolution. *Environ Sci Technol* **2007**, *41* (3), 963-970; DOI 10.1021/es061438n.
112. Amos, B. K.; Ritalahti, K. M.; Cruz-Garcia, C.; Padilla-Crespo, E.; Löffler, F. E. Oxygen effect on *Dehalococcoides* viability and biomarker quantification. *Environ Sci Technol* **2008**, *42* (15), 5718-5726; DOI 10.1021/es703227g.
113. Isalou, M.; Sleep, B. E.; Liss, S. N. Biodegradation of high concentrations of tetrachloroethene in a continuous flow column system. *Environ Sci Technol* **1998**, *32* (22), 3579-3585; DOI 10.1021/es9803052.
114. Cápiro, N. L.; Löffler, F. E.; Pennell, K. D. Spatial and temporal dynamics of organohalide-respiring bacteria in a heterogeneous PCE–DNAPL source zone. *J Contam Hydrol* **2015**, *182*, 78-90; DOI 10.1016/j.jconhyd.2015.08.007.
115. Adamson, D. T.; McDade, J. M.; Hughes, J. B. Inoculation of DNAPL source zone to initiate reductive dechlorination of PCE. *Environ Sci Technol* **2003**, *37* (11), 2525-2533; DOI 10.1021/es020236y.
116. Bradley, P. M.; Richmond, S.; Chapelle, F. H. Chloroethene biodegradation in sediments at 4°C. *Appl Environ Microb* **2005**, *71* (10), 6414-6417; DOI 10.1128/AEM.71.10.6414-6417.2005.
117. Yang, Y.; Cápiro, N. L.; Marcet, T. F.; Yan, J.; Pennell, K. D.; Löffler, F. E. Organohalide respiration with chlorinated ethenes under low pH conditions. *Environ Sci Technol* **2017**, *51* (15), 8579-8588; DOI 10.1021/acs.est.7b01510.
118. Cope, N.; Hughes, J. B. Biologically-enhanced removal of PCE from NAPL source zones. *Environ Sci Technol* **2001**, *35* (10), 2014-2021; DOI 10.1021/es0017357.
119. Sleep, B. E.; Seepersad, D. J.; Mo, K.; Heidorn, C. M.; Hrapovic, L.; Morrill, P. L.; McMaster, M. L.; Hood, E. D.; LeBron, C.; Sherwood Lollar, B. Biological enhancement of tetrachloroethene dissolution and associated microbial community changes. *Environ Sci Technol* **2006**, *40* (11), 3623-3633; DOI 10.1021/es051493g.

120. Behrens, S.; Azizian, M. F.; McMurdie, P. J.; Sabalowsky, A.; Dolan, M. E.; Semprini, L.; Spormann, A. M. Monitoring abundance and expression of "*Dehalococcoides*" species chloroethene-reductive dehalogenases in a tetrachloroethene-dechlorinating flow column. *Appl Environ Microb* **2008**, *74* (18), 5695-5703; DOI 10.1128/AEM.00926-08.
121. Costerton, J. W.; Lewandowski, Z.; Caldwell, D. E.; Korber, D. R.; Lappin-Scott, H. M. Microbial biofilms. *Annu Rev Microbiol* **1995**, *49* (1), 711-745; DOI 10.1146/annurev.mi.49.100195.003431.
122. Lens, P. N. L.; De Beer, D.; Cronenberg, C. C. H.; Houwen, F. P.; Ottengraf, S. P. P.; Verstraete, W. H. Heterogeneous distribution of microbial activity in methanogenic aggregates: pH and glucose microprofiles. *Appl Environ Microb* **1993**, *59* (11), 3803-3815; DOI
123. Holmes, V. F.; He, J.; Lee, P. K. H.; Alvarez-Cohen, L. Discrimination of multiple *Dehalococcoides* strains in a trichloroethene enrichment by quantification of their reductive dehalogenase genes. *Appl Environ Microb* **2006**, *72* (9), 5877-5883; DOI 10.1128/aem.00516-06.
124. Lee, P. K. H.; Macbeth, T. W.; Sorenson, K. S.; Deeb, R. A.; Alvarez-Cohen, L. Quantifying genes and transcripts to assess the in situ physiology of "*Dehalococcoides*" spp. in a trichloroethene-contaminated groundwater site. *Appl Environ Microb* **2008**, *74* (9), 2728-2739; DOI 10.1128/aem.02199-07.
125. Müller, J. A.; Rosner, B. M.; Von Abendroth, G.; Meshulam-Simon, G.; McCarty, P. L.; Spormann, A. M. Molecular identification of the catabolic vinyl chloride reductase from *Dehalococcoides* sp. strain VS and its environmental distribution. *Appl Environ Microb* **2004**, *70* (8), 4880-4888; DOI 10.1128/aem.70.8.4880-4888.2004.
126. Suchomel, E. J.; Ramsburg, C. A.; Pennell, K. D. Evaluation of trichloroethene recovery processes in heterogeneous aquifer cells flushed with biodegradable surfactants. *J Contam Hydrol* **2007**, *94* (3-4), 195-214; DOI 10.1016/j.jconhyd.2007.05.011.
127. Löffler, F. E.; Sanford, R. A.; Ritalahti, K. M. Enrichment, cultivation, and detection of reductively dechlorinating bacteria. *Methods Enzymol* **2005**, *397*, 77-111; DOI 10.1016/s0076-6879(05)97005-5.
128. Roberts, J. In *Optimizing injection methods using high quality anaerobic injection water and dealing with low pH groundwater during bioremediation of chlorinated solvents*, Remtec Remediation Technology Summit, Denver, CO, March 7 - 9, 2017; Denver, CO, 2017.
129. Liang, X.; Molenda, O.; Tang, S.; Edwards, E. A. Identity and substrate specificity of reductive dehalogenases expressed in *Dehalococcoides*-containing enrichment cultures maintained on different chlorinated ethenes. *Appl Environ Microb* **2015**, *81* (14), 4626-4633; DOI 10.1128/aem.00536-15.
130. Ritalahti, K. M.; Amos, B. K.; Sung, Y.; Wu, Q. Z.; Koenigsberg, S. S.; Löffler, F. E. Quantitative PCR targeting 16s rRNA and reductive

dehalogenase genes simultaneously monitors multiple *Dehalococcoides* strains. *Appl Environ Microb* **2006**, *72* (4), 2765-2774; DOI 10.1128/aem.72.4.2765-27774.2006.
131. Yu, S.; Semprini, L. Kinetics and modeling of reductive dechlorination at high PCE and TCE concentrations. *Biotechnol Bioeng* **2004**, *88* (4), 451-464; DOI 10.1002/bit.20260.
132. Cápiro, N. L.; Wang, Y.; Hatt, J. K.; Lebrón, C. A.; Pennell, K. D.; Löffler, F. E. Distribution of organohalide-respiring bacteria between solid and aqueous phases. *Environ Sci Technol* **2014**, *48* (18), 10878-10887; DOI 10.1021/es501320h.